# ENCAPSULATION OF ULTRASOUND EXTRACTED BIOACTIVE COMPOUNDS OF BANANA PEEL WITH GRAPE POMACE

Thesis Submitted for the Award of the Degree of

## DOCTOR OF PHILOSOPHY

in

**Fruit Science**

By

**Khalangre Atul Baliram**

**Registration Number: 12106544**

**Supervised By**

**Dr. Anis Ahmad Mirza (19474)**

Department of Horticulture (Professor)

Lovely professional University, Punjab

**Co-Supervised by**

| **Dr. Ajay Kumar Sharma** | **Dr. Ahammed Shabeer T.P.** |
|---|---|
| Fruit science | Agriculture Chemistry |
| ICAR-National Research Centre for Grapes | ICAR-National Research Centre for Grapes |



**LOVELY PROFESSIONAL UNIVERSITY, PUNJAB**
**2024**

# DECLARATION

I, hereby declare that the presented work in the thesis entitled "**Encapsulation of ultrasound extracted bioactive compounds of banana peel with grape pomace**" in fulfilment of degree of **Doctor of Philosophy (Ph. D.)** is outcome of research work carried out by me under the supervision of Dr. Anis Mirza, working as Professor, in the Department of Horticulture, School of Agriculture, of Lovely Professional University, Punjab, India. In keeping with general practice of reporting scientific observations, due acknowledgements have been made whenever work described here has been based on findings of other investigator. This work has not been submitted in part or full to any other University or Institute for the award of any degree.

Name of the scholar: **Khalangre Atul Baliram**

Registration No.: **12106544**

Department/school: **Department of Horticulture, School of Agriculture**.

**Lovely Professional University**,

**Punjab, India**

# CERTIFICATE

This is to certify that the work reported in the Ph. D. thesis entitled "**Encapsulation Of Ultrasound Extracted Bioactive Compounds Of Banana Peel With Grape Pomace**" submitted in fulfillment of the requirement for the award of degree of **Doctor of Philosophy (Ph.D.)** in the Department of Horticulture, School of agriculture, Lovely Professional University, Phagwara, India is a research work carried out by  Khalangre Atul Baliram, 12106544, is bonafide record of his original work carried out under my supervision and that no part of thesis has been submitted for any other degree, diploma or equivalent course.

Name of supervisor : Dr. Anis Mirza
Designation : Professor
Department/school : Department of Horticulture
University : Lovely Professional
University, Punjab

| Name of Co-Supervisor | : | Dr. Ajay Kumar Sharma | Name of Co-Supervisor | : | Dr. Ahammed Shabeer T.P. |
|---|---|---|---|---|---|
| Designation | : | Principal Scientist | Designation | : | Senior Scientist |
| Department | ; | Post Harvest Technology | Department | ; | Agriculture Chemistry |
| Research Centre | : | ICAR-National Research Centre for Grapes, Pune. | Research Centre | : | ICAR-National Research Centre for Grapes, Pune. |

## CERTIFICATE-II

This is to certify that the thesis entitled "**Encapsulation of Ultrasound Extracted Bioactive Compounds of Banana Peel with Grape Pomace**" submitted by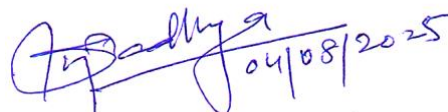 **Khalangre Atul Baliram (Registration No.: 12106544)** to the Lovely Professional University, Phagwara, in partial fulfillment of the requirements for the degree of **DOCTOR OF PHILOSOPHY (Ph.D.)** in the discipline of **Horticulture (Fruit Science)**, has been approved by the Advisory Committee after an oral examination of the student in collaboration with an external examiner.
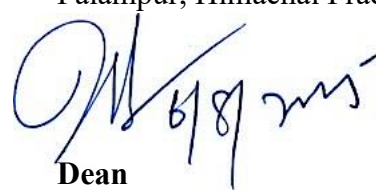
**Chairperson, Advisory Committee**
Department of Horticulture
Lovely Professional University
Phagwara – 144411

**External Examiner**
**Dr. Suresh Kumar Upadhyay**
Professor and Head,
Department of Horticulture &
Agroforestry, College of Agriculture,
CSK HP Agricultural University,
Palampur, Himachal Pradesh

**Head**
Department of Horticulture
Lovely Professional University
Phagwara – 144411

**Dean**
School of Agriculture
Lovely Professional University
Phagwara – 144411

**Place: LPU, Phagwara**

**School of Agriculture**

**Lovely Professional University, Phagwara**

| | | |
|---|---|---|
| **Title** | : | Encapsulation of ultrasound extracted bioactive compounds of banana peel with grape pomace |
| **Name of student** | : | Khalangre Atul Baliram |
| **Registration number** | : | 12106544 |
| **Year of Admission** | : | 2021 |
| **Name of Research Guide** | : | Dr Anis Mirza |
| **Name of Research Co-Guide** | : | Dr. Ajay Kumar Sharma |
| | | Dr. Ahammed Shabber TP |

# Abstract

Current research work focuses on the sustainable utilization of two major agricultural by-products, banana peel (BP) and grape pomace (GP), which are often discarded despite their rich bioactive compound content. The primary aim of the research is to harness these compounds through extraction and encapsulation, transforming them into functional ingredients for food and pharmaceutical industries. The study utilizes ultrasound-assisted extraction (UAE) to extract bioactive compounds from BP and explores the encapsulation of these compounds using GP as a carrier material. The work also investigates the drying processes for both BP and GP, which are crucial for preserving their bioactive components and enhancing the efficiency of the encapsulation process. By valorising these waste products, this research contributes to sustainable agricultural practices and adds value to food waste.

**Background and Rationale**

Food waste presents a significant global challenge, with about half of the world's fruit and vegetable production being lost or wasted annually. Agricultural by-products, particularly those generated from processing industries, contribute heavily to this waste. Banana peel (BP) and grape pomace (GP) are two such by-products that are produced in large volumes. While they contain high levels of bioactive compounds, including phenols, flavonoids and antioxidants, they are frequently

discarded. These compounds, which have known health benefits such as antioxidant, anti-inflammatory and antimicrobial properties, have significant potential applications in food and nutraceutical industries. However, due to the high moisture content of these by-products, their utilization is challenging without proper drying and preservation techniques.

Banana is one of the most produced and consumed fruits worldwide, with India being the largest producer. The processing of bananas results in substantial amounts of BP waste, which constitutes 30-40% of the fruit's total weight. BP is rich in valuable bioactive compounds, such as dopamine, phenolic acids and flavonoids. However, its high moisture content (90-92%) makes it highly perishable, leading to microbial spoilage and environmental concerns when disposed of improperly. Without drying, the bioactive compounds in BP degrade quickly, limiting its potential use in functional products. Grape pomace (GP), the solid remains of grapes after wine production, also contains high amounts of polyphenols, tannins, and dietary fiber. Similar to BP, GP is often discarded, despite its rich bioactive composition. GP accounts for 20-25% of the total weight of processed grapes, and its moisture content can range from 50-80%, making it prone to spoilage.

This research explores the drying, extraction and encapsulation of BP bioactive compounds with GP. The drying process is essential for preserving bioactive components, reducing moisture content and ensuring that BP and GP can be further processed and stored without significant degradation. The study then focuses on extracting these compounds from BP using ultrasound-assisted extraction (UAE) and encapsulating them with GP as a carrier material. By employing these sustainable methods, the research aims to convert waste into valuable products for the food and pharmaceutical sectors.

**Objectives**

**Physicochemical characterization of BP and GP:** To analyse the composition of BP and GP, including their bioactive content, moisture levels and antioxidant activity. To investigate the drying behaviour of BP and GP using different drying techniques, with a focus on preserving bioactive compounds and reducing moisture content to ideal levels for further processing.

**Encapsulation of BP bioactive compounds with GP:** To encapsulate BP bioactive compounds extract extracted using ultrasonicator, with GP as a carrier material through spray drying, ensuring the stability of the compounds.

**Physicochemical characterization of the encapsulated powder:** To evaluate the encapsulated powder, including its moisture content, phenolic retention, antioxidant activity and encapsulation efficiency.

## State of Purpose

The purpose of this research is to address the global challenge of food waste by valorising two abundant agricultural by-products—BP and GP—through optimized drying, extraction and encapsulation methods. By improving the preservation and utilization of these by-products, the study aims to create functional ingredients with enhanced stability, suitable for use in the food and nutraceutical industries. The research emphasizes the importance of drying BP and GP, which is essential for maximizing the retention of their bioactive compounds and making them more accessible for industrial applications.

## Hypothesis

The central hypothesis of this research is that drying BP and GP at optimized conditions will preserve their bioactive compounds, which can then be efficiently extracted using UAE. Furthermore, encapsulating the extracted bioactive compounds with GP through spray drying will result in a stable, functional powder with high retention of bioactive compounds and antioxidant activity. The hypothesis also posits that the encapsulation process will improve the stability and bioavailability of the bioactive compounds, making them more suitable for use in food and nutraceutical products.

## Methodology

### Drying of banana peel (BP) and grape pomace (GP)

The drying of BP and GP is a critical step in this research. BP, with its high moisture content, must be dried effectively to prevent microbial growth and spoilage while preserving its bioactive compounds. GP also requires drying to reduce moisture content and facilitate its use as a carrier material in the encapsulation process.

Drying of BP:

Hot air drying was also employed to achieve faster drying times while maintaining the quality of the bioactive compounds. In hot air drying, BP was exposed to temperatures between 50°C and 70°C, with drying times ranging from 24 to 48 hours depending on the temperature. The drying rate, moisture content, and retention of bioactive compounds were monitored to determine the optimal drying conditions.

Drying of GP:

Hot air drying was employed for GP, using temperatures of 60°C to 80°C to reduce moisture content more quickly while preserving phenolic compounds. The drying process was optimized to ensure that the moisture content was reduced to below 10%, ensuring the stability of the bioactive compounds for subsequent encapsulation.

**Extraction of Bioactive Compounds from BP Using UAE**

UAE was employed to extract bioactive compounds from BP after drying. The ultrasound process uses high-frequency sound waves to create cavitation bubbles that break down the cell walls of BP, allowing for the efficient release of phenolic compounds, catecholamines such as dopamine, L-dopa and L-tyrosine. The extraction process was optimized by adjusting parameters such as solvent concentration (ethanol-water mixtures), sonication time, sonication power and solid to liquid ratio. UAE was chosen for its ability to preserve heat-sensitive compounds and its efficiency in reducing extraction time compared to conventional methods.

**Encapsulation of BP Bioactive Compounds Using GP**

After extraction, the bioactive compounds from BP were encapsulated using GP as a carrier material through spray drying. Spray drying is a widely used encapsulation method that transforms the liquid mixture of BP extract and GP into a fine, dry powder by atomizing it in a hot air chamber. The encapsulation process was optimized to ensure high encapsulation efficiency, encapsulation yield and retention of bioactive compounds such as dopamine, L-dopa and L-tyrosine contents, with parameters such as feed concentration, inlet temperature and the ratio of BP extract to GP.

**Physicochemical characterization of the Encapsulated Powder**

The encapsulated powder was characterized for its physicochemical properties, including bulked density, tapped density, porosity and flowability, cohesiveness, solubility, moisture content, phenolic retention, antioxidant activity, dopamine, L-dopa and L-tyrosine content.

## Results and Discussion

### Physicochemical Characterization of BP and GP

Both BP and GP were found to be rich in bioactive compounds. BP contained high levels of phenolic compounds and flavonoids, while GP exhibited a high concentration of phenolic, flavonoids and anthocyanin contents. The moisture content of BP was reduced through drying to facilitate its processing and to preserve its bioactive compounds. GP also demonstrated strong antioxidant activity, making it an ideal carrier material for the encapsulation process.

### Effect of Drying on BP and GP

The drying process significantly influenced the retention of bioactive compounds in both BP and GP. Hot air drying at 60°C provided an optimal balance between drying speed and phenolic retention. In GP, hot air drying at 70°C reduced moisture content to below 10% and preserved the antioxidant activity of polyphenols. The drying processes were optimized to ensure that both BP and GP could be stored and processed further without significant degradation of their bioactive components.

### Extraction of BP Bioactive Compounds

The UAE process, optimized for a 50% ethanol solution, a sonication time of 11.8 minutes, solid to liquid ratio 8 mg/100mL and sonication power of 400 W, extracted high yields of phenolic compounds from dried BP. The UAE method was more efficient than conventional solvent extraction, reducing the extraction time and preserving antioxidant activity. These results highlight the advantages of UAE for bioactive compound extraction in industrial applications.

### Encapsulation of BP Bioactive Compounds with GP

Encapsulating BP bioactive compounds using GP resulted in a stable, free-flowing powder with high encapsulation efficiency. The encapsulated powder exhibited high retention of phenolic compounds, dopamine, L-dop and L-tyrosine content, making it suitable for use in functional foods and nutraceuticals. The use of GP as the carrier material enhanced the nutritional profile of the encapsulated product while contributing to the overall stability of the bioactive compounds.

**Conclusion**

This research demonstrates the potential for utilizing agricultural by-products, specifically BP and GP, through optimized drying, extraction and encapsulation processes. The successful drying of BP and GP preserved their bioactive compounds, enabling their efficient extraction using UAE and subsequent encapsulation into a stable, functional powder. The encapsulated powder, rich in bioactive compounds, offers potential applications in the food and pharmaceutical industries, contributing to sustainable practices by reducing food waste and adding value to agricultural by-products.

This study's findings underscore the importance of optimizing drying methods to preserve bioactive compounds in agricultural by-products. Further research should explore the scalability of these processes for industrial applications and investigate the health benefits of the encapsulated powder through in vivo studies. By demonstrating the feasibility of using BP and GP for functional food development, this research provides a pathway toward more sustainable and efficient use of food resources.

# TABLE OF CONTENTS

# LIST OF TABLES

# LIST OF FIGURES

# LIST OF PICTURES

# LIST OF FLOW CHARTS

# Introduction

At present, nearly half of all the fruit and vegetables produced globally are wasted, around 1.3 billion tons of waste annually (UNEP, 2022). Fruits and vegetables losses occur throughout the supply chain, with 40-50% waste during the postharvest phase for fruits and vegetables in both developing and developed countries (FAO, 2024). The fruit and vegetable processing industries generate a wide range of waste, including leaves, peels, unusable pulp, seeds, cull fruits and stones, much of which is ultimately discarded (Fernandez et al., 2018). These postharvest and agro-industrial wastes contain significant amounts of bioactive compounds. Reducing these losses can be achieved by using these by-products to create functional foods that are sources of naturally occurring bioactive compounds with antioxidant qualities (Socaci, 2017).

Banana ranks as the world's second-largest fruit in terms of global production, making up around 16% of the total fruit production. In 2022, about 179.3 million tons of bananas were produced worldwide (FAOSTAT, 2022). Notably, India is the largest banana producer, contributing 33.62 million tons (FAOSTAT, 2022). Banana hold significant global importance both as a staple food and an economic crop, providing essential vitamins (B6, C), minerals (K, Mn), dietary fibre and bioactive compounds. Besides being consumed fresh, bananas are used in various processed forms, such as banana chips and puree, exported globally (Gafuma et al., 2018). This extensive production and processing generate large amounts of agricultural waste, including peduncles, pseudo stems, rachis, peels, rejected fruits and flowers (García Batista et al., 2020). On average, a banana weighs 125 g, with 75% water content and 25% dry matter (Hikal et al., 2022). Annually, 31.5 million tons of banana peel (BP) waste is generated, accounting for 30-40% of total weight of the fruit (Sharma et al., 2016; Alzate Acevedo et al., 2021; Voora et al., 2020). This necessitates proper preservation of BP without altering its bioactive composition for further industrial exploitation. BP decomposes slowly, taking about 2 years and producing greenhouse gases, impacting climate change (Tibolla et al., 2018; Mishra et al., 2022). BP is a richer natural source of phytochemicals than the pulp, containing carbohydrates, pectin, fibres, cellulose, hemicellulose, phenols, flavonoids and other bioactive compounds (Ibrahim et al.,

2013; Emaga et al., 2011). Phenolic compounds in BP range from 0.5 to 60 GAE mg/g, including gallic acid, tannic acid, catechin, epicatechin, carotenoid, anthocyanins and catecholamines (Singh et al., 2016). These compounds having role in antimicrobial and antioxidant activities (Chabuck et al., 2013; Fidrianny et al., 2014). Traditionally, peels are used for various ailments, including anaemia, diarrhoea, inflammation, ulcers, stress regulation, cough, and burns (Kumar et al., 2012; Singh et al., 2016). The moisture content (90-92%) in BP complicates handling, adds unwanted weight, and accelerates microbial growth and spoilage, affecting bioactive compounds (Dhake et al., 2023). Hence, preserving BP with minimal moisture is essential for future exploration of its bioactive components. Drying is an oldest preservation method that reduces moisture content in commodities (Kim et al., 2002; Mphahlele et al., 2019). It involves mass transfer due to heat, evaporating moisture within the material (Jha & Sit, 2020). Drying offers significant advantages over other techniques. Traditional method of drying is sun drying, has disadvantages such as large space and labour requirements, dependence on sunlight, and high contamination risk (Kooli et al., 2007). Alternative drying method, hot air tray drying, address these challenges with simplicity and efficiency (Dönmez & Kadakal, 2024). Temperature is a key factor, affecting drying time and phytochemical constituents (Sokač et al., 2022). Effective drying conditions must balance time efficiency and phytochemical preservation.

The extraction of phytochemicals is crucial for maximizing agricultural resource utilization. Bioactive compounds, such as polyphenols, flavonoids and essential oils, offer health benefits, including antioxidant, anti-inflammatory and antimicrobial properties (Dai & Mumper, 2010). Traditional extraction methods, like solvent extraction, require large solvent volumes and extended processing times, potentially degrading sensitive compounds (Azmir et al., 2013). Ultrasound-assisted extraction (UAE) offers enhanced efficiency and selectivity, using ultrasonic waves to induce cavitation, which disrupts cell walls and facilitates bioactive release (Chemat et al., 2017). UAE reduces extraction time and solvent consumption while increasing target compound yields. Studies show UAE effectively extracts phenolic compounds from grape pomace and citrus peels, yielding higher concentrations than conventional methods (Ghafoor et al., 2009; Wang et al., 2021). UAE operates at lower temperatures, preserving bioactivity of heat-sensitive compounds (Zhou et al., 2017).

This makes UAE particularly advantageous for processing fruit by-products, aligning with green chemistry and sustainable development goals.

The quick release, lower solubility, limited permeation, lower bioavailability and instability against environmental stresses are some of the criteria that limit the direct inclusion of phenolics in pure form in food goods (Esfanjani & Jafari, 2016). The activity and health advantages of phenolic compounds are limited by their volatility during food production, transport, storage, or in the gastrointestinal tract (Munin & Edwards-Lévy, 2011). Encapsulation is a feasible approach for stabilizing bioactive compounds. Spray drying is the most commonly used encapsulation method due to its versatility and cost-effectiveness, producing stable, high-quality particles that are widely favoured in the food industry (Mahdavi et al., 2014; Kaderides et al., 2015; Shishir & Chen, 2017). Effective encapsulation requires suitable wall materials like polysaccharides, lipids and proteins, which ensure controlled release of phytochemicals. The properties of microcapsules depend on the encapsulation method, process parameters and wall material (Kaderides & Goula, 2017). Ideal wall materials have film-forming properties, good emulsification, fine drying properties, lower viscosity at high concentrations and cheaper. Various encapsulation agents exist, but using a carrier with inherent nutritional value can further enhance the final product's benefits.

Grape (*Vitis vinifera* L.) is a major fruit crop globally, with an estimated production of 74,942,573 metric tons in 2022 (FAOSTAT, 2022). Over 50% of grapes are processed, primarily for wine production, generating substantial solid waste called pomace. Grape pomace (GP) consists of skin, seed, rachis and pulp traces, summing up to 20-25% of processed grapes (Muñoz-Bernal et al., 2021). Grape skins, accounting for over 80% of wet GP, contain polyphenolic compounds and dietary fibres, making them valuable raw materials for nutraceuticals (Sant'Anna et al., 2014; Hogervorst et al., 2017). GP is rich in phytochemicals (phenols, flavonoids, tannins, flavan-3-ols, stilbenes, anthocyanins, cyanidins and proanthocyanidins) with health benefits such as antioxidant, antiaging, antitumor and antimicrobial properties (Bordiga et al., 2019; Antonić et al., 2020; Muñoz-Bernal et al., 2021; Šelo et al., 2023). However, high moisture content (50-80%) in GP affects storage stability, leading to spoilage by mold and yeast (Doymaz & Akgün, 2009; Sokač et al., 2022).

Drying GP reduces moisture content, producing a stable raw material without altering bioactive composition (Doymaz & Akgün, 2009). This dried form of grape pomace can be utilised in encapsulation of phenolics so that it adds more nutrients and phytochemicals to enhance the encapsulated product.

Considering these points, the current research work entitled "Encapsulation of ultrasound extracted bioactive compounds of banana peel with grape pomace" aims to achieve the following objectives:

1. Physicochemical characterization of the banana peel and grape pomace.
2. Encapsulation of banana peel extract with grape pomace.
3. Physicochemical characterization of the encapsulated powder.

## Review of literature

BP is a major agricultural waste generated from the banana production and processing industry. BP is a richest source of the various bioactive compounds and their antioxidant activities but moisture content is limiting factor, makes it vulnerable to faster degradation. The study was aimed to solve this issue and better utilization of these bioactive compounds from the banana peel. Where the new carrier material i.e., grape pomace for encapsulation was used to replace the traditional carrier agent maltodextrin. This chapter gives insights on the literature used for the current study entitled "Encapsulation of ultrasound extracted bioactive compounds of banana peel with grape pomace".

2.1 Physico-chemical characteristics of banana peel.

2.2 Physico-chemical characteristics of grape pomace.

2.3 Effect of drying methods on drying characteristics.

2.4 Effect of drying methods on physico-chemical, bioactive properties.

2.5 Optimization of extraction of bioactive compounds using ultrasound assisted extraction method.

2.6 Encapsulation of bioactive compound with different carrier materials using spray dryer and physico-chemical characterization of encapsulated powder.

**2.1 Physico-chemical characteristics of banana peel.**

Wachirasiri et al. (2009) conducted a study on the preparation of banana peel from the Musa ABB banana cultivar and found that the banana peel contained 91% moisture.

Babbar et al. (2010) estimated the total phenol content (TPC) and antioxidant activities (AA) of different fruit residues. The TPC and AA of banana peel was reported to be $3.8 \pm 0.24$ mg GAE/g DW and $5.67 \pm 0.32$ mg TE/g DW, respectively.

Sundaram et al. (2011) evaluated the phenolic content in banana peel of cultivar Bhusawal keli during different ripening stages of banana such as green, ripe, over ripe. The total phenolic content in green, ripe and over ripe stages were $17.43 \pm 0.90$, $10.91 \pm 0.47$ and $8.44 \pm 0.1$ mg GAE/g DM, respectively.

Singhal and Ratra (2013) investigated the biochemical contents of *Musa acuminata* peel extract. They reported antioxidant activity in methanolic and hexane extracts to be 321.29 and 323.41 μg/mL, respectively. The TFC in methanolic and hexane extracts were 75.97 and 71.95 mg rutin/g, respectively, and the total phenolic content in methanolic and hexane extracts were 114.4 and 74.08 mg GAE/g, respectively.

Rebello et al. (2014) prepared peel flour from Musa AAA and reported a TPC of $29.02 \pm 0.8$ mg GAE/g, with FRAP, ABTS and ORAC antioxidant activities of $14.0 \pm 1.7$, $242.2 \pm 34.8$, and $435.5 \pm 60.2$ μM Trolox-eq/g, respectively.

Awele et al. (2016) investigated the antioxidant potential of two different banana varieties (Dwarf Cavendish and Musa omuni). The TPC, TFC and antioxidant activity ranged from 336.83-383.83 mg GAE/100g, 242.83-252.82 mg rutin/100g, and 25.44%-30.27%, respectively.

Aboul-Enein et al. (2016) studied the banana peel and found that moisture content was 88.10%, with the highest total phenolic and flavonoid content being 17.89 mg/g DW and 21.04 mg/g DW, respectively, in methanolic extract (80%).

Agama-Acevedo et al. (2016) evaluated the physico-chemical properties of plantain BP. The moisture in peel was 860 g/kg, total phenol contains were 7.71 mg GAE/g, condensed tannins were 31.0 mg GAE/g and hydrolysable tannins were 21.0 mg GAE/g.

Hernández-Carranza et al. (2016) studied fruit by products of banana. Upon analysis the banana peel contained TPC of 490 mg GAE/100g, TFC of 752 mg CE/100g, DPPH free radical scavenging activity 999 mg TE/100g dw and FRAP antioxidant capacity 24.6 mM Fe2+/100g dw.

Syukriani et al. (2021) carried out an experiment on characterisation of banana fruit of cultivar raja. Results showed that the moisture ranged between 6.21 to 39.33%, 1.33-1.86% of ash content and 2% of protein content. vitamin C in peel was 32.3 mg/100g, fruit (7.18 mg/100g) and flesh (4.99 mg/100g). Whereas peel contains higher potassium (73.03%) and calcium (16.12%) content and pulp content more phosphorus (10.52%), magnesium (6.58%) and chlorine (4.37 %) than peel.

Islam et al. (2023) studied enzyme-assisted extraction of banana peels and under optimized conditions, found the TPC, TFC, DPPH and ABTS antioxidant activities were 25.37 mg GAE/g DM, 13.99 mg QE/g DM, 88.25% and 74.27%, respectively.

## 2.2 Physico-chemical characteristics of grape pomace.

Parry et al. (2011) studied the chemical composition of fermented and non-fermented grape pomace. Fermented red grape pomace of variety Tino Cao and non-fermented white grape pomace of variety Chardonnay showed total phenol content 72.0 ±3.0 and 47.7 ±4.4 GAE mg/g, respectively. Antioxidant capacity of chardonnay and Tina Cao pomace was evaluated by ORAC (331.1±6.0 and 386.4±8.3 µmol TE/g, respectively), ABTS (393.6±7.2 and 806.7±12.2 µmol TE/g, respectively) and $DPPH_{EC50}$ (154.2±4.4 and 94.6±12.0 10 min mg eq/L, respectively).

González-Centeno et al. (2013) characterized grape pomace of different grape pomace cultivars for polyphenols and antioxidant activity. Grape pomace of cultivar Chardonnay, Macabeu, Parellada and Premsal Blanc contained total phenolic content of 3891±383, 3093±266, 4654±255 and 3639±200 mg GA/g dm, respectively, total proanthocyanidins of 71.9±2.0, 50.8±0.0, 92.1±4.1 and 73.2±4.8 mg tannins/g dm, respectively and antioxidant activity was accessed by ABTS (92.4±1.0, 71.6±1.6, 134.0±4.3 and 93.8±4.0 mg Trolox/g dm, respectively), CUPRAC (124.2±9.8, 106.3±5.1, 209.1±12.8 and 139.79.7 mg Trolox/g dm, respectively), FRAP (76.1±4.8, 49.0±5.0, 124.8±10.7 and 68.3±6.2 mg Trolox/g dm, respectively) and ORAC (93.7±9.0, 58.1±7.6, 122.2±7.3 and 62.8±6.2 mg Trolox/g dm, respectively).

Iora et al. (2015) examined grape pomace of three cultivars i.e., Merlot, Tanat and Cabernet for its physicochemical composition. Moisture content was 9.35±0.13, 4.02±0.25 and 3.46±0.23 %, respectively. Total phenolic content was 3762.42±121.06, 3014.55±9.09 and 5101.82±119.03 mg GAE/100g, respectively, total flavonoid content was 2121.84±28.71, 1648.28±72.99 and 2983.91±51.76 mg CTE/100g, respectively and total monomeric anthocyanin content was 1576.37±77.03 1246.85±64.27 and 2092.93±71.57 mg cya-3-glu/100g, respectively.

Ky and Teissedre (2015) characterized the grape skin of different grape cultivars for polyphenolic content and antioxidant activity. Aqueous extracts of skin of Grenache, Syrah, Carignan, Mourvèdre and Alicante cultivars of grape showed 109.72±0.19, 146.50±1.19, 120.83±1.12 mg GAE/g DW of total phenol content, respectively,

112.28± 2.67, 156.63 ± 2.63, 161.61 ± 1.32, 104.79 ± 2.00 and 221.4 ± 3.47 mg/g DW of Total tannin content, respectively and 8.70 ± 0.01, 16.01 ± 0.01, 14.62 ± 0.75, 5.65 ± 0.01 and 21.40 ± 0.20 mg/g DW of total anthocyanin contents, respectively. Whereas 70% aqueous alcoholic extracts showed 195.15 ± 0.28, 224.92 ± 0.18, 203.47 ± 0.83, 219.88 ± 0.18 and 188.94 ± 0.69 mg GAE/g DW of total phenolic contents, respectively, 256.07 ± 3.65, 312.46 ± 10.77, 345.34 ± 4.18, 268.6 ± 11.68 and 232.65 ± 3.14 mg/g DW of total tannins and 53.66 ± 0.83, 86.68 ± 1.71, 88.44 ± 0.59, 46.64 ± 0.39 and 54.41 ± 2.66 mg/g DW of total anthocyanins, respectively.

Ribeiro et al. (2015) evaluated the pomace of grape cultivars of Cabernet Sauvignon (CS), Merlot (ME), Terci (TE) and mixture of 65% Bordeaux, 25% Isabel and 10% BRS Violet (MI) generated after winemaking for moisture content. The moisture content in CS, ME, TE and MI were 13.63±0.14, 6.59±0.21, 8.52±0.15 and 2.85 ±0.08 g/100g dw, respectively.

Ahmed et al. (2020) studied the bioactive composition of pomace of selected ten varieties of grapes. Grape pomace of varieties Alfonso, Antepkarasi, Büzgülü, Ekşikara, Çalkarası, Dimlit, Hönüsü, Marcaş, Redglob and Topacık contains 97.86 ± 3.17, 88.44±2.28, 85.61±1.67, 127.18±4.35, 138.41±6.71, 76.48±3.98, 78.57±2.56, 147.51±3.85, 91.14±2.47 and 75.41±1.73 mg GAE/100g of total phenol contents, respectively and 87.61±2.58, 85.47±5.21, 71.18±1.43, 95.47±3.51, 96.71±2.64, 81.18±2.76, 82.27±3.83, 98.47±1.65, 86.71±1.51 and 80.38±2.77 % of antioxidant activity, respectively. Whereas moisture content was 21.17±0.76, 24.32±0.52, 25.18±0.68, 23.57±0.91, 20.64±0.57, 25.71±1.03, 28.47±0.48, 23.51±0.54, 21.89±1.13 and 24.61±1.17 %, respectively.

Rodrigues et al. (2023) characterized the biochemical composition of fermented red grape pomace. 50% ethanolic extract of grape pomace showed TPC of 38±3.64 mg GAE/g DW, TFC of 14.94±2.29 mg Cat/g DW and reducing capacity of 22.25±3.00 mg/mL and 50 % acetone extract showed TPC of 45.18±9.51 mg GAE/g DW, TFC of 18.29±3.07 and reducing capacity of 14.93±3.81 mg/mL.

**2.3 Effect of drying methods on drying characteristics**

Goyal et al. (2007) conducted the study on drying of plum slices. The drying was performed at temperatures ranging from 55 to 65°C after pre-treating the plum slices with different methods. The drying behaviour of the plum slices was effectively

described by the logarithmic model, which showed a higher $R^2$ value. Moisture diffusivity increased as the drying temperature rose.

Niamnuy et al. (2012) performed drying of soybean using a gas infrared combined with a hot air vibrating dryer (GFIR-HAVD) at temperatures of 50, 70, 130 and 150°C. The drying data were fitted to a simple kinetic model, revealing that effective moisture diffusivity was dependent on the drying temperature. The $E_a$ for the drying process was 13.88 kJ/mol.

Akdaş and Başlar (2015) Mandarin slices were dried using both an oven and a vacuum dryer at temperatures of 55, 65 and 75°C. Out of the seven models tested, the page model provided the best fit, with $R^2$ ranging from 0.992 to 0.999. For oven drying, the $D_{eff}$ was between $0.353 \times 10^{-7}$ to $1.370 \times 10^{-7}$ m²/s, while for vacuum drying, it was between $0.952 \times 10^{-7}$ and $2.764 \times 10^{-7}$ m²/s. The Ea was 56.447 kJ/mol for oven drying and 49.713 kJ/mol for vacuum drying.

Baslar et al. (2014) carried an experiment to study the dying of pomegranate arils using forced air circulating method at temperatures 55, 65 and 75 °C. Logarithmic model was good fit to data with highest $R^2$ (0.9989-0.9999) and lowest RMSE values (0.0054-0.0142). The effective moisture diffusivity values at temperatures 55, 65 and 75 °C were $5.39 \times 10^{-11}$, $1.12 \times 10^{-10}$ and $1.70 \times 10^{-10}$ m²/s, respectively. Activation energy was 44.798 kJ/mol was required to complete drying process of pomegranate arils.

Kumar (2015) investigated the drying of blanched ripened banana peel in tray dryer to study the drying behaviour. High $R^2$ (0.99460, 0.99652), and the lowest $X^2$ value (0.000218, 0.000231) and RMSE (0.014778, 0.015177) the logarithmic model was proved as best fit.

Teles et al. (2017) dried the pinot noir grape pomace using convective dryer at temperature 40, 50 and 60°C with air velocity 0.42 m/s. Page model fitted well to describe drying of grape pomace with highest $R^2$ values (0.986-0.996). moisture content was decreased to $1.47 \pm 0.01$; $1.59 \pm 0.01$ and $1.64 \pm 0.01$ % DW for temperatures 40, 50 and 60°C. $D_{eff}$ ranged between $1.143 \times 10^{-8} - 6.341 \times 10^{-9}$ m²/s.

Akar and Barutçu Mazi, (2019) conducted a study on drying of kiwifruit, with hot air (HAD), vacuum (VD), freeze (FD) and hot air-microwave (HA–MVD) drying. For

MVD and FD, the Page and Weibull models were found to be the best fits, while for VD, the logarithmic model provided the best fit, demonstrating the highest $R^2$ values and lowest RMSE values.

Moura et al. (2021) studied the drying of trapia residues at temperature 50, 60, 70 and 80 °C with 0.6 cm thickness of trapia peel and seed. Among selected ten mathematical models midilli model fitted well to the drying kinetics ($R^2$=0.9960). Effective moisture diffusivity ranged between m $5 \times 10^{-10}$ to $16.1 \times 10^{-10}$ m$^2$/s. $E_a$ ranged between 18 to 24.2 kJ/mol where activation energy for seed was higher than peel.

Ampah et al. (2022) dried 0.6 cm thick and 10 cm$^2$ area slices of mango fruits (Kent, Keitt, Haden and Palmer) using mechanical dryer at temperature 55, 65 and 75 °C. the moisture content of all samples decreased with increase in temperature. Palmer variety showed highest moisture (87.2 % w.b.) and lowest moisture (8.7 % w.b.). midilli, page, wang and singh and logarithmic model showed best fit for describing drying behaviour of mango varieties. Effective moisture diffusivity value for Kent, Keitt, Haden and Palmer were $5.90 \times 10^{-7}$, $6.40 \times 10^{-7}$, $6.57 \times 10^{-7}$, and $7.33 \times 10^{-7}$ m2/s, respectively. Activation energy ranged between 19.90 to 25.50 kJ/mol. Haden variety showed highest activation energy among all varieties.

Popescu et al. (2023) dried the tomato peel of variety Rila using the hot air dryer at temperatures 50-75°C. The experimental data was fitted to different ten mathematical model among which the two term and handerson and pabis model fitted well to the data. The $D_{eff}$ was between $1.01 \times 10^{-9}$ to $1.53 \times 10^{-9}$ m$^2$/s.

Dhake et al. (2023) studied drying of banana peel green. The peels were treated with 0.5% and 1.0% potassium metabisulfite, while untreated peels served as the control. Drying was performed at 40 to 60°C using a tray dryer. The drying times for the samples ranged from 360 to 510 minutes. The page model proved best fit, showing the high $R^2$ values and lowest $x^2$ and RMSE. $D_{eff}$ increased with higher drying temperatures, between $5.069 \times 10^{-8}$ to $6.659 \times 10^{-8}$ m$^2$/s for the control, $6.013 \times 10^{-8}$ to $7.653 \times 10^{-8}$ m$^2$/s for 0.5% KMS, and $4.969 \times 10^{-8}$ to $6.510 \times 10^{-8}$ m$^2$/s for 1.0% KMS.

Dönmez and Kadakal (2024) dried the Gilaburu (*Viburnum opulus* L.) fruits using the hot air dryer at temperatures 50 to 70 °C. Among all these models page model best

fitted to drying at 70°C with highest $R^2$ values (0.992) and lowest $x^2$ value (0.001070552) and RMSE value (0.0304) and parabolic model fitted well to data drying at 50 and 60 °C with highest $R^2$ value (0.9996and 0.9915) and lowest $x^2$ values (0.000044974 and 0.00019453) and RMSE values (0.0066 and 0.0133). Deff values were ranged between $3.38 \times 10^{-10} – 4.01 \times 10^{-11}$ m²/s and activation energy required was 133.814 kJ/mol.

Conte et la. (2024) dried the grape pomace of cultivar Montepulciano using natural convection at room pressure at temperatures 50, 60 and 70°C at relative humidity 5%. Three mathematical models (Fick, Dual-stage type A, Dual stage type B) were fitted to the experimental data among which dual-stage type B model showed best fit and $R^2$ value (0.972).

**2.4 Effect of drying methods on physico-chemical, bioactive properties.**

Niamnuy et al. (2012) investigated the degradation kinetics of soybean isoflavones during drying using a gas infrared combined with hot air vibrating drying system at temperatures of 50, 70, 130 and 150 °C. All degradation processes followed first-order kinetics. Among the isoflavones, the degradation rate constant was highest for MGI, followed by AGI, GI and GE.

Demiray et al. (2013) examined the degradation kinetics of bioactive compounds in tomato quarters (Cv. Rio Grande) using a cabinet dryer at temperatures of 60, 70, 80, 90 and 100°C. All degradation processes followed first-order kinetics. The k values were found to range from 0.078 to 0.448 per hour for lycopene, 0.084 to 0.380 per hour for β-carotene, and 0.076 to 0.472 per hour for ascorbic acid. The activation energy was approximately 47 kJ/mol for both lycopene and ascorbic acid, while it was 40 kJ/mol for β-carotene.

Akdas and Baslar (2014) studied the degradation kinetics of phytochemicals in mandarin slices during drying under oven and vacuum drying at temperatures 55, 65 and 75 °C. degradation of total phenol content, total flavonoid content, antioxidant activity and vitamin C followed the first order kinetic model with $R^2$ 0.838 -0.979. degradation of total phenols and flavonoids was higher under vacuum drying but the degradation of vitamin C was two times higher in oven drying. The antioxidant activity showed increase in degradation with increase in drying temperature during vacuum drying and in oven drying it showed higher rate degradation at all

temperatures. Overall, the oven drying showed more colour changes and required more energy for drying.

Başlar et al. (2014) studied the effect of forced air circulating drying at temperature 55, 65 and 75 °C on pomegranate arils, bioactive compounds. The degradation of TPC, TFC, TAC and AA was studied by fitting to first order kinetics model. Drying rate constant for total phenol content ranged between $13.696 \pm 0.333$ to $27.653 \pm 2.108$ per hour, for TAC between $18.630 \pm 1.685$ to $74.368 \pm 7.669$ per hour, for antioxidant activity $10.351 \pm 0.593$ to $38.550 \pm 2.168$ per hour and for total flavonoid $22.632 \pm 1.594$ to $50.338 \pm 1.827$ per hour. The half-life for all parameters was decreased significantly, the activation energy for total phenol content, total anthocyanin content, antioxidant activity and total flavonoids was 31.76, 39.10, 34.236 and 37.85 kJ/mol, respectively.

Demiray and Tulek (2017) investigated degradation kinetics of carrot colour during hot air drying at temperatures of 45, 55 and 65°C. The colour of carrot slices was assessed using hunter parameters: L (lightness/darkness), a (redness/greenness) and b (yellowness/blueness). During the drying process, the L, a and b values decreased, while the total colour change ($\Delta E$) increased. The degradation of L, a and b values followed first-order kinetics, whereas $\Delta E$ adhered to zero-order kinetics. The dried carrot slices were subsequently used as an ingredient in instant soups, meals and were also utilized to develop an oil-free snack with high nutritional value.

Teles et al. (2017) carried out an experiment of drying of pinot noir grape pomace using convective drying method at temperature 40 to 60°C with air velocity of 0.42 m/s. the temperature 60°C showed better preservation of phenolic compounds and antioxidant activity.

Jha and sit (2020) conducted an experiment to examine the effect of convective drying on *Terminalia chebula* fruit. The drying was performed at temperatures between 40 and 60°C. The diffusion model was best fit. $D_{eff}$ values were between $1.02596 \times 10^{-11}$ to $7.72720 \times 10^{-11}$ m²/s. The degradation of phytochemicals fitted to first-order kinetics, with activation energies for all parameters ranging from 3.74 to 42.52 kJ/mol. Vitamin C showed a higher degradation rate compared to the other phytochemicals at all temperatures.

Ouyang et al. (2021) investigated effect of hot air drying at temperature 60-100°C with 1.5 m/s air flow for 6-17 hour's time on degradation of phytochemicals in pumpkin. Final moisture content in dried pumpkin was 10.50±0.29%. insoluble phenolic content accounted for around 74.9 % of total phenolic content in fresh pumpkin and it was deceased to 49.4 (100°C) and 59.7 % (60°C) in dried pumpkin. With increase in drying temperature the retention of total phenolic content, insoluble phenolic content and ascorbic acid decreased significantly but soluble phenolic content increased might be due to conversion of insoluble phenolic content to soluble phenolic content at higher temperature. The degradation of ascorbic acid followed first order kinetic ($R^2$=0.985–0.999) and total phenolic content followed zero order kinetics ($R^2$=0.887–0.997).

Sokač et al. (2022) studied effect of different drying methods such as vacuum drying (35, 50 and 70°C), conventional drying (70°C) and open sun drying on bioactive compounds of grape pomace. Polyphenols were highly stable during whole process of drying but some of the degradation was observed in vacuum drying at temperatures 35 and 50 °C. whereas, tartaric acid and tannins was more prone to degradation in all methods of drying but showed more stability in vacuum drying at 70 °C.

Elik et al., (2023) studied drying of orange peels using conventional hot air drying (HAD) and radio frequency assisted hot air drying (RF-HAD). RF-HAD drying resulted in shorter drying time as compared to HAD. Electrode gap of 70 mm and 30 mm thickness shoed better-quality properties in terms of colour, TPC, carotene content. Ascorbic acid, antioxidant activities, water retention capacity and flow behaviour compared to HAD.

Popescu et al. (2023) studied the effect of hot air drying at temperatures 50, 55, 60, 65, 70 and 75 °C on the ripe tomato peels of variety Rila extract quality i.e. carotenoid content. The lycopene degradation was 5% at 55 °C which was increased to 94% at 110 °C, similarly the β- carotene degradation at 55 °C was 51% and which rose to 83% at the 110°C.

Dönmez and Kadakal (2024) studied effect of hot air drying at temperatures 50, 60 and 70°C on bioactive compounds in gilaburu fruits. The TPC and antioxidant activities were degraded by 73.64% and 84.08 % when dried at 70°C. trans-reservetrol was 1.26±0.05 g/100g DW in fresh fruits which degraded to 0.31±0.03,

0.30±0.01 and 0.21±0.01 g/100g DW when dried at 50, 60 and 70°C, respectively. Higher degradation was observed in niacin content drying at all temperatures.

**2.5 Optimization of extraction of bioactive compounds using ultrasound assisted extraction method.**

Rodrigues and Pinto (2007) conducted an experiment to extract phenolics from coconut shell powder using ultrasonicator. The extraction process was optimized by varying factors such as toasting time (20 to 60 minutes), toasting temperature (100 to 200°C), and extraction time (20 to 60 minutes). A 50% ethanol-water solution with a pH of 4.5, adjusted with HCl, was used as the solvent.

Rodrigues et al. (2008) extracted phenolic compounds from coconut shell powder using an ultrasonicator. The extraction process was optimized by varying several factors such as temperature, solution-to-solid ratio, pH and extraction time, with a 24-experimental design applied through response surface methodology. A 50% ethanol-water solution was used for extraction. A temperature of 30°C, a solution-to-solid ratio of 50, an extraction time of 15 minutes, and a solvent pH of 6.5, yielded 22.44 mg/g phenols.

Carrera et al. (2012) extracted phenolic compounds from the grape variety Tempranillo using ultrasound method. Effect different extraction variables such as extraction temperature (0–75 °C), duty cycle (0.2 s, 0.6 s and 1 s), the quantity of sample (0.5–2 g), output amplitude (20, 50 and 100%) and the total extraction time (3–15 min) were evaluated. Three dependent parameters were evaluated such as phenol, tannin and anthocyanin. The extraction showed higher recoveries of these parameters as compared common method of extraction with very shorter time i.e., 6 min. and common method took 60 min. for extraction.

İnce et al. (2013) extracted polyphenols from melissa using microwave and ultrasound extraction. In both method of extraction, the effect of extraction time, solid to solvent ratio on extraction of polyphenols were studied. The water was used as solvent for extraction. For ultrasound effect of different powers (50-80%) were also studied. Finally, the highest total phenol content of 145.8 mg GAE/g was extracted for microwave at 5 min. and 1:30 mg/mL and 105.5 mg GAE/g at 20 min. of sonication with 1:30 solid to liquid ratio at 50 % sonication power.

Şahin and Şamlı (2013) optimized extraction bioactive compounds from olive leaf through ultrasound assisted extraction. The 500 mg solid to 10 mL solvent ratio, 60 min. time and 50% ethanol concentration yielded 201.2158 mg, 25.0626 CAE/g DL TPC and 95.5610 % antioxidant capacity.

Rodrigues et al. (2015) performed an experiment to extract anthocyanin and polyphenols from the jaboticaba peel using sonicator. Three independent parameters pH (2-5), ethanol concentration (12-38 % v/v), extraction time (20-60 min.) were optimized. The final optimal conditions 46 % ethanol, at pH1 for 10 min sonication 92.8 mg/g dry peel of GAE, 7.8 mg/g dry peel EAE and 4.9 mg/g dry peel of C3GE.

Altemimi et al. (2016) carried out an experiment to study the ultrasound-assisted extraction of phenols form the peaches and pumpkins. The effect of three independent parameters extraction temperatures, power levels and extraction on phenolic contents from peaches and pumpkins was evaluated using box-Behnken design of response surface methodology. Optimum condition for phenolic compounds in pumkins were 41.45°C extraction temperature, 44.60% sonication power for 25.6 min extraction time and for radical scavenging activity were 40.99°C extraction temperature, 56.01 % sonication powder for 25.71 min extraction time. whereas, for phenolic compounds in peach extract 41.53°C extraction temperature, 43.99% of sonication power for 27.86 min extraction time and for radical scavenging activity were 41.60°C extraction temperature, 44.88% of sonication power for 27.49 min. of extraction time.

Rodsamran and Sothornvit (2019) carried out an experiment to optimize extraction of natural phenolic compounds from lime peel using ultrasound-assisted extraction (UAE) and microwave-assisted extraction (MAE). MAE achieved the best results with 55% ethanol concentration, 140 W power and 45 seconds of extraction. UAE achieved best result at 55% solvent concentration, 38% amplitude level, and 4 minutes of time. UAE proved more effective, yielding 54.4 mg GAE/g of total phenolic content and higher antioxidant activity while reducing extraction time by 33% compared to MAE.

Pollini et al. (2020) extracted the bioactive compounds from the moringa leaves using the sonicator. The independent parameters such as solvent (0-50 %), solvent/dry leaves ratio (30 and 60 mL/g DM), temperature (30-60°C) and time (10-60 min.) were optimized for the phenolic content recovery and antioxidant activity in extract.

Th solvent concentration and solvent to dry leaves ratio has more influence on the extraction parameters. The optimized conditions 50 % water, 60:1 solvent/dry leaves, at 60 °C temperature yielded 13.79 mg GAE/g dry matter of total phenolic content and antioxidant activity of 43.32 %.

Wang et al. (2020) studied the extraction of phenolic compounds for potato peel using direct ultrasound assisted extraction, indirect ultrasound assisted extraction and conventional shaking extraction in 50% ethanol solvent. Among all methods direct ultrasound extraction showed higher and faster extraction of phenolic contents from potato peels.

Park et al. (2022) optimized the extraction of the flavonoids from Ruby S apple peel using the ultrasonicator. The study assessed the effects of temperature (20–40°C), time (15–45 minutes) and solvent concentration (50–90% ethanol) on TPC, TFC and DPPH radical scavenging activity. The highest yield of extract, TPC, TFC and AA was achieved at 20°C, 25.30 minutes and 50% ethanol. Major flavonoids extracted included hyperoside, isoquercetin, and phloridzin.

Phaiphan (2022) extracted pectin from banana peel waste using ultrasound method of extraction. Effect of Extraction temperature 35-45°C, pH 1-2 and extraction temperature of 10-20 min. on yield of pectin was evaluated. The highest yield of pectin was achieved at 33.12°C extraction temperature, 17.12 min. sonication time and 3.68 pH.

## 2.6 Encapsulation of bioactive compound with different carrier materials using spray dryer and physico-chemical characterization of encapsulated powder.

Robert et al., (2010) encapsulated the bioactive compounds of pomegranate juice and ethanolic extract with maltodextrin and soy protein isolates using spray dryer. Four different experiments were designed using $2^2$ statistical factorial design where pomegranate juice with maltodextrin, pomegranate juice with soy protein isolate, pomegranate extract with maltodextrin, pomegranate extract with soy protein isolate encapsulated with two independent parameters, coating material concentration and inlet air temperature. Results revealed that encapsulation of polyphenols with soy protein isolates showed better encapsulation efficiency but for anthocyanins maltodextrin showed better encapsulation efficiency. Encapsulated powder with

maltodextrin showed better preservation of polyphenols and anthocyanins than the soy protein isolates.

Paini et al. (2015) encapsulated the polyphenols extracted from the olive pomace with high pressure-high temperature agitated reactor using the spray dryer. Optimization of encapsulation carried out by studying the effect of inlet temperature (130-160 °C) and feed flow (5-10 mL/min). The optimal conditions 130°C inlet temperature, 100g/L maltodextrin concentration and 10mL/min feed flow showed the 94% of microencapsulation yield, 76% encapsulation efficiency, 39.5 $mg_{CAE}/g_{DP}$ polyphenol sontents and 33.8 $mmol_{DPPH}/L_{extract}$ antiradical power. Microcapsules were stable at 5°C in dark condition for 70 days whereas storage at 25 °C showed 21% degradation and sunlight exposure showed 66% degradation.

Vu et al. (2020) encapsulated phenolic extract from banana peel was with different coating materials using a spray dryer. The study examined the effects of extract-to-coating material ratio (1:1 to 1:7), inlet temperature (130-180°C), feed rate (3-15 mL/min), and five different coating materials (maltodextrin-40, maltodextrin-100, maltodextrin-180, gum Arabic, soy protein isolate, and a mixture of maltodextrin-100 and gum arabic in an 8:2 ratio) on the physical, phytochemical and antioxidant properties of the encapsulated powder. While the inlet temperature (140-180°C) and feed rate (3-15 mL/min) did not impact the TPC and AA, they affected the moisture and yield. The extract-to-coating material ratio influenced the concentration of total phenols, antioxidant activity and powder yield but did not affect moisture content. Optimal conditions were identified as 150°C inlet temperature, 9 mL/min feed rate, a 1:1 extract-to-coating material ratio and using the maltodextrin M100 and gum arabic mixture.

Escobar-Avello et al. (2021) encapsulated the polyphenolic extract of grape cane with hydroxy beta-cyclodextrin using a spray dryer. Spray dryer conditions were set as inlet temperature 130°C, outlet temperature 71°C, air inlet 35-40 $m^3$/h and airflow 473 L/h. Spray dryer was equipped with 0.7 mm nozzle and feed flow rate was kept 6-7 mL/min. The encapsulated powder showed encapsulation efficiency of 80.5 ± 1.1 % and highest value of restrytisol (97.0 ±0.6 %) and lowest value of (*E*)-resveratrol (32.7 ±2.8%). The AA of the encapsulated powder was 5300±472 µmol TE/g DW.

Ghandehari Yazdi et al. (2021) encapsulated the phenolic compounds extracted form pistachio green hull using spray dryer. In this study effect of inlet air temperature, dilution factor, wall: core ratio and rate of feeding on the physicochemical parameters of encapsulated powder were optimized using response surface methodology statistical tool. Encapsulated powder using optimal conditions showed the total phenolic content value (32.1 mg GAE/g) and 81 % encapsulation efficiency. The antioxidant activity of the free pistachio green hull showed 10 % higher than encapsulated powder. There was the 4% degradation in phenolic content in encapsulated powder was observed during storage study for 60 days.

Araújo et al. (2022) encapsulated the extracts of the spent coffee grounds using spray dryer and freeze dryer. The encapsulation efficiency in terms of phenols in encapsulated powder for both methods of encapsulation was greater reaching around 83.43%. Freeze dried powder was better than spray dried powder in terms of moisture and bulk density. Powder prepared using the combination of arabic gum and maltodextrin showed the longer preservation of all bioactive compounds in encapsulated powder.

**Materials and Methodology**

The present study entitled "Encapsulation of ultrasound extracted bioactive compounds of banana peel with grape pomace" was carried out at research laboratories of the ICAR-National Research Centre for Grapes, Pune during the year 2022-2024. This chapter provides detailed insights into the materials and methodologies used to successfully conduct the research work. The experimental flow chart as given below:
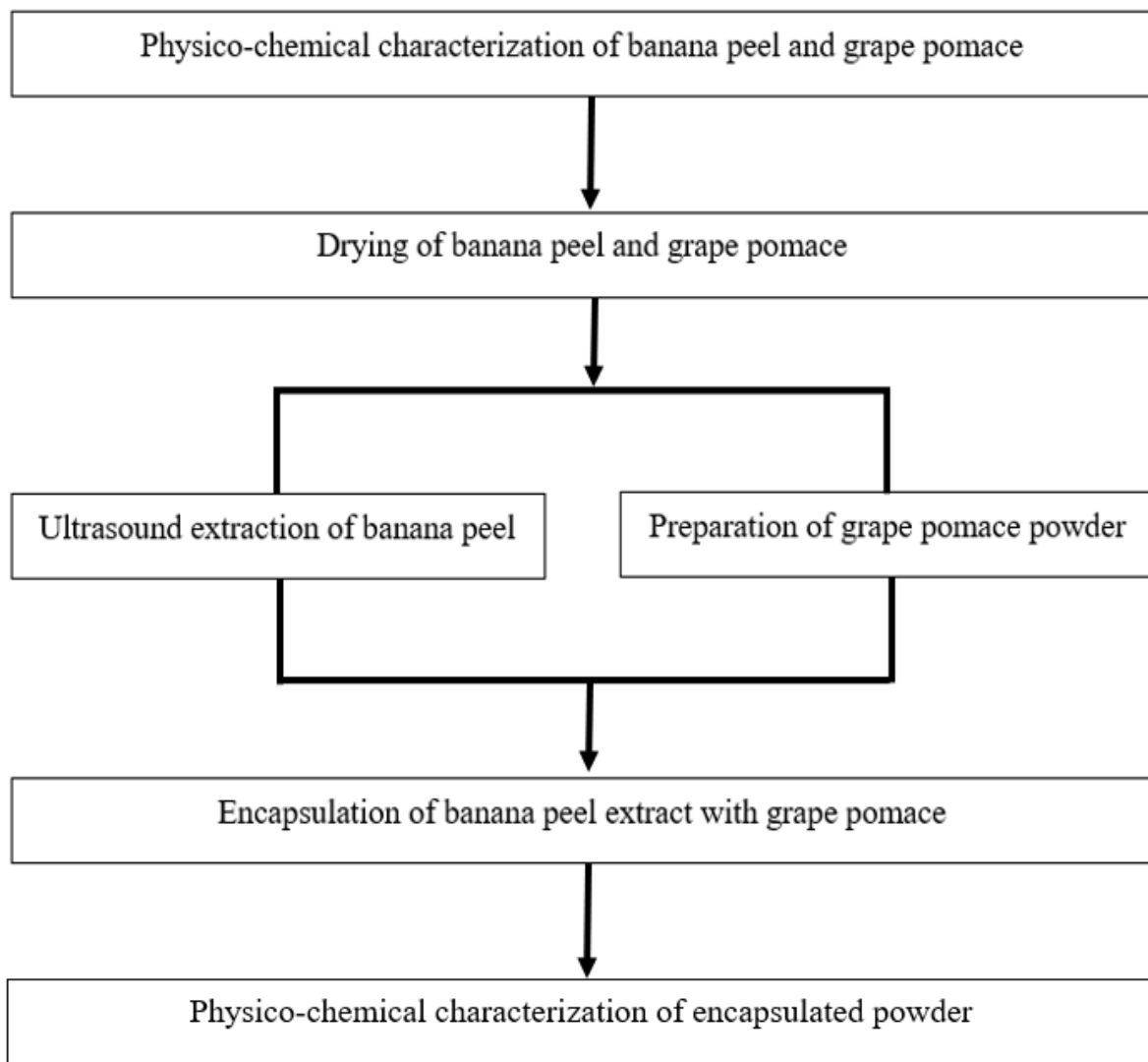


**Flow chart 3.1: Flow chart on experimental plan.**

## 3.1 Materials

The banana peels (cv. Grand Nain) were sourced from the local fruit processing industry at Pune, India and grape pomace (cv. Manjari Medika) was sourced from the research winery unit of division of post-harvest technology, ICAR-National Research Centre for Grapes, Pune, India. The collected peels and pomace were sorted and graded for any contaminants and wilted portions, and stored at -20°C frozen condition by packing in HDPE bags for not more than 30 days for further use in experiments.



(a)                                                    (b)

**Picture 3.1: Banana peels (a) and Grape pomace (b)**

## 3.2.1 Physicochemical characterization of banana peel

### 3.2.1.1 Physical properties

#### 3.2.1.1.1 Banana peels recovery (%)

The banana peels recovery percentage were estimated by taking 1 kilogram of banana fruit. Banana peels were peeled off from the pulp of the fruits, and percent recovery was calculated using the given formula in triplicates.

$$\text{Banana peel recovery (\%)} = \frac{Weight\ of\ peels\ recoverd}{Initial\ weight\ of\ fruits} \times 100$$

#### 3.2.1.1.2 Moisture content (%)

It was measured by placing unit mass of sample in Moisture analyser (MA 50/1. R. WH Moisture Analyzer, RADWAG Weighing Solutions, Poland). The results were displayed as percent loss in weight by heating it at 110°C.

### 3.2.1.2 Biochemical properties

### 3.2.1.2.1 Preparation of banana peel extract

To extract banana peel components, the peels were ground in liquid nitrogen to achieve a fine and uniform mixture. Subsequently, 1 gram of this fine mixture was combined with a solvent consisting of 80% methanol in type-I water, in triplicate. The mixture was vortexed to ensure homogenization and then subjected to bath sonication for 10 minutes at 25°C. Following sonication, centrifuged for 15 min. at 300 RPM. The supernatant was carefully collected and stored in a refrigerator for further analysis (Islam et al., 2023).

### 3.2.1.2.2 Total phenolic contents (mg GAE/100g)

Total phenolic contents were estimated by FC's reagent method. The absorbance was taken at 750 nm, where results are articulated by comparing it with the standard curve of linearity points of gallic acid (1, 2, 5, 7, 10, 20, 50 mg/kg). Obtained results were given in mg Gallic Acid Equivalent per 100 g DW (mg GAE/100g DW) (Islam et al., 2023).

### 3.2.1.2.3 Total flavonoid contents (mg QE/100g)

Total flavonoid contents were analysed using some modification of aluminium colorimetric method using quercetin as standard (Islam et al., 2023). Measuring absorbance at 510nm. The results were articulated by comparing it with calibration curve of quercetin and expressed as mg Quercetin Equivalents per 100g (mg QE/100g).

### 3.2.1.2.4 Antioxidant activity (%)

Antioxidant activity of sample was determined by using DPPH radical scavenging activity. The extract (100 μL) was added in 3900 μL of DPPH (dissolved in 95 % methanol) and kept of incubation for 90 min. Then the absorbance for sample ($A_2$) was recorded at 510 nm. The absorbance ($A_1$) of DPPH was initially taken and recorded. The results were calculated using following formula and expressed as percent inhibition:

$$\text{Antioxidant activity (\%)} = \frac{A1-A2}{A1} \times 100$$

## 3.2.2 Physicochemical properties of grape pomace

### 3.2.2.1 Physical properties

#### 3.2.2.1.1 Grape pomace recovery (%)

Grape pomace recovery was calculated by extracting the juice from 1 kg of grapes. The percentage recovery was calculated using the given formula in triplicates.

$$\text{Grape pomace recovery (\%)} = \frac{Weight\ of\ pomace\ recoverd}{Initial\ weight\ of\ grape\ pomace} \times 100$$

#### 3.2.2.1.2 Moisture content (%)

As given in section 3.2.2.

### 3.2.2.2 Biochemical properties

#### 3.2.2.2.1 Preparation of grape pomace extract

All collected samples were fine grounded using mortar and pestle in liquid nitrogen. For the extraction of RGP components protocol given by (Ribeiro et al., 2015) was followed with some changes. 1 gram of the grounded mixture was taken in solvent (Methanol 80% in type I water), in triplicate. Mixture was then shaken for 24 hours at 25 °C on shaker (Jeto tech/IS-971RF, Korea) and tubes containing the mixture was then centrifuged (Kubota/7000, Japan) at 5000 RPM for 20 min. The supernatant was carefully collected for further analysis.

#### 3.2.2.2.2 Total phenolic contents (mg GAE/100g)

Please refer section 3.2.3

#### 3.2.2.2.3 Total flavonoid contents (mg CE/100g)

Please refer section 3.2.4, where standard catechin hydrate was used and results given as mg catechin equivalents per 100 g (mg CE/100g)

#### 3.2.2.2.4 Antioxidant activity (%)

Please refer section 3.2.5

#### 3.2.2.2.5 Total anthocyanin contents (mg/100g)

TAC was estimated by pH differential method by dissolving sample extract in pH 1.0 potassium chloride (0.025 mol/L) and pH 4.5 sodium acetate (0.4 mol/L) buffer.

Absorbance for each sample was taken at 520 nm and 700 nm (Rockenbach et al., 2011). Obtained results were expressed as milligram per 100g of dry matter of RGP sample (mg/100g DM). Formula used for calculation was as given below:

$$A = (A520\text{-}A700)\ pH1.0 - (A520\text{-}A700)\ pH4.5$$

$$TAC\ (mg/kg) = (A \times MW \times DF \times 1000)/(e \times l)$$

$$TAC\ (mg/100g) = TAC\ (mg/kg)/10$$

### 3.2.3 Drying and degradation kinetics of banana peel

### 3.2.3.1 Drying of banana peels

Drying of BP was carried out using hot air dryer (local made and assembled at ICAR-NRC for Grapes, Pune, India) at 40, 50, 60 and 70°C with 1.5 m/s airflow parallel to the sample surface during drying. For each temperature, the same quantity of peel was used for drying, i.e., the initial weight of BP samples was kept at 100 g. During the drying period, the weight of the sample was recorded at every 30-minute interval up to equilibrium moisture condition (same weight for two consecutive readings). Similarly, to study degradation of total phenol content (TPC), total flavonoid contents (TFC) and antioxidant activity (AA) in BP during drying, separate samples were kept for drying and at every 60 minutes 50 g of sample was taken and packed in sample bags to store at -20 °C for further analysis. The BPs were spread as single layer on removable stainless-steel grids (40×90 cm).



**Picture 3.2: Hot air tray drying of banana peels.**

**Table 3.1: Treatment details of banana peel drying.**

| Treatments | Temperature (°C) |
|------------|------------------|
| **BP1** | 40 |
| **BP2** | 50 |
| **BP3** | 60 |
| **BP4** | 70 |
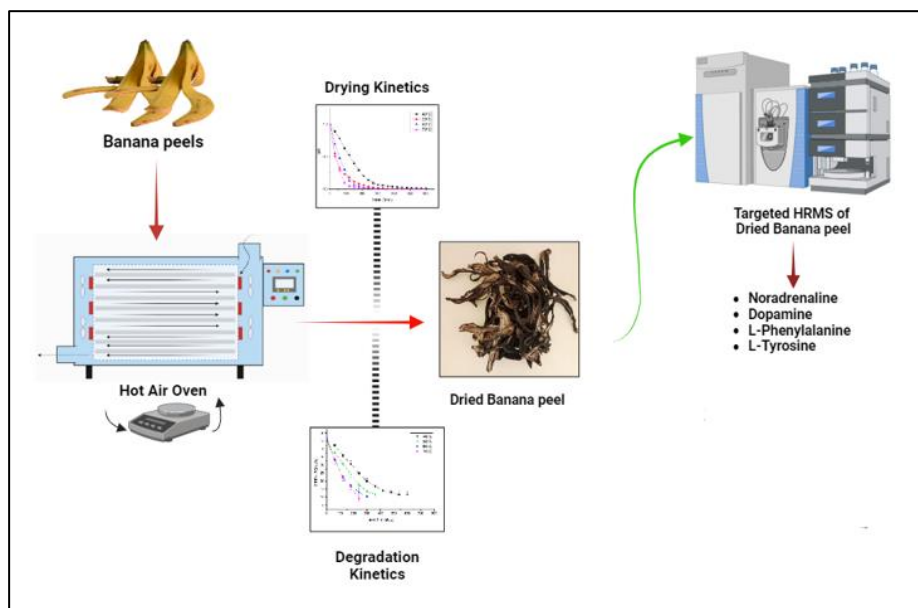


**Figure 3.1: Banana peel drying experiment flow diagram**.

### 3.2.3.2 Mathematical modelling for drying kinetics

Mathematical modelling of the drying data is important to study the drying behaviour of BP. There are various models are available for drying of sample, the models which have close alignment with drying curves that are obtained from data of drying of sample are more suitable. To access the goodness of fit of model with the drying curves three statistical parameters considered, those are Coefficient of determination ($R^2$), Root Mean Square Error (RMSE) and Chi-square test ($x^2$). Many studies were found in which these parameters were used for fitting mathematical models (Abbaspour-Gilandeh et al., 2019; Goyal et al., 2007; Guiné et al., 2015; Kooli et al., 2007; Kumar K, 2015; Mghazli et al., 2017; Khalangre et al., 2024). In this study of thin layer drying of BP, six different

distinct mathematical models were selected for analysis and fitting of the experimental drying data of BP that was dried using hot air tray dryer at 40, 50, 60, 70 and 80 °C carried out.

The ratio of moisture content of BP at different time level is called as moisture ratio and determined using:

$$MR = \frac{M_t - Me}{M_0 - M_e} \tag{01}$$

In this experiment the GP were dried till two successive constant readings of weight of GP, the $M_e$ is negligible than $M_t$ and $M_0$. So, we can simplify above equation (01) by changing $(M_t-M_e)/(M_o-M_e)$ to $M_t/M_0$.

$$MR = \frac{M_t}{M_0} \tag{02}$$

**Table 3.2: Six mathematical models that used for modelling of drying data of BP**

| Sr. No. | Model name | Model Equation | References |
|---------|-----------|----------------|------------|
| 1 | Newton | MR=*exp(-kt)* | Westerman et al., 1973 |
| 2 | Page | MR=*exp(-kt$^n$)* | Page, 1949 |
| 3 | Hander and pabis | MR = *aexp(-kt )* | Saeed et al., 2008 |
| 4 | Verma et al | MR = *aexp (-kt) + (1-a ) exp(-gt)* | Verma et al., 1985 |
| 5 | Approximation of diffusion | MR = *aexp (-kt)+ (1-a ) exp(-kbt)* | Yaldiz et al., 2001 |
| 6 | Midilli et al | MR = *aexp(-kt$^n$)+bt* | Midilli et al., 2002 |

The statistical fit was estimated by $R^2$, RMSE and $X^2$ using add in tool in Microsoft excel. For the greater fit of model, the $R^2$ should be high near to 1 and $X^2$ and RMSE should be lowest close to 0. The all-selected parameters were calculated by using given equations (03, 04 and 05, respectively),

$$R^2 = 1 - \left[\frac{\sum_{i-1}^{N}(MR_{pre,i}-MR_{exp,i})^2}{\sum_{i-1}^{N}(\overline{MR}_{pre}-MR_{exp,i})^2}\right] \tag{03}$$

$$X^2 = \frac{\sum_{i=1}^{N}(MR_{exp,i}-MR_{pre,i})^2}{N-z} \tag{04}$$

$$RMSE = \sum_{i=1}^{N}\left[\sqrt{\frac{(MR_{exp,i}-MR_{pre,i})^2}{N}}\right] \tag{05}$$

In which, experimental moisture ratio ($MR_{exp,i}$), predicted moisture ratio ($MR_{pre,i}$), no. of observation ($N$) and no. of drying constants ($z$).

### 3.2.3.3 Effective Moisture Diffusivity ($D_{eff}$)

Different drying curves of moisture ratio versus drying time were generated using Fick's second law for each drying temperature. Effective moisture diffusivity was calculated by using theses curves.

$$MR = \frac{8}{\pi^2}\sum_{n=0}^{\infty}\frac{1}{(2n+1)^2}\exp-\left(\frac{(2n+1)^2\pi^2 D_{eff}t}{4L^2}\right) \tag{04}$$

In this context, $D_{eff}$ represents the effective diffusivity (m²/s), and $L$ corresponds to the thickness (mm). simplification of equation gives

$$MR = \frac{8}{\pi^2}\exp\left(-\frac{\pi^2 D_{eff}t}{4L^2}\right) \tag{05}$$

By plotting natural logarithms of MR against the drying time from the data the $D_{eff}$ was calculated. This plot yielded a straight line characterized by a negative slope, and the relationship between K and $D_{eff}$ is expressed by:

$$K = \frac{\pi^2 D_{eff}}{4L^2} \tag{06}$$

### 3.2.3.4 Activation Energy ($E_a$)

Arrhenius equation was used for modelling of the relationship between drying temperature and $D_{eff}$, which is expressed as follows:

$$D_{eff} = D_0 \exp\left(-\frac{Ea}{RT}\right) \qquad (06)$$

In the above equation, where $D_0$ represents the $D_{eff}$ at infinite temperature (m²/s), $Ea$ denotes the activation energy required for diffusion of one mole of moisture (kJ/mol), gas constant ($R = 8.314 \times 10^{-3}$ kJ/mol) and T signifies the temperature in Kelvin (K).

### 3.2.3.5 Biochemical analysis of Banana peel

### 3.2.3.5.1 Preparation of dried banana peel extract

The extraction of samples was carried out as per the method given in section 3.2.1.2.1.

### 3.2.3.5.2 Total phenol contents (mg GAE/100g)

Total phenolic contents in banana peel, as given in section 3.2.1.2.2.

### 3.2.3.5.3 Total flavonoids contents (mg QE/100g)

Total flavonoid contents in banana peel were estimated by using aluminium chloride method, where quercetin used as standard to quantify total flavonoid contents in banana peel as given in section 3.2.1.2.3.

### 3.2.3.5.4 Antioxidant activity (%)

Antioxidant activity in banana peel was estimated by using DPPH % radical scavenging activity as given in section 3.2.1.2.4.

### 3.2.3.6 Degradation kinetics

For degradation studies of bioactive compounds of banana peels, the sample at every 60 minutes interval were analysed and data was generated. The changes in the concentration of phytochemicals were fitted to first order kinetic model. The equation of first order kinetics model is as described below:

$$c = c_0 e^{\pm kt} \qquad (09)$$

In which, C stands for the values of bioactive compounds at different interval of time during drying. $C_0$ indicates the initial values of all these parameters before starting the drying. K stands for the rate constant of first order kinetics.

The Half-life ($t_{1/2}$) for bioactive compounds was calculated as follows:

$$t_{1/2} = ln\ (2)/k \tag{10}$$

The Arrhenius equation was used to find the temperature dependence for degradation of bioactive compounds which is given below:

$$k = k_0 e^{Ea/RT} \tag{11}$$

### 3.2.3.7 Targeted phytochemical analysis of dried banana peel using high resolution-LC-Orbitrap-MS

The BP (fresh and dry) was extracted and relatively quantified for the targeted bio-active compounds such as noradrenaline, dopamine, L-phenylalanine and L-tyrosine by a targeted work flow using LC-Orbitrap-MS analysis. Each targeted compounds are quantified as mg /kg dopamine equivalent (mg/kg DE).

### 3.2.3.7.1 Sample preparation

100 mg of well homogenised sample of fresh banana peel and finely grounded dried powder (10 mg) of banana peel was extracted with 1000 µL (0.1%) acidified methanol. The sample and solvent were mixed well by vertexing and sonicated for 15 min. using a bath sonicator at 25°C. The mixture was then subjected to centrifugation at 10000 rpm for 5 minutes and supernatant was collected in eppendorf tube. 100 µL of filtered extract (0.22 µm PTFE membrane) was taken in a vial containing 500 µL of acidified water and 400 µL of acetonitrile and processed for analysis by LC-Orbitrap-MS.

### 3.2.3.7.3 LC-MS [UHPLC-Orbitrap MS] conditions

The analysis was performed using Ultimate 3000-series Ultrahigh Performance Liquid Chromatograph (UHPLC) hyphenated to Orbitrap Q-Exactive mass spectrometer (MS) (Thermo Fisher Scientific, Bremen, Germany) as given by Chintagunta et al. (2022). The mobile phase consisted of (A) - water (100%), and (B) - ACN (95:5,

ACN:Water v/v) with 0.1% formic acid in both phases. The gradient program was set as: 0–1 min: 0% B, 1–10 min:100% B, 10–15 min:100% B and 15.1–20 min:0% B with a 0.4 mL/min flow rate. Chromatographic separations were performed using a Waters HSS-T3 (100 × 2.1 mm, 1.7µm) column.

### 3.2.3.7.4 Data processing

Data processing of the raw files obtained by analysis on LC-Orbitrap-MS was carried out according to Chintagunta et al. (2022) with some changes in process. For the identification of compounds high resolution accurate mass (HRAM) database of phenols specifically created for this study. The confirmation of analytes was carried out by measuring HRAM of the characteristic fragment ions and precursor. The threshold intensity was more than 5000. Reference standard of dopamine (purity >99%, sourced from Sigma Aldrich, USA) was used to validate MS spectra, retention time and MS/MS fragments. Trace Finder software (version 3.3, Thermo Fisher Scientific) was used for LC-MS data files (n=3) were processing, which identified compounds by comparing them with the anthocyanin database, and its derivatives. By using the response of reference standard of dopamine, the relative quantification of identified compounds was carried out.

### 3.2.4 Drying and degradation kinetics of grape pomace

### 3.2.4.1 Drying of grape pomace

Drying of Grape Pomace (GP) was carried out using hot air tray dryer (local made and assembled at ICAR-NRC for Grapes, Pune, India) at 40, 50, 60 and 70°C with 1.5 m/s airflow parallel to the sample surface during drying. For each temperature, the same quantity of GP was used for drying, i.e., the initial weight of GP samples was kept at 50 g. During the drying period, the weight of the sample was recorded at every 30-minute interval up to equilibrium moisture condition (same weight for two consecutive readings). Similarly, to study degradation of TPC, TFC, AA and TAC in GP during drying, separate samples were kept for drying and at every 60 minutes 30 g of sample was taken and packed in sample bags, kept at -20 °C for further analysis. The GP was spread as single layer in Petri plate of 10 cm diameter and 1.5 mm thickness.

**Picture 3.3: Grape pomace hot air drying**

**Table 3.3: Treatment details of grape pomace hot air drying**

| Treatments | Temperature (°C) |
|------------|------------------|
| GP1 | 40 |
| GP2 | 50 |
| GP3 | 60 |
| GP4 | 70 |
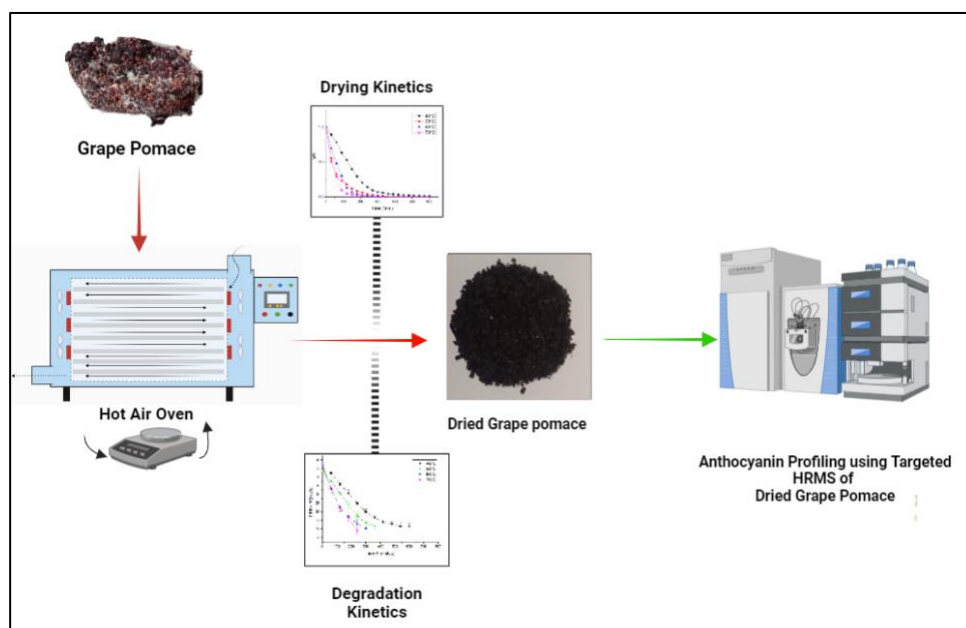


**Figure 3.2: Grape pomace drying experiment flow diagram.**

## 3.2.4.2 Mathematical modelling

Mathematical modelling of data was done as per given in section 3.2.3.2

**3.2.4.3 Effective moisture diffusivity ($D_{eff}$)**

$D_{eff}$ was estimated as per given in section 3.2.3.3.

**3.2.4.4 Activation energy ($E_a$)**

Activation energy was estimated as per given in section 3.2.3.4.

**3.2.4.5 Biochemical analysis of grape pomace.**

**3.2.4.5.1 Sample preparation**

Sample was prepared and extracted as per the method given in section 3.2.2.2.1.

**3.2.4.5.2 Total phenol contents (mg GAE/100g)**

As given in section 3.2.1.2.2.

**3.2.4.5.3 Total flavonoids contents (mg CE/100g)**

Total flavonoid contents in grape pomace were estimated by using aluminium chloride method, where catechin hydrate used as standard for grape pomace as given in section 3.2.1.2.3.

**3.2.4.5.4 Total anthocyanin contents (mg/ 100g)**

The total anthocyanin contents in grape pomace, as per given in section 3.2.2.2.5.

**3.2.4.5.5 Antioxidant activity (%)**

Antioxidant activity in grape pomace was estimated, as given in section 3.2.1.2.4.

**3.2.4.6 Degradation kinetics**

The degradation kinetics for grape pomace was estimated as per given in section 3.2.3.6.

**3.2.4.7 Impact of drying temperature on anthocyanin profiling of dried grape pomace by high resolution-UHPLC-Orbitrap-MS analysis**

The evaluation of effect of different drying temperature on anthocyanin profiles of GP was carried out using HRMS. The fresh GP and dried GP at 40, 50, 60, 70 and 80°C was extracted and relatively quantified against certified reference standard of cyaniding-3-*O*-glucoside (C3G) for anthocyanin profiles by a targeted work flow using LC-Orbitrap-MS analysis. Each targeted compounds are quantified as milligram per kilogram cyanidin-3-*O*-glucoside equivalent (mg.kg$^{-1}$ C3GE.).

**3.2.4.7.1 Sample preparation**

The extraction of fresh (100 mg) and dried (10 mg) homogenised and finely grounded GP was carried out using 1000 µL of 0.1% acidified methanol. The sample and solvent mixture was thoroughly mixed using a vortex, followed by bath sonication for 15 minutes at 25°C temperature. The obtained mixture was then centrifuged at 10,000 rpm for 5 minutes. The supernatant was collected in 2 ml Eppendorf tube. Finally, a vial was prepared by mixing 100 µL of filtered extract (0.22 µm PTFE membrane), 500 µL of acidified water and 400 µL of acetonitrile. This mixture was then processed for analysis by injecting in LC-Orbitrap-MS.

**3.2.4.7.2 LC-MS [UHPLC-Orbitrap MS] analysis**

As given in section 3.2.3.7.3.

**3.2.4.7.3 Data processing**

Data processing of the raw files obtained by analysis on LC-Orbitrap-MS was carried out according to Chintagunta et al. (2022) with some changes in process. For the identification of compounds high resolution accurate mass (HRAM) database of grape anthocyanin having 250 different anthocyanin specifically created for this study. The confirmation of analytes was carried out by measuring HRAM of the characteristic fragment ions and precursor. The threshold intensity was more than 5000. Reference standard of Cyanidin-3-O-glucoside (purity >99%, sourced from Sigma Aldrich, USA) was used to validate MS spectra, retention time and MS/MS fragments. Trace Finder software (version 3.3, Thermo Fisher Scientific) was used for LC-MS data files (n=3)

were processing, which identified compounds by comparing them with the anthocyanin database, and its derivatives.

### 3.2.5 Preparation of grape pomace powder

The grape pomace powder was prepared from dried grape pomace at 60 $^{\circ}$C by separating seeds from the dried grape pomace. Milling of separated grape pomace was carried out using Labtec CT410 sample mill (FOSS Analytical Co., Ltd., China) to get fine powder. Further to achieve desired particle size of 0.2 mm the grape pomace powder was sieved using a fine mesh of 0.2mm.



| | |
|---|---|
| a) | b) |
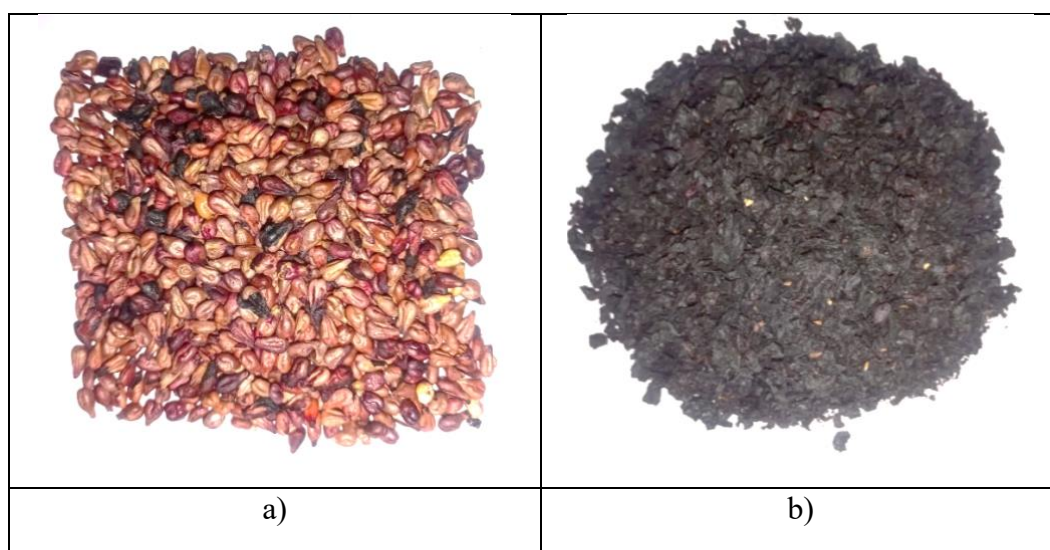
**Picture 3.4: Grape seeds (a) and grape skin (b)**

```
┌─────────────────────────┐
│   Dried grape pomace    │
└─────────────────────────┘
             │
             ▼
┌─────────────────────────┐
│  Sorting of skin and seeds │
└─────────────────────────┘
             │
             ▼
┌─────────────────────────┐
│   Dry milling of skin   │
└─────────────────────────┘
             │
             ▼
┌─────────────────────────┐
│        Sieving          │
└─────────────────────────┘
             │
             ▼
┌─────────────────────────┐
│  Grape pomace powder    │
└─────────────────────────┘
```
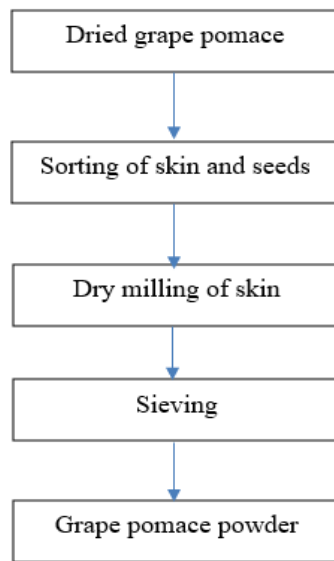
**Flow chart 3.2: Preparation of grape pomace powder**



**Picture 3.5: Dry milling of grape skin**



**Picture 3.6: Sieving of milled powder**

**Picture 3.7: Fine grape pomace powder**

### 3.2.6 Extraction of bioactive compounds from banana peel

### 3.2.6.1 Ultrasound assisted extraction

Probe sonicator with 500 Watts maximum sonication power and 20 kHz frequency model Q500 Sonicator (Qsonica sonicator, Newtown, USA). The sonicator was having the Ti-Al-V probe for sonication with 13 mm size and 100 mm length. The experiment of extraction was carried out using the pulse mode where two modes such pulse mode on and pulse mode off time of the sonication. The sonicator has the facility to adjust the sonication power from 0 to 100% to set the desirable level of sonication power. For the extraction of the dried banana peels were grounded and particle size of 0.2 mm was achieved by sieving it using a mesh. The solvent was made by mixing ethanol with distilled water with varying concentration. During the process of extraction 200 ml mixture of banana peel powder and solvent was taken in a beaker and probe was dipped to 20 mm depth. the resulted extracts were evaporated using rocket evaporator (Genovac Inc, USA) to 40 ml.



**Picture 3.8: Probe sonicator**

### 3.2.6.2 Experimental design

Using a Face centred central composite (FCCCD) design of response surface methodology experiment was designed. 30 numbers of experiments were generated using 6 centre points and three levels (-1, 0, +1). The independent variables considered were extraction time, sonication power, solvent concentration and powder to solvent ratio between 5 to 10 minutes, 200 to 400 Watts, 50 -100% and 2 to 8 g/ml, respectively (Table 3.4). Depending upon these independent variables the impact on depending responses such as, total phenol contents (mg/100g), dopamine content (mg/100g), L-dopa content (mg/100g) and L-tyrosine content (mg/100g) were evaluated.

**Table 3.4: Details of the experimental treatments banana peel extraction**

| Treatments | A: Time (Minutes) | B: Peels to Solvent ratio | C: Power (Watts) | D: Solvent concentration (%) |
|---|---|---|---|---|
| 1 | 10 | 5 | 300 | 50 |
| 2 | 15 | 8 | 400 | 100 |
| 3 | 5 | 8 | 200 | 100 |
| 4 | 10 | 5 | 300 | 75 |
| 5 | 10 | 5 | 300 | 75 |
| 6 | 15 | 8 | 200 | 50 |
| 7 | 10 | 5 | 400 | 75 |
| 8 | 5 | 8 | 400 | 50 |
| 9 | 5 | 2 | 400 | 50 |
| 10 | 5 | 2 | 200 | 50 |
| 11 | 10 | 5 | 300 | 75 |
| 12 | 15 | 8 | 400 | 50 |
| 13 | 10 | 5 | 300 | 75 |
| 14 | 10 | 5 | 300 | 100 |
| 15 | 5 | 2 | 200 | 100 |
| 16 | 15 | 2 | 200 | 50 |
| 17 | 15 | 2 | 400 | 100 |
| 18 | 15 | 2 | 400 | 50 |
| 19 | 10 | 5 | 200 | 75 |
| 20 | 5 | 8 | 400 | 100 |
| 21 | 5 | 2 | 400 | 100 |
| 22 | 5 | 5 | 300 | 75 |
| 23 | 15 | 8 | 200 | 100 |
| 24 | 10 | 8 | 300 | 75 |
| 25 | 10 | 5 | 300 | 75 |
| 26 | 15 | 2 | 200 | 100 |
| 27 | 5 | 8 | 200 | 50 |
| 28 | 10 | 2 | 300 | 75 |

| 29 | 10 | 5 | 300 | 75 |
|---|---|---|---|---|
| 30 | 15 | 5 | 300 | 75 |

### 3.2.6.3 Optimisation of process parameters

Optimisation of process parameters was caried out based on numerical optimization approach of design expert software, with targeting maximization of total phenolic contents, dopamine content, L-dopa content and L-tyrosine content. The experiment was performed at the optimal process condition based on numerical optimisation and hence response parameter validated using standard deviation.

### 3.2.6.4 Response analysis

### 3.2.6.4.1 Total phenol contents (mg GAE/100g)

As given in section 3.2.3.

### 3.2.6.4.2 Dopamine content, L-tyrosine content and L-dopa content (mg/100g)

### 3.2.6.4.2.1 Sample preparation

The concentrated extract was diluted using mixture of methanol and water and injected to system for analysis.

### 3.2.6.4.2.2 Standard preparation

A mixture of certified reference standards of dopamine, L-tyrosine and L-dopa was used for quantification. Individual stock solution of each compound of 1000 µg/mL concentration was prepared in methanol and stored at -20°C. The mixture sock of dopamine, L-tyrosine and L-dopa was prepared in methanol with concentration of 100 mg/L, then, from the mixture stock solution of 10 and 1 mg/L concentration were prepared by serial dilution in methanol and stored at 0°C. A seven-point calibration of solvent standard between 0.005 to 0.200 mg/L was prepared in methanol: water (1:1) and used for quantification.

### 3.2.6.4.2.3 LC-MS/MS conditions

Dopamine, L-tyrosine and L-dopa analysed using a Shimadzu UFLC XR system, paired with an API 4000 mass spectrometer (triple quadrupole/linear ion trap, QqQLIT) from Applied Biosystems (Foster City, USA). A Luna® 5 µm HILIC 200 Å LC column 150 mm × 4.6 mm, was used for chromatographic separation. The mobile phase comprised two solvents: pure water with 0.1% formic acid (A) and acetonitrile with 0.1%

formic acid (B). The flow rate was maintained at 0.6 mL/min over a 10-minute gradient program. The initial mobile phase composition of 80% B was held for 2 minutes, followed by a gradual decrease to 12% B from 3 to 6 minutes. This was then reduced to 80% B at 6.5 minutes and maintained until the end of the run. The injection volume was set at 10 μL, and the column oven was kept at 40°C. Quantification was conducted in positive ion mode with multiple reaction monitoring (MRM) transitions optimized for electrospray ionization (ESI). The system operated with a spray gas (GS1) at 25 psi, drying gas (GS2) at 50 psi, a source temperature of 600°C, and an electrospray voltage of 4.5 kV. The data was processed and analysed using Analyst software (version 1.7.1). All conditions were maintained consistently throughout the analysis to ensure reliable results. At optimized instrumental condition, the mass parameters of target analytes are provided in Table 3.5.

**Table 3.5: Mass parameters of dopamine, L-dopa and L-tyrosine**

| Compound | Q1 mass (Da) | Q3 Mass (Da) | DP (Volts) | CE (Volts) | CXP (Volts) |
|---|---|---|---|---|---|
| Dopamine-I | 154.100 | 137.100 | 30 | 15 | 5 |
| Dopamine-II | 154.100 | 91.000 | 30 | 10 | 7 |
| L-dopa-I | 198.000 | 152.000 | 60 | 15 | 13 |
| L-dopa-II | 198.000 | 181.000 | 60 | 32 | 13 |
| L-tyrosine-I | 182.000 | 136.000 | 14 | 14 | 6 |
| L-tyrosine-II | 182.000 | 136.000 | 14 | 18 | 4 |

### 3.2.6.4.2.4 Analytical method quality control

The method developed for the targeted analytes was verified considering factors such as the limit of detection (LOD), limit of quantification (LOQ), matrix interference and linearity. The LOD and LOQ were determined to establish the method's sensitivity. The LOD for each analyte was determined by evaluating the signal-to-noise ratio (S/N) of 3 relative to the background noise from blank samples, while the LOQ was calculated using an S/N ratio of 10. Linearity of response for the analytes was verified using a

seven-point calibration curve, with concentrations ranging from 0.005 to 0.200 mg/L in solvent standards and used for quantification.

### 3.2.7 Encapsulation of banana peel extract with grape pomace powder

### 3.2.7.1 Ultrasonic homogenisation of banana peel extract into grape pomace powder

The coating matrix solution was prepared by dissolving grape pomace powder in deionized water. Once the powder was fully dispersed, the banana peel extract was incorporated into the solution. To ensure thorough mixing and uniform distribution of the extract within the grape pomace solution, a bath sonicator with a maximum nominal output power of 100 W and a frequency of 20 kHz was used for 10 minutes. This process facilitated the homogenization of the solution.

### 3.2.7.2 Spray drying

The banana peel and grape pomace solution was dried using spray dryer (Techno Search Instruments Pvt. Ltd., Mumbai, India) equipped with a concurrent flow and nozzle atomizer. The atomizer, with a 1.0 mm internal diameter, utilized controlled compressed air.

**Picture 3.9: Spray dryer**

### 3.2.7.3 Experimental design

Face centred central composite design (FCCCD) based RSM design was used to set the number of experiments. In all experiments, the atomizer pressure, the feed rate, the feed solids concentration, and the feed temperature were be kept at $1.5 \pm 0.1$ bar, $1.2 \pm 0.05$ ml/min, $25.00 \pm 0.5\%$ w/w, and $30.0 \pm 2.0$ °C, respectively. The independent variable considered are inlet air temperature (A), amount of pomace (B), wall to core material ratio (C) and the aspirator air flow rate (D) and was ranged between 180 and 220 °C, 10 to 50 %, 1:1 and 1:5, and 80 to 100 Nm$^3$/s, respectively. Based on such variation of independent parameters was evaluated.

Based on FCCCD design, the number of experiments for the encapsulation process refers to 30 (table 3.6). Six numbers of experiment are in the central points, six numbers of experiments corresponding to axial and remaining 18 were factorial design-based experiments.

**Table 3.6: Details of experimental treatments for spray drying**

| Treatments | A: Inlet air temperature (°C) | B: Pomace (%) | C: Wall to core material ratio | D: Aspirator flow rate (Nm3/hr) |
|---|---|---|---|---|
| 1 | 180 | 5 | 5 | 100 |
| 2 | 200 | 17.5 | 5 | 90 |
| 3 | 180 | 5 | 5 | 80 |
| 4 | 220 | 5 | 5 | 100 |
| 5 | 200 | 17.5 | 3 | 90 |
| 6 | 180 | 30 | 5 | 100 |
| 7 | 180 | 5 | 1 | 80 |
| 8 | 220 | 30 | 5 | 80 |
| 9 | 180 | 30 | 1 | 100 |
| 10 | 200 | 17.5 | 3 | 90 |
| 11 | 200 | 30 | 3 | 90 |
| 12 | 200 | 17.5 | 3 | 90 |
| 13 | 200 | 17.5 | 3 | 90 |
| 14 | 220 | 30 | 5 | 100 |
| 15 | 180 | 17.5 | 3 | 90 |
| 16 | 220 | 5 | 1 | 100 |
| 17 | 200 | 17.5 | 1 | 90 |
| 18 | 200 | 17.5 | 3 | 80 |
| 19 | 180 | 5 | 1 | 100 |
| 20 | 200 | 17.5 | 3 | 90 |
| 21 | 180 | 30 | 1 | 80 |
| 22 | 180 | 30 | 5 | 80 |
| 23 | 220 | 5 | 1 | 80 |
| 24 | 200 | 17.5 | 3 | 100 |
| 25 | 220 | 17.5 | 3 | 90 |
| 26 | 220 | 30 | 1 | 80 |
| 27 | 220 | 5 | 5 | 80 |
| 28 | 200 | 17.5 | 3 | 90 |
| 29 | 220 | 30 | 1 | 100 |
| 30 | 200 | 5 | 3 | 90 |

### 3.2.7.4 Optimisation of process parameters

Optimisation of process parameters was caried out based on numerical optimization approach of design expert software, with targeting maximization of encapsulation efficiency and encapsulation yield. The experiment was performed at the optimal process condition based on numerical optimization and hence response parameter was validated using standard deviation.

### 3.2.7.5 Response analysis

### 3.2.7.5.1 Encapsulation efficiency (%)

The given formula used for calculation (Kaderides *et al.*, 2015)

$$Ef = \frac{TPC - SPC}{TPC} \times 100 \qquad (12)$$

Where, TPC is total phenol content and SPC is surface phenol content.

### 3.2.7.5.2 Encapsulation yield (%)

It is estimated by dividing weight of total powder yielded by the mass to be dried..

### 3.2.7.5.3 Dopamine, L-dopa and L-tyrosine content (mg/100g)

The analysis of these targeted analytes was carried out using method described in section 3.2.6.4.2.

### 3.2.8 Physicochemical characterization of the encapsulated powder.

### 3.2.8.1 Physical properties of encapsulated powder

### 3.2.8.1.1 Powder yield (%)

The yield of the encapsulated powder was calculated by given formula

$$Powder\ yield = \frac{weight\ of\ encapsulated\ powder\ (g)}{weight\ of\ formulation\ to\ be\ dried\ (g)} \times 100 \qquad (13)$$

### 3.2.8.1.2 Bulked density (ρB)

Take one gram of powder in a ten ml graduated measuring cylinder. Allow the powder to be settled in the cylinder without tapping if needed flatten the top of powder and note down the reading for the calculation

$$Bulk\ density\ (\rho B) = \frac{Known\ mass\ of\ powder\ (M)}{Volume\ (V)} \qquad (14)$$

### 3.2.8.1.3 Tapped density (ρT)

Same as the bulk density where the powder was tapped 100 time and volume of powder was recorded. Tapped density was calculated by given formula

$$\text{Tapped density } (\rho T) = \frac{Known\ mass\ of\ powder\ (M)}{Volume\ (V)} \tag{15}$$

### 3.2.8.1.4 Particle density ($\rho_p$)

The particle density was determined using the method described by Jinapong et al. (2008). A 10 ml graduated cylinder with stopper filled with 1 g of powder followed by adding 5 ml of petroleum ether and shaken for 1 minute. Subsequently, the cylinder wall was rinsed with an additional 1 ml of petroleum ether. The particle density was then calculated using the formula provided.

$$\text{Particle density } \left(\boldsymbol{\rho_p}\right) = \frac{Weight\ of\ pwder\ (M)}{Total\ volume\ of\ petrolium\ ether\ with\ suspended\ particles\ (ml)-6}$$

(16)

### 3.2.8.1.5 Porosity ($\varepsilon$) and flowability

The porosity ($\varepsilon$) was calculated by as given below,

$$\varepsilon = \frac{\rho_p - \rho T}{\rho_p} \times 100 \tag{17}$$

whereas, the flowability was expressed as carr index (CI) as given by jinapong et al., (2008).

$$CI = \frac{\rho T - \rho B}{\rho T} \times 100 \tag{18}$$

**Table 3.7: Classification of powder flowability based on Carr index (CI)**

| CI(%) | Flowability |
|-------|-------------|
| <15   | Very good   |
| 15-20 | Good        |
| 20-35 | Fair        |
| 35-45 | Bad         |
| >45   | Very bad    |

**3.2.8.1.6 Cohesiveness (Housner ratio)**

Cohesiveness was calculated using given formula as hausner ratio and termed the cohesiveness of powder (Jinapong et al., 2008)

$$HR = \frac{\rho T}{\rho B} \qquad (19)$$

**Table 3.8: Classification of cohesiveness of powder based on Hausner ratio**

| HR | Cohesiveness |
|--------|--------------|
| <1.2 | Low |
| 12-1.4 | Intermediate |
| >1.4 | High |

**3.2.8.1.7 Solubility**

Powder solubility was assessed using a modified version of the method outlined by Eastman and Moore (1984). 1 g sample was mixed with 100 ml distilled water and mixed well in shaker at 1500 RPM for 5 min. Mixture was then centrifuged 5000 RPM for 5 min. and allowed to settle for 30 minutes. 25 ml aliquot was then dried in an oven at 105°C for 5 hours. The solubility percentage was determined by using given formula.

$$\text{Solubility (\%)} = \frac{\text{weight of petridish dried with sample} - \text{weight of empty petri dish}}{\text{weight of petridish dried with sample}} \times 100 \quad (20)$$

**3.2.8.1.8 Moisture contents (%)**

Moisture content of encapsulated powder was estimated using moisture analyser, as given in section 3.2.2.

**3.2.8.2 Biochemical properties of encapsulated powder**

**3.2.8.2.1 Total phenol contents (mg/100g)**

Total phenol contents in encapsulated powder estimated using folin-ciocalteu's reagent method, as given in section 3.2.1.2.2.

**3.2.8.2.2 Total flavonoids content (mg/100g)**

Total flavonoid contents in encapsulated powder estimated using aluminium chloride method, as given in section 3.2.1.2.3

### 3.2.8.2.3 Total anthocyanin contents (mg/100 g)

Total anthocyanin contents in encapsulated powder estimated using pH differential method, as given section 3.2.2.2.5.

### 3.2.8.2.4 Antioxidant activity (%)

Antioxidant activity of encapsulated powder estimated using DPPH % radical scavenging method, as given in section 3.2.1.2.4.

### 3.2.8.2.5 Dopamine Content, L-tyrosine content and L-dopa content (mg/100g)

Dopamine content, L-tyrosine content and L-dopa content in encapsulated powder estimated as given in section 3.2.6.4.2.

*Chapter-4*

# Results and discussion

The present study entitled, **"Encapsulation of ultrasound extracted bioactive compounds of banana peel with grape pomace"** was undertaken in the department of horticulture, school of agriculture, lovely professional university, punjab and ICAR-national research centre for grapes, pune during the year 2022-2024.

The present study was carried out to optimize the extraction of bioactive compounds in banana peel and encapsulation of extracts with novel carrier agents developed from grape pomace to stabilize the bioactive compound in extract and develop a nutraceutical product. The current chapter deals with the results of all experiments carried out to optimize drying of banana peel and grape pomace, optimize extraction of banana peel bioactive compound and finally encapsulating extract with grape pomace powder using spray dryer. Obtained data was statistically analysed and obtained results are discussed in various sections.

## 4.1 Physicochemical characterization of banana peel.

The physicochemical analysis of banana peel revealed several key properties that highlight its potential for by-product utilization (Table 4.1). The peel recovery was 38±0.81 %, indicating that the peel constitutes a substantial portion of the banana fruit, which can be significant for waste valorisation in the food industry. The high moisture content of 92.06±1.28 % is typical of fresh fruit peels, making them highly perishable and prone to microbial spoilage. This also affects the extraction efficiency of bioactive compounds, necessitating drying or preservation methods for long-term storage and utilization (Sulaiman et al., 2011).



**Picture 4.1: Banana peel of variety "Grand Nain".**

In terms of bioactive compounds, the TPC of banana peel was found to be 373.25±2.99 mg GAE/100g and TFC was 169.38±2.18 mg QE/100g. These phytochemicals are known for their potent antioxidant properties, which contribute to potential health benefits when incorporated into food or nutraceutical products (Vu et al., 2018). The antioxidant activity (AA) of banana peel, measured at 45.57±1.45 %, further supports its application as a natural antioxidant source, capable of scavenging free radicals and potentially contributing to oxidative stress reduction (Bennett et al., 2010). These compounds position banana peel as a valuable ingredient in the development of functional foods, pharmaceuticals, and cosmetic products.

Overall, the significant levels of these compounds in banana peel suggest its strong potential as a sustainable source of natural antioxidants. However, the high moisture content highlights the importance of implementing drying techniques before industrial use to prevent spoilage and maintain the stability of bioactive compounds.

**Table 4.1: Physicochemical parameters of banana peel.**

| Sr. No. | Parameters | Mean± SD |
|---------|------------|----------|
| 1. | Peel recovery (%) | 38±0.81 |
| 2. | Moisture (%) | 92.06±1.28 |
| 3. | TPC (mg GAE/100g) | 373.25±2.99 |
| 4. | TFC (mg QE/100g) | 169.38±2.18 |
| 5. | AA (%) | 45.57±1.45 |

## 4.2 Physicochemical characterisation of grape pomace

The physicochemical analysis of grape pomace revealed several important characteristics that underscore its potential for various applications. The peel recovery was 43.72±0.70%, indicating that a significant portion of the grape fruit is retained as pomace. The moisture content was measured at 72.15±0.86%, a typical trait for fruit pomace, making proper drying or preservation methods necessary to prevent microbial spoilage and degradation of valuable compounds during storage (Khalangre et al., 2024).

**Picture 4.2: Grape pomace of variety "Manjari Medika".**

TPC was 584.95±0.95 mg GAE/100g in grape pomace which is very high amount. Studies have highlighted the antioxidant capacity of grape pomace, which can contribute to health benefits when utilized in nutraceuticals or functional foods (Makris et al., 2007). The TFC of 146.10±1.20 mg QE/100g further underscores the bioactive potential of grape pomace, as flavonoids play a key role in reducing oxidative stress and inflammation.

Additionally, the TAC was recorded at 60.29±0.343 mg/100g. Anthocyanins, known for their vibrant pigments and strong antioxidant activity, are increasingly utilized as natural colorants and antioxidants in food and cosmetic products. The high anthocyanin content in grape pomace positions it as a valuable source for these applications (García-Lomillo & González-SanJosé, 2017). The AA was measured at 89.66±0.93%, demonstrating the strong capacity of grape pomace to neutralize free radicals and prevent oxidative damage. This highlights its potential in developing functional foods and supplements aimed at combating oxidative stress-related health issues.

In conclusion, grape pomace is rich in phenolics, flavonoids and anthocyanins, contributing to its significant antioxidant activity. These results emphasize the potential for grape pomace to be utilized in food, cosmetic and pharmaceutical industries, where natural bioactive compounds are increasingly in demand for their health-promoting properties.

**Table 4.2: Physicochemical parameters of grape pomace.**

| Sr. No. | Parameters | Mean±SD |
|---------|-----------|---------|
| 1. | Peel recovery (%) | 43.72±0.70 |
| 2. | Moisture (%) | 72.15±0.86 |
| 3. | TPC (mg GAE/100g) | 584.95±0.95 |
| 4. | TFC (mg QE/100g) | 146.10±1.20 |
| 5. | TAC (mg/100g) | 60.29±0.343 |
| 6. | AA (%) | 89.66±0.93 |

## 4.3 Drying of banana peel

### 4.3.1 Drying Kinetics

The drying of BP was carried out at 40, 50, 60 and 70 ˚C, it was observed that decrease in time of drying with increase in temperature. Similar observation in behaviour of drying was found in pomegranate peel (Wanderley et al., 2023), trapia residues (Moura et al., 2021) and mango (Ampah et al., 2022). Initial moisture content in BP was 92.65 % wet basis (w.b.) and after drying it was reached on an average 1.65 % w.b., the moisture content was reduced to 98.21 % with respect to initial. Wanderley et al. (2023) reported initial moisture content for pomegranate bark and seeds as 70.74 % and 36.60 % w.b. respectively, which was reduced greatly to 7.14-11.84 and 1.26-2.42 % w.b., respectively. The reduction in moisture content was 89 to 96.55 % respectively with respect to initial value which is also in line with findings of current study.

**Picture 4.3: Banana peels dried at 40 (a), 50(b), 60 (c) and 70 (d)°C**
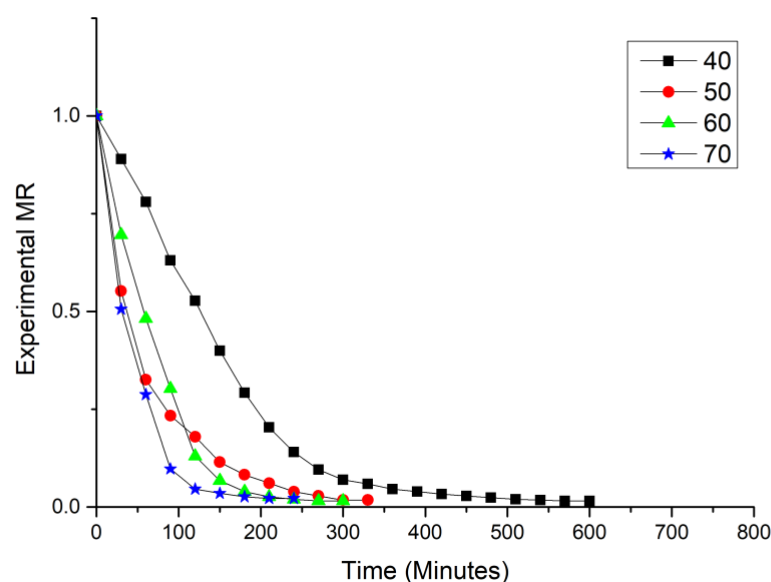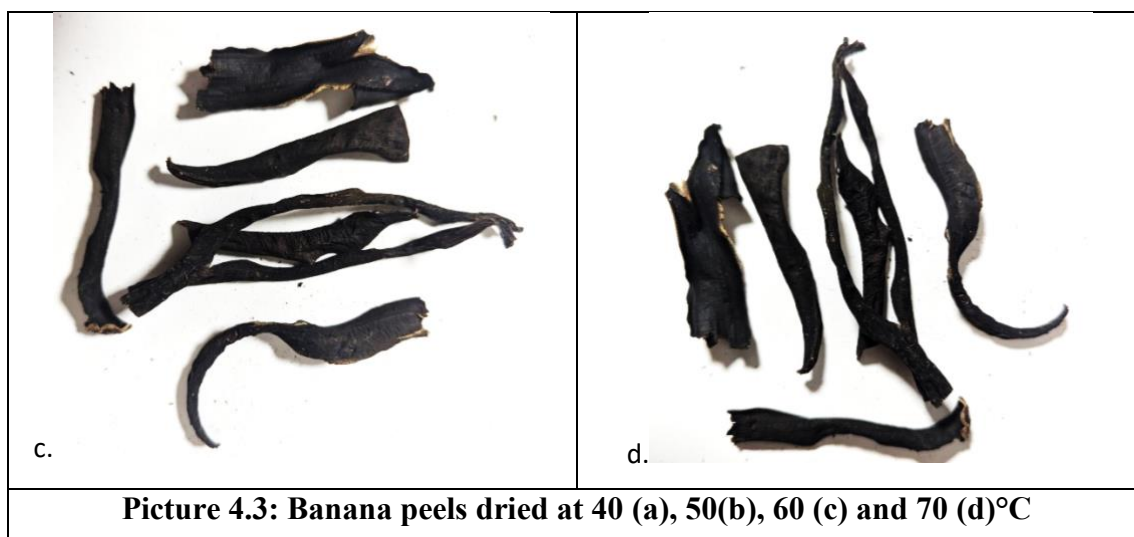


**Figure 4.1: Changes in Moisture ratio during drying of banana peel at 40, 50, 60 and 70°C.**

Table 2 shows the data on results of mathematical models fitted to drying data of BPs at 40, 50, 60 and 70 °C. All the mathematical models that were used for experiment were found fitting satisfactorily, showing higher values of $R^2$ i.e., > 0.94, lower RMSE and chai-square ($X^2$) values. Among all selected models, best fit for experimental data was observed for Midilli et. al. model with average $R^2$ value 0.9967, average RMSE value 0.0130 and average chi-square ($x^2$) value 0.0145 (Fig. 4.3). The accompanying residual plot (Fig. 4.3) portrays residuals closely clustered

around zero, exhibiting a random distribution. This observation underscores the quality of fit achieved (Wisniak & Polishuk, 1999). Similarly, Moura et al., 2021 reported best fit of drying kinetics data to Midilli et al. model for drying of trapia peels. Jha & Sit, 2020 reported drying kinetics model best fitted to approximation of diffusion for deseeded fruits of terminalia. However, for drying of pomegranate peel, best fit was observed with Diffusion of Approximation and Verma models (Wanderley et al., 2023).

Changes in rate constant of drying indicated the impact of different external factors, (Madamba et al., 1996) and serves as an approximate indicator of effective diffusivity during the falling rate period of the drying process (Oliveira et al., 2012). Figure 4.1 presents moisture ratio versus drying time of the best fit midilli et al. model for drying of BP. During the drying process, it was observed that there was no constant rate period, because rate of transfer of moisture from outer surface of material is faster as there is no resistance to displacement of moisture. But when it comes to reduce moisture of inner part of the material, the rate of transfer of moisture in material was much lower. This was because of resistance to moisture transfer from inner side to outer surface (Moura et al., 2021; Oliveira et al., 2012; Wanderley et al., 2023).

Initially there was high moisture content present in BP which resulted in higher drying rate between 100 to 150 minutes, which lead to formation of highest angular coefficients of curve (Gaware et al., 2010). This mechanism of transfer of water from liquid state to vapour form is often characterized by effective diffusion. This is greatly depending upon the temperature, pressure and moisture content of material (Mghazli et al., 2017). Similar type of behaviour was observed by Abbaspour-Gilandeh et al. (2019) during drying of walnut kernels, by Wanderley et al. (2023) for drying of peel and seeds of pomegranate, and by Jha & Sit (2020) for drying of deseeded *Terminalia chebula* fruits.

**Table 4.3: Mathematical models fitting data for drying of banana peels**

| Sr. No. | Model | Temp | Parameters | $R^2$ | Average $R^2$ | RMSE | Average RMSE | $X^2$ | Average $X^2$ |
|---|---|---|---|---|---|---|---|---|---|
| 1 | Newton | 40 | K=0.006720548 | 0.944382448 | 0.974444664 | 0.0504 | 0.0333 | 0.2334 | 0.1590 |
|  |  | 50 | K=0.016614696 | 0.981867771 |  | 0.0302 |  | 0.2003 |  |
|  |  | 60 | K=0.014238208 | 0.976549620 |  | 0.0344 |  | 0.0853 |  |
|  |  | 70 | K=0.022659107 | 0.994978818 |  | 0.0182 |  | 0.1171 |  |
| 2 | Page | 40 | K=0.000722620 n=1.431689803 | 0.995808663 | 0.995819131 | 0.0138 | 0.0145 | 0.5661 | 0.20908 |
|  |  | 50 | K=0.042364968 n=0.785703535 | 0.998373483 |  | 0.0090 |  | 0.0058 |  |
|  |  | 60 | K=0.004562974 n=1.254629236 | 0.993892105 |  | 0.0175 |  | 0.0920 |  |
|  |  | 70 | K=0.004067835 n=1.400007472 | 0.995202272 |  | 0.0178 |  | 0.1722 |  |
| 3 | Hander and pabis | 40 | k=0.007263838 a=1.09101649 | 0.960349041 | 0.979466401 | 0.0425 | 0.0305 | 0.1567 | 0.1257 |
|  |  | 50 | k=0.016053241 a=0.96769615 | 0.983777620 |  | 0.0286 |  | 0.1523 |  |
|  |  | 60 | k=0.014623533 a=1.03127494 | 0.978752322 |  | 0.0327 |  | 0.0754 |  |
|  |  | 70 | k=0.022699646 a=1.00208373 | 0.994986620 |  | 0.0182 |  | 0.1183 |  |
| 4 | Verma et al | 40 | k=0.012464907 a=7.174746434 g=0.014299140 | 0.995609877 | 0.989648012 | 0.0141 | 0.0222 | 0.1723 | 0.1560 |
|  |  | 50 | k=0.016606087 a=8.685635504 g=0.016604712 | 0.981867716 |  | 0.0302 |  | 0.2005 |  |
|  |  | 60 | k=0.009447014 a=4.997235577 g=0.008563619 | 0.986068826 |  | 0.0265 |  | 0.0699 |  |
|  |  | 70 | k=0.019712439 a=10.02868543 g=0.019419274 | 0.995045630 |  | 0.0181 |  | 0.1813 |  |
| 5 | Approximation of diffusion | 40 | k=0.004083824 a=10.08923278 b=0.948104569 | 0.963312584 | 0.981578353 | 0.0409 | 0.02897 | 0.0909 | 0.1329 |
|  |  | 50 | k=0.01661453  a=13.89845494 b=0.999999765 | 0.981867771 |  | 0.0302 |  | 0.2003 |  |
|  |  | 60 | k=0.009141927 a=15.95391760 b=0.971974286 | 0.986086557 |  | 0.0265 |  | 0.0693 |  |
|  |  | 70 | k=0.019781529 a=20.30323600 b=0.993184510 | 0.995046498 |  | 0.0181 |  | 0.1713 |  |
| 6 | Diffusion | 40 | a=1.091016487 b=0.007263838 | 0.960349041 | 0.979466401 | 0.0425 | 0.0305 | 0.1567 | 0.1257 |
|  |  | 50 | a=0.967696152 b=0.016053241 | 0.983777620 |  | 0.0286 |  | 0.1523 |  |
|  |  | 60 | a=1.03127494  b=0.014623533 | 0.978752322 |  | 0.0327 |  | 0.0754 |  |
|  |  | 70 | a=1.00208373  b=0.022699646 | 0.994986620 |  | 0.0182 |  | 0.1183 |  |
| 7 | Midilli et al. | 40 | k=0.000468669 a=0.985639841 b=3.48918E-05 n=1.518518338 | 0.998033932 | 0.99665431 | 0.0094 | 0.0130 | 0.0158 | 0.0145 |
|  |  | 50 | k=0.042450809a=1.003912245    b=9.74956E-06    n=0.789601009 | 0.998148997 |  | 0.0096 |  | 0.0076 |  |
|  |  | 60 | k=0.991539748 a=0.003971331 b=2.47699E-05 n=1.286262854 | 0.994217320 |  | 0.0171 |  | 0.0200 |  |
|  |  | 70 | k=0.016180753 a=0.998133817 b=7.27887E-05 n=1.088535095 | 0.996216990 |  | 0.0158 |  | 0.0145 |  |

## 4.3.2 Fitting of drying curves

The fitting of drying curve was done by using moisture ratio data, as per fig. 4.1. Moisture ratio varies for drying time during drying of BP at 40, 50, 60 and 70 °C. As per the results it was observed that there was decrease in drying time as the temperature increased, this happened because the higher temperature tends to increase rate of transfer of water molecules from BP. This tendency influenced by reducing drying time from 600 to 240 minutes with temperature from 40 to 70°C. Initially when there were higher contents of moisture in BP, the rate of transfer of moisture was found to be very high which was decreased as the moisture content of BP decreased. By plotting the dimensionless moisture ratio versus drying time, it was observed that during progression of drying time, moisture ratio was decreased rapidly (fig.4.1). It was found that initially drying rate was very high, because there was higher moisture content. Later, when moisture content of BP decreased the drying rate also decreased. Drying rate was observed to be decreasing till the BP reaches the equilibrium moisture level in the falling rate period. Studies on drying of deseeded fruits of *Terminalia chebula*, the similar results were observed by Jha & Sit, (2020). The moisture content of BP was decreased from 92.648 % w.b. to the final average moisture content of 1.448 % w.b. at varying temperature. Similar results were observed for changes in moisture content during drying of wastes of different fruits (Elik et al., 2023; Abbaspour-Gilandeh et al., 2019; Jiang et al., 2023).
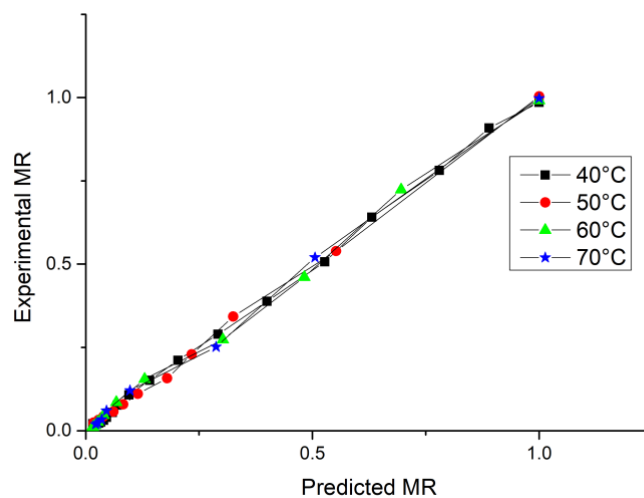


**Figure 4.2: Experimental MR vs Predicted MR of "Midilli et al." model.**
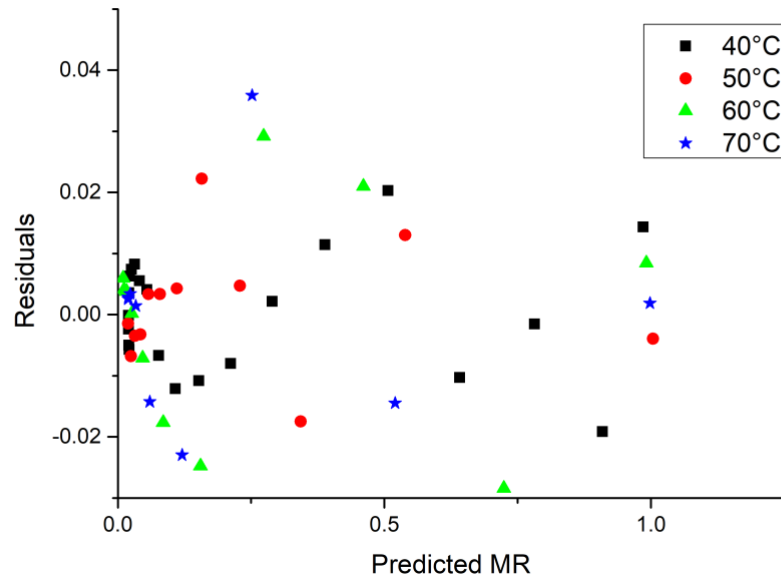
**Figure 4.3: Plot for residual analysis of "Midilli et al." model**

### 4.3.3 Effective Moisture Diffusivity of drying

Diffusivity is nothing but used for the calculation of mass transfer during various food process such as drying, cooling or freezing or thermal processing (Kaveh et al., 2017). As shown in fig. 4.4, the average moisture diffusivity was calculated by taking the mean of the effective moisture diffusivity of changing moisture levels during the process of drying. The values of the $D_{eff}$ of current experiment are depicted in table 3. The trend of Values of $D_{eff}$ was increased with drying temperature. Similar behaviour of increase in $D_{eff}$ with increase in drying temperature during drying was observed in case of mango (Ampah et al., 2022) and drying of deseeded terminalia fruits (Jha & Sit, 2020). The values for moisture diffusivity were ranged between $4.22 \times 10^{-10}$ to $9.126 \times 10^{-10}$ for temperature 40 to 70 °C. For the drying of agricultural and food commodities, $D_{eff}$ between $10^{-8}$ to $10^{-12}$ (Zogzas et al., 1996; Kaveh et al., 2018). The values for $D_{eff}$ for drying of mango fruits (Ampah et al., 2022) and mango peels (Sant'anna et al., 2014) were also in the same range.
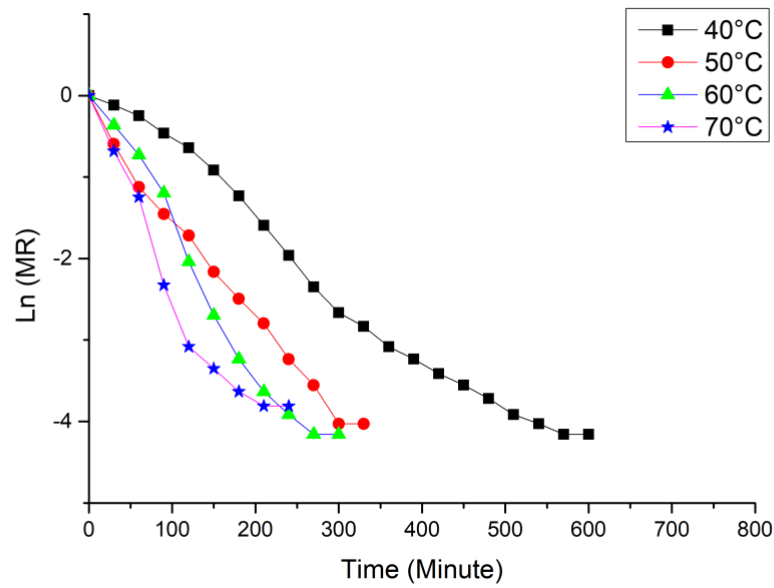
**Figure 4.4: Plot for natural logarithm of experimental moisture ratio vs Time in minute**

### 4.3.4 Activation energy of drying

The value for activation energy of current drying experiment observed is given in table 4. By plotting natural logarithms of effective moisture diffusivity against the inverse of temperature in kelvin (fig. 4.4), $E_a$ was calculated. For drying of BP, the value for activation energy was 22.776 kJ/mol similar as between 12.7-110 kJ/mol, which is required for fruits and vegetables (Zogzas et al., 1996; Kaveh et al., 2017). For drying of grape pomace, the $E_a$ reported was 26.440 kJ/mol (Fernando et al., 2012). Similarly, for drying of slices of crab-apple of 3 mm and 5 mm thickness, $E_a$ reported was 17.46 and 23.82 kJ/mol (Jiang et al., 2023).

**Table 4.4: Parameters of effective moisture diffusivity for drying of BP along with coefficient of determination ($R^2$)**

| Temperature °C | Deff (m²/s) | $R^2$ | Ea (kJ/mol.) |
|---|---|---|---|
| 40 | $4.22 \times 10^{-10}$ | 0.9761 | |
| 50 | $6.8382 \times 10^{-10}$ | 0.9942 | |
| 60 | $8.4438 \times 10^{-10}$ | 0.966 | 22.776 |
| 70 | $9.126 \times 10^{-10}$ | 0.9129 | |
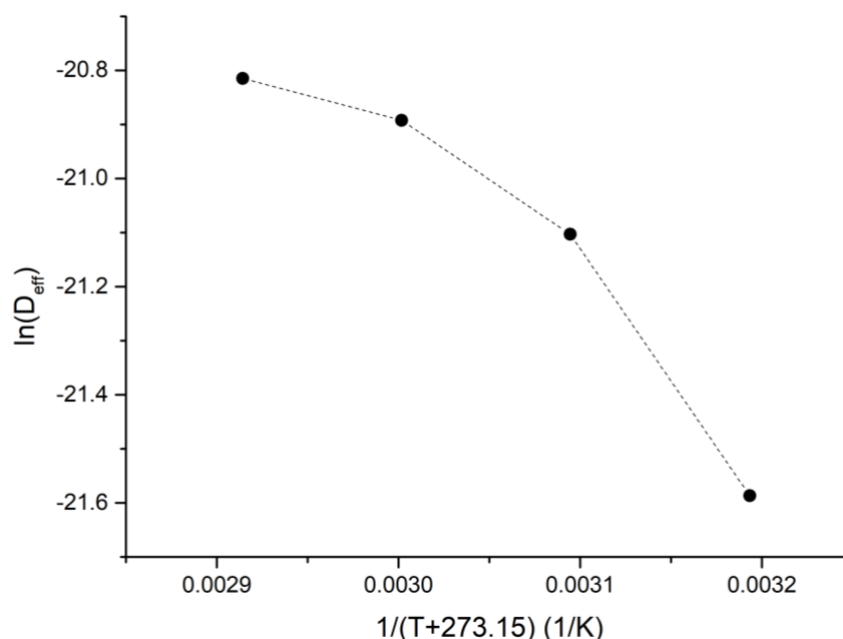
**Figure 4.5: Natural logarithm of D$_{eff}$ vs. 1/t for banana peel drying**

## 4.3.5 Impact of temperature on degradation kinetics for TPC, TFC and AA in drying

Every plant material contains phenolic compounds and antioxidants. These compounds have many health benefitting properties. Because of this nature, these compounds are the deciding factors for the quality and usefulness of material for different processing purposes. But these compounds are highly sensitive and easily get degraded when exposed to temperature. The degradation kinetics of TPC, TFC and AA during drying of BP observed in the experiment are showed in fig. 4.6, 4.7 and 4.8  The values for k, $R^2$ and $t_{1/}$ are as shown in table 4.5. Considering the values of k, it can be concluded that the rate of degradation for TFC is faster than TPC. Changes in the values of antioxidant activities was mainly due the degradation in TFC and TPC, but there might be other factors also involved. Similarly, as the rate of degradation for antioxidant activity higher in comparison to TFC and TPC with a lowest half-life.  For all the parameters, the half-life ($t_{1/2}$) decreased with increase in temperature. The $t_{1/2}$ for TPC was 10.697 h at 40 °C indicate that there was no much degradation in phenolic compounds during drying at this temperature. At 70 °C, the half-life for AA was found to be lowest whereas for TPC, the half-life higher than other parameters suggesting that the antioxidant activity is not solely depending upon the TPC in BPs. But we can observe in

the table 5 that the half-life for TFC at 70° is not having significant difference with AA at 70°C which suggest that the degradation rate of AA is dependent on TFC content to some extent. The larger value of $E_a$ indicated the temperature dependence of the degradation of compounds (Vardin & Yilmaz, 2018). The highest value for $E_a$ for the antioxidant activity observed was 26.83, which tells us that the temperature is the major factor which causes degradation in antioxidant activity in BP drying. This is in line with reported $E_a$ value in drying of terminalia fruits (Jha & Sit, 2020). The lower value of $E_a$ for TPC and TFC indicates that the degradation of these compounds could be depended on different parameters such as pH, moisture, oxygen, light and also presence of various enzymes etc. Presence of polyphenol oxidase in banana peels also affect the concentration of phenolic compounds. Among all these factors temperature is the major factor which leads to degradation of these compounds during drying (Jha & Sit, 2020).

**Table 4.5: Parameters of degradation kinetics for TPC, TFC and AA for banana peel drying**

| Parameters | Temperature (°C) | k | $R^2$ | $t_{1/2}$ (Hrs.) | Ea (kJ/mol.) |
|---|---|---|---|---|---|
| TPC | 40 | 0.0933 | 0.9859 | 10.7 | 11.62 |
| | 50 | -0.0944 | 0.9958 | 7.4 | |
| | 60 | -0.1194 | 0.9615 | 5.8 | |
| | 70 | -0.1334 | 0.995 | 5.2 | |
| TFC | 40 | -0.0863 | .9766 | 8.0 | 14.68 |
| | 50 | -0.1195 | 0.9218 | 5.8 | |
| | 60 | -0.1233 | 0.9839 | 5.6 | |
| | 70 | -0.1473 | 0.9513 | 4.7 | |
| AA | 40 | 0.0601 | 0.9291 | 11.5 | 26.83 |
| | 50 | -0.093 | 0.9791 | 7.5 | |
| | 60 | -0.1203 | 0.923 | 5.8 | |
| | 70 | -0.1495 | 0.9779 | 4.6 | |
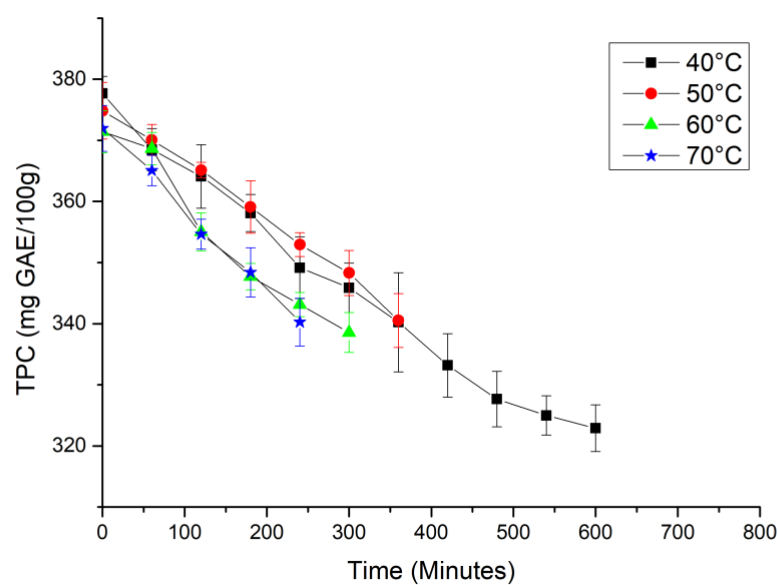
**Figure 4.6: Changes in Total phenol contents of Banana peel during drying at different temperatures.**
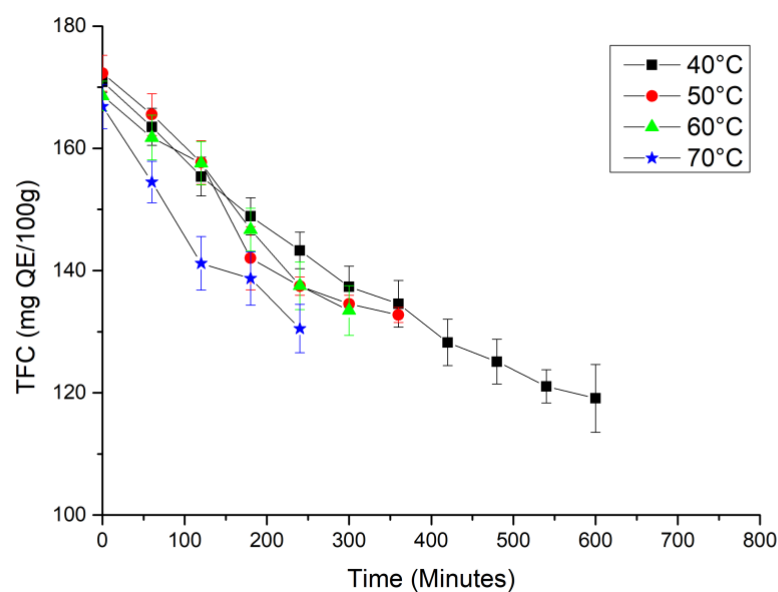


**Figure 4.7: Changes in Total Flavonoid contents of Banana peel during drying at different temperatures.**
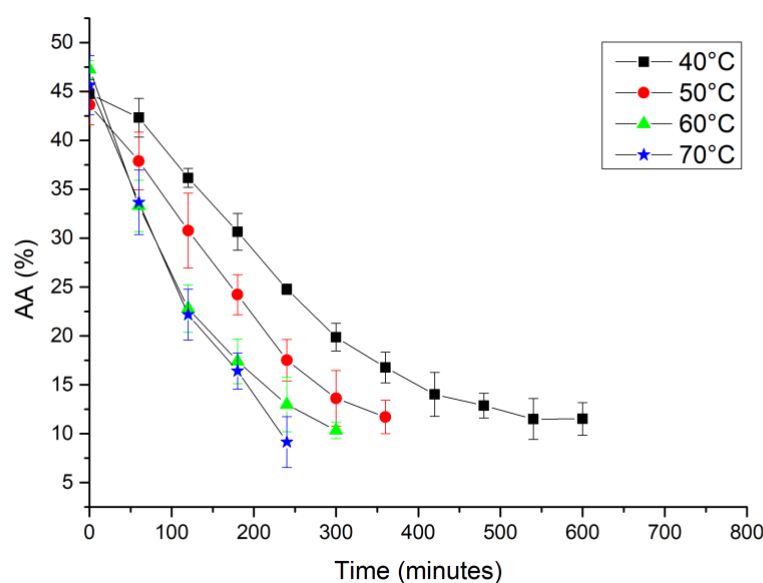
**Figure 4.8: Changes in Antioxidant activity of Banana peel during drying at different temperatures.**

## 4.3.6 Impact of drying temperature on targeted bio-active compounds in banana peel

Table 4.6 displays data on targeted bio-active compound relative concentration from a targeted flow analysis of both fresh and dried BP using LC-Orbitrap-MS analysis. The XIC were shown in figure 4.10. The analysis focused on the compound's noradrenaline, dopamine, L-phenylalanine and L-tyrosine, with their relative concentrations in fresh BP noted as 2.556, 32.084, 3.894 and 2.083 mg/kg DE dry weight basis (d.b.), respectively (fig. 4.9). Dopamine and noradrenaline are catecholamines known for their roles in brain function. Catecholamines, as a group, play essential roles in brain state regulation, vigilance, reward processing, and learning and memory processes (Ranjbar-Slamloo & Fazlali, 2020). L-phenylalanine and L-tyrosine are amino acid compounds involved in the first two steps of dopamine biosynthesis, with dopamine serving as a precursor for noradrenaline production. This highlights the interconnectedness of these compounds in the biochemical pathways related to neurotransmitter synthesis.. The data indicates a decrease in the concentration of these compounds with increasing drying temperature. At 40°C, the decrease in the concentration of noradrenaline, dopamine, L-phenylalanine and L-tyrosine compared to fresh BP was 3.951%, 11.92%, 25.78% and 23.57%, respectively. At 50°C, this decrease was 22.22%, 27.94%, 32.34% and 49.83%, respectively. When the drying temperature

rose to 60°C, the percentage degradation was increased to 53.63%, 43.26%, 53.90% and 55.16%, respectively, compared to fresh BP. At 70°C, the percentages were further increased to 64.04%, 50.73%, 66.49% and 77.00%, respectively, compared to fresh BP. This observation indicate that the rate of degradation of L-phenylalanine and L-tyrosine is higher compared to noradrenaline and dopamine across all drying temperatures. This higher degradation rate might be attributed to the conversion of L-phenylalanine and L-tyrosine into some amount of dopamine during drying, as these compounds play direct roles in dopamine biosynthesis. This observation is also complimentary to decrease in TPC content in drying and the rate of degradation is directly proportional to increase in drying temperature. Similarly, Pu et al. (2018) observed a decrease in the concentration of catechin and other compounds in dried jujube fruits compared to fresh ones during the drying process.
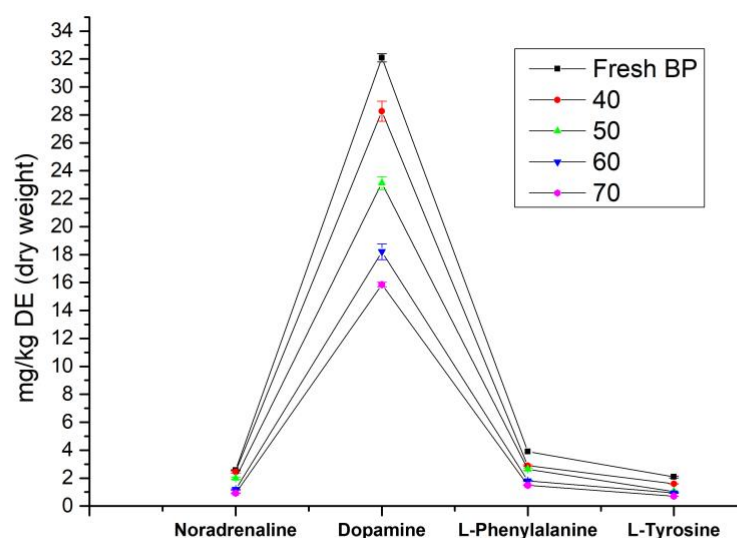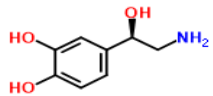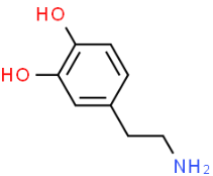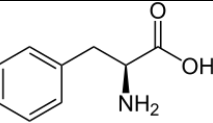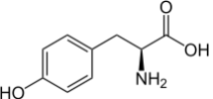


**Figure 4.9: Impact on concentration of Noradrenaline, Dopamine, L-phenylalanine and L-tyrosine of different drying temperature using LC-Orbitrap-MS.**

**Table 4.6: Concentration and other targeted flow parameters Fresh BP and Dried BP powder Dried at different temperature i. e., 40, 50, 60 and 70°C**

| Identified compound | Sub Class of phenolic compound | Structure of compound | m/z | Fresh BP (mg/kg DE) | BP dried at 40°C (mg/kg DE) | BP dried at 50°C (mg/kg DE) | BP dried at 60°C (mg/kg DE) | BP dried at 70°C (mg/kg DE) |
|---|---|---|---|---|---|---|---|---|
| Noradrenaline ($C_8H_{11}NO_3$) | Catecholamine |  | 170.08 | 2.56 | 2.46 | 1.99 | 1.19 | 0.92 |
| Dopamine ($C_8H_{11}NO_2$) | Catecholamine |  | 154.09 | 32.09 | 28.26 | 23.12 | 18.20 | 15.86 |
| L-Phenylalanine | Amino Acid |  | 166.09 | 3.90 | 2.89 | 2.63 | 1.80 | 1.49 |
| L-Tyrosine | Amino Acid |  | 182.08 | 2.08 | 1.59 | 1.04 | 0.93 | 0.70 |
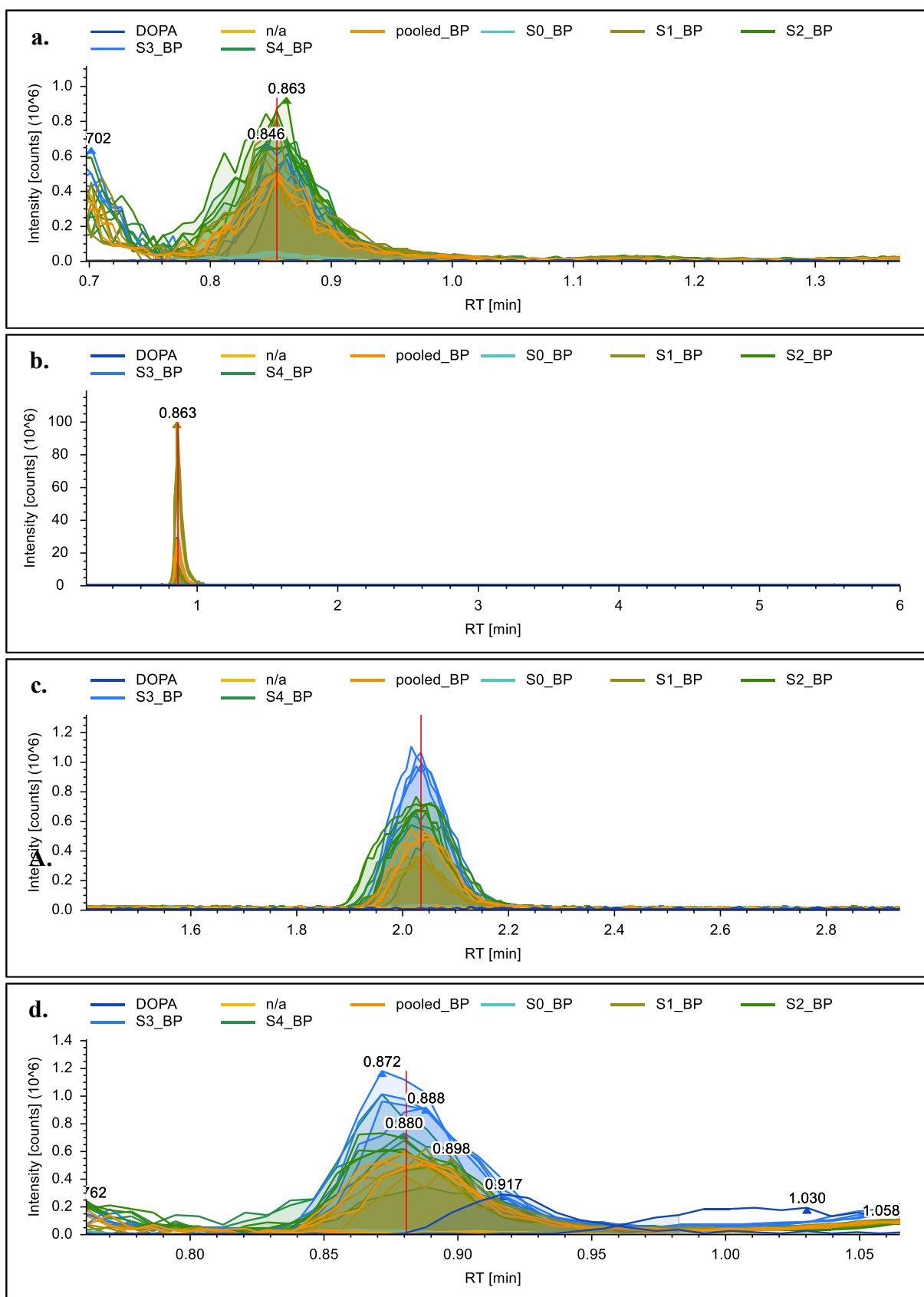
**Figure 4.10:** Chromatograms for of the a. Noradrenaline, b. Dopamine, c. L-phenylalanine, d. L-tyrosine (*DOPA- standard dopamine, n/a- blank, pooled_BP- mixture of all samples, S0_BP- Fresh Banana peel, S1_BP- Banana peel dried at 40°C, S2_BP- Banana peel dried at 50°C, S3_BP- Banana peel dried at 60°C and S4  BP- Banana peel dried at 70°C.*)

**4.4 Drying of grape pomace**

**4.4.1 Drying kinetics**

The GP was found to be containing 72.69 % initial moisture content and, on an average, the dried GP with a moisture content of 3.74 % with a 94.85 % decrease in moisture content in dried GP as compared to fresh GP. Sridhar & Charles (2022) reported a 92.58% decrease in moisture content in dry Kyoho fruit skin as compared to fresh and 88.70 % decrease in moisture content during drying of mango by Wanderley et al. (2023) which are in conformity with current study. Time required to dry GP at 40, 50, 60, 70 and 80°C was 840, 540, 390, 330 and 180 minutes, respectively (fig. 1). Similar observation was recorded during drying study of mango (Ampah et al., 2022), pomegranate peel and seeds (Wanderley et al., 2023), potato peels (Brahmi et al., 2023) and grape (Kyoho) skin (Sridhar & Charles, 2022). Similar results for faster drying at higher temperature were observed during dehydration of grape seed by Clemente et al. (2014) and by Sridhar & Charles (2022) during drying of kyoho grape fruit skin. Also, the rate of changes in moisture levels during drying depends upon the nature of material to dried (Sridhar & Charles, 2022). Overall, during the period of drying there was continues decrease in the moisture ratio until reaches equilibrium with surrounding which shows that the drying of GP completed in falling rate period. This suggests that diffusion of moisture is the major factor that regulates the drying process. Drying of different agricultural commodities shows similar results (Avhad & Marchetti, 2016; Sridhar & Charles, 2022). Initially, the high moisture content in the GP led to a higher drying rate between 100 and 250 minutes, resulting in the formation of highest angular coefficients of the curves. This mechanism, where water transitions from liquid to vapour, is often characterized by effective diffusion, which is significantly influenced by temperature, pressure, and the moisture of the material. Similarly, phenomenon was observed by, Abbaspour-Gilandeh et al., (2019) during the drying of walnut kernels, Wanderley et al., (2023) for the drying of peels and seeds of pomegranate, and  Jha & Sit (2020) for the drying of deseeded Terminalia fruits.

**Picture 4.4: Grape pomace dried at (a)40, (b)50, (c)60, (d) 70 and (e)°80 C**
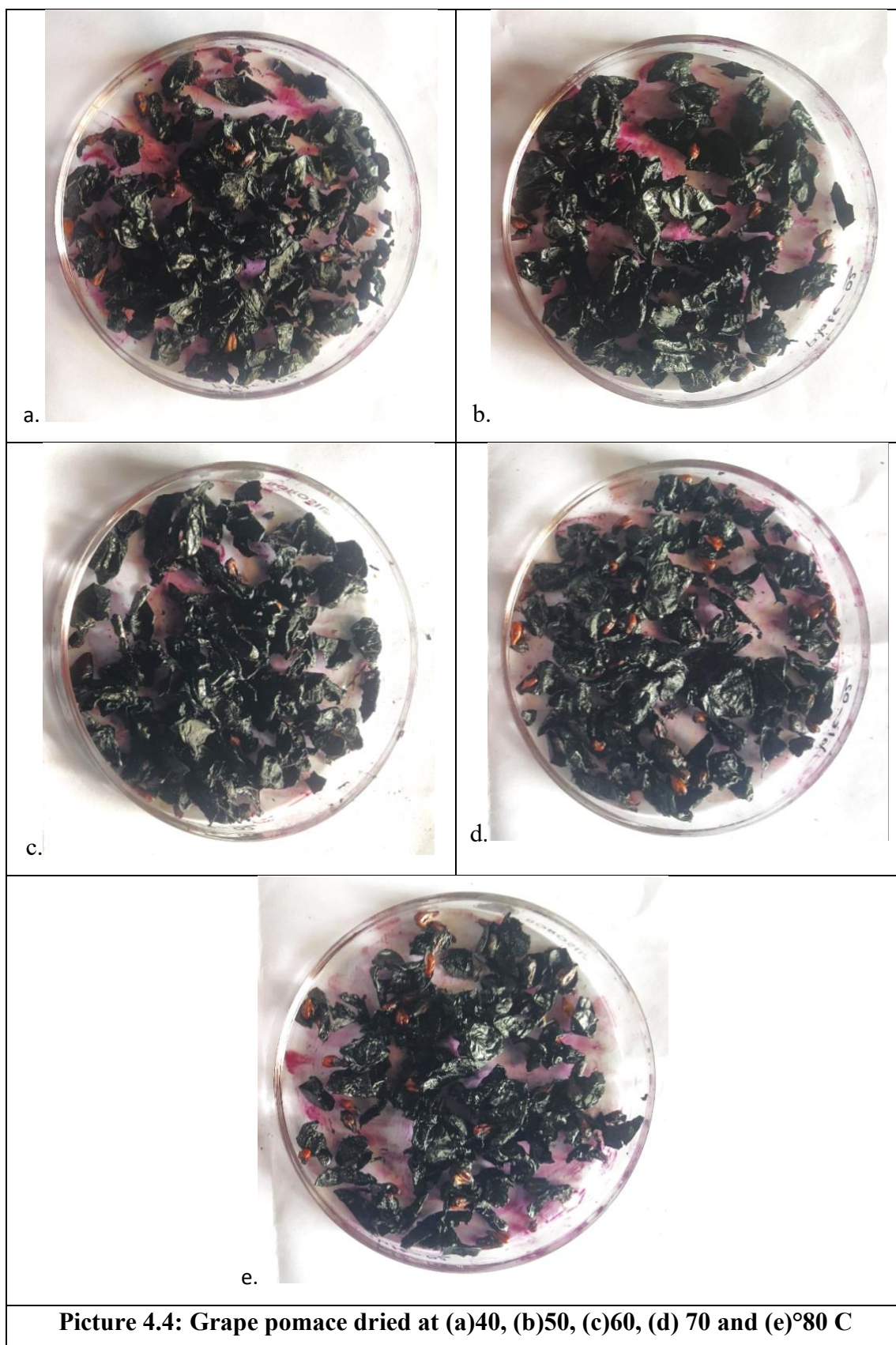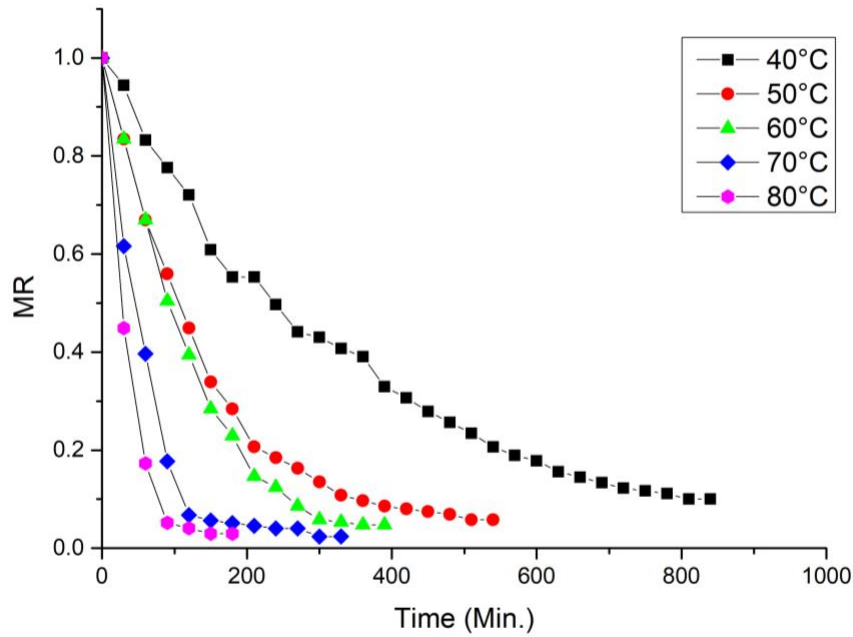
**Figure 4.11.: Changes in moisture ratio (MR) during drying at different drying temperatures.**

## 4.4.2 Mathematical modelling and fitting of curves

Evaluation of drying kinetics was performed with MR of drying of GP at different temperature such as 40, 50, 60, 70 and 80°C (fig. 4.11) and the data of experiment was fitted with selected mathematical models (Table 4.7). The value for drying constant ($k$), increased with drying temperature for newton, page, handerson and pabis and logarithmic models. The $k$ reflects the influence of temperature and $D_{eff}$ during falling rate period of drying process (Madamba et al., 1996; Oliveira et al., 2012). All the selected mathematical models were found to be fitting well to the experimental data showing higher $R^2$ values >0.97, lower RMSE (< 0.022) and $x^2$ (<0.292). Midilli et al. fitted well for the current study having highest average $R^2$ (0.9931), lowest RMSE (0.0124) and $x^2$ (0.0117) values. This result was validated by doing rigorous residual analysis by plotting experimental MR vs. predicted MR (Fig. 4.12) which showed strong corelation ($R^2$ =0.9931) and plot of residuals versus predicted MR (Fig. 4.13) clustering of residuals closely to zero with some random distribution. These are the proofs of quality of models fit (Wisniak & Polishuk, 1999). However, Sridhar & Charles (2022) reported the page and two-term model as a best fit for kinetics data of drying of kyoho GP. Ampah et al. (2022) also reported the best

fit for Midilli, Page, Wang and Singh and Logarithmic models for experimental data of drying of different varieties of mango. Therefore, for drying of GP Midilli et al. model most useful for predicting different parameters of drying of GP using hot air tray dryer.
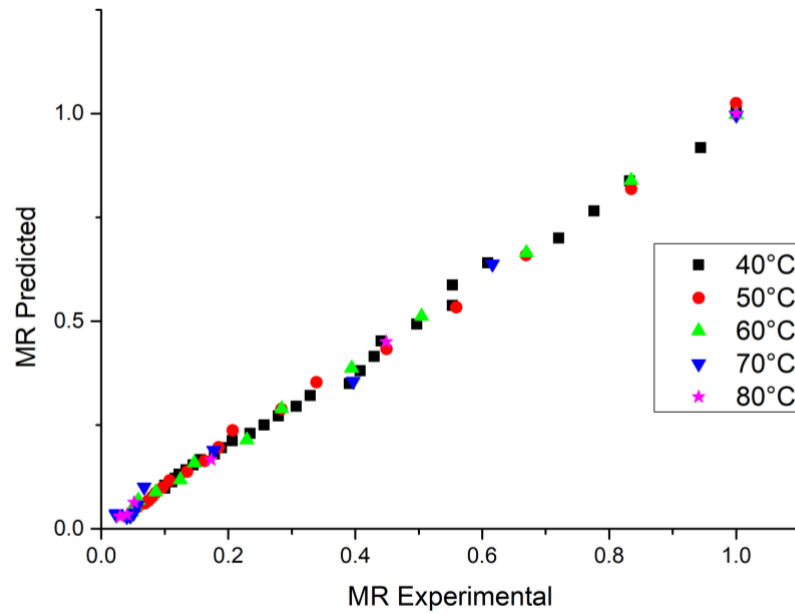


**Figure 4.12: MR predicted vs MR experimental**
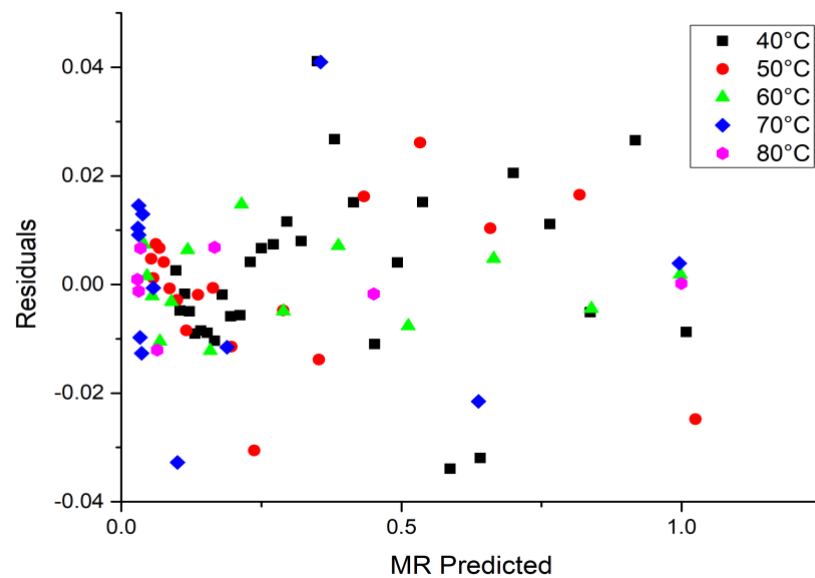


**4.13: Residuals vs MR predicted**

**Table 4.7: Mathematical models data for drying of grape pomace**

| Sr. No. | Model | Temp | Parameters | $R^2$ | Average $R^2$ | RMSE | Average RMSE | $X^2$ | Average $X^2$ |
|---|---|---|---|---|---|---|---|---|---|
| 1 | Newton | 40 | K=0.002874148 | 0.981288541 | 0.98533883 | 0.0156 | 0.0216 | 0.0155 | 0.0986 |
| | | 50 | K=0.006733120 | 0.986633969 | | 0.0189 | | 0.1157 | |
| | | 60 | K=0.008088284 | 0.978448219 | | 0.0266 | | 0.0415 | |
| | | 70 | K=0.017328336 | 0.990703594 | | 0.0284 | | 0.3854 | |
| | | | K=0.028133430 | 0.996273185 | | 0.0172 | | 0.1149 | |
| 2 | Page | 40 | K=0.003162409 n=0.983926392 | 0.981829022 | 0.98991978 | 0.0154 | 0.0173 | 0.0152 | 0.1948 |
| | | 50 | K=0.007518463 n=0.978662948 | 0.987017420 | | 0.0186 | | 0.0909 | |
| | | 60 | K=0.003430803 n=1.172176192 | 0.996689496 | | 0.0104 | | 0.0340 | |
| | | 70 | K=0.010567151 n=1.116555625 | 0.999209810 | | 0.0262 | | 1.2361 | |
| | | 80 | K=0.019986543 n=1.089028500 | 0.997001535 | | 0.0154 | | 0.2708 | |
| 3 | Handerson and Pabis model | 40 | k=0.002869396 a=0.998501730 | 0.981307531 | 0.98665937 | 0.0156 | 0.2131 | 0.0154 | 0.2917 |
| | | 50 | k=0.006761734 a=1.004126644 | 0.986692749 | | 0.0188 | | 0.1194 | |
| | | 60 | k=0.008415479 a=1.042064846 | 0.984599623 | | 0.0225 | | 0.0293 | |
| | | 70 | k=0.017542992 a=1.012684501 | 0.985554707 | | 0.0273 | | 0.3480 | |
| | | 80 | k=0.028226585 a=1.004120107 | 0.996304792 | | 0.0171 | | 0.1169 | |
| 4 | Verma et al | 40 | k=0.003217032 a=0.700313668 g=0.002230667 | 0.981685641 | 0.98800486 | 0.0154 | 0.0192 | 0.0154 | 0.1700 |
| | | 50 | k=0.006799751 a=1.008923090 g=0.096768002 | 0.986745659 | | 0.0188 | | 0.1247 | |
| | | 60 | k=0.006704009 a=1.190792277 g=0.002583709 | 0.986787535 | | 0.0208 | | 0.0772 | |
| | | 70 | k=0.020303136 a=1.252168302 g=0.051731638 | 0.992393598 | | 0.0257 | | 0.8833 | |
| | | 80 | k=0.031372529 a=1.142683700 g=0.815414458 | 0.997291960 | | 0.0146 | | 0.2114 | |
| 5 | Approximation of diffusion | 40 | k=0.002876806 a=0.982091107 b=0.917135295 | 0.981289642 | 0.98734968 | 0.0156 | 0.0200 | 0.0154 | 0.1206 |
| | | 50 | k=0.006733097 a=1.046132603 b=0.999969936 | 0.986633969 | | 0.0189 | | 0.1157 | |
| | | 60 | k=0.005362876 a=7.112893438 b=0.936665707 | 0.987720196 | | 0.0201 | | 0.0831 | |
| | | 70 | k=0.007462756 a=0.013230957 b=2.411658311 | 0.991504718 | | 0.0272 | | 0.0809 | |
| | | 80 | k=-0.035597467a=1.947640600 b=1.351342179 | 0.996986409 | | 0.0154 | | 0.3006 | |
| 6 | Midilli et al. | 40 | k=0.003456978a=1.008727157b=1.22922E-05 n=0.974697488 | 0.980776547 | 0.99308618 | 0.0158 | 0.0123 | 0.0174 | 0.0116 |
| | | 50 | k=0.008252933a=1.024796550b=5.63953E-05 n=0.974697488 | 0.993222039 | | 0.0134 | | 0.0111 | |
| | | 60 | k=0.002676039a=0.998137637b=6.117E-05 n=1.230060175 | 0.998340295 | | 0.0075 | | 0.0058 | |
| | | 70 | k=0.007215573a=0.996092165 b=0.000109531 n=1.216011785 | 0.996000611 | | 0.0186 | | 0.0416 | |
| | | 80 | k=0.013694711a=0.999809076b=0.000166695 n=1.199029065 | 0.999564752 | | 0.0058 | | 0.0039 | |

### 4.4.3 Effective moisture diffusivity ($D_{eff}$)

$D_{eff}$ was calculated by plotting natural logarithm of MR versus time required as shown in fig. 4.14 for GP under different drying temperatures. The values for $D_{eff}$ for 40 to 80 °C were ranged from $1.54 \times 10^{-10}$ to $1.12 \times 10^{-09}$ $m^2.s^{-1}$ (table 4.8) and all observed values are positive. It is observed that the values for $D_{eff}$ showed increasing trend with drying temperature. Similar trend in increase in diffusivity with drying temperature was observed for drying of mango (Ampah et al., 2022) and drying of kyoho (grape) skin (Sridhar & Charles, 2022). It is reported that for drying of agricultural and food commodities, values for $D_{eff}$ between $10^{-8}$ to $10^{-12}$ (Kaveh et al., 2018; Zogzas et al., 1996). The values for $D_{eff}$ observed in current experiment also within this range. Ampah et al. (2022) and Sant'anna et al. (2014) also estimated the values for $D_{eff}$ within the same range for drying of mango fruit and peels, respectively.
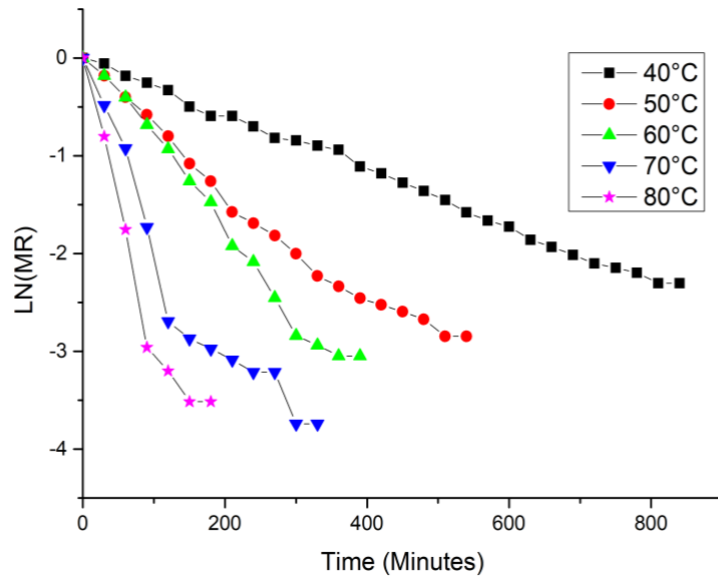


**Figure 4.14: Natural logarithm of MR vs time for the determination of effective moisture diffusivity**

### 4.4.4 Activation energy ($E_a$)

Activation energy ($E_a$) is nothing but the energy required to displace one mole of water from sample and expressed as kJ.mol$^{-1}$. $E_a$ calculated by plotting the natural logarithm of $D_{eff}$ against inverse of temperature in kelvin (K) (fig. 4.15). The value for activation energy for drying of GP was 42.79 kJ.mol$^{-1}$ (table 4.8). For drying of

various fruits and vegetables commodities, the $E_a$ was observed to be in the range of 12.7-110 kJ.mol$^{-1}$ (Kaveh et al., 2017; Zogzas et al., 1996). For drying of kyoho (grape) skin, the $E_a$ observed was 33.78 kJ.mol$^{-1}$ (Sridhar & Charles, 2022).
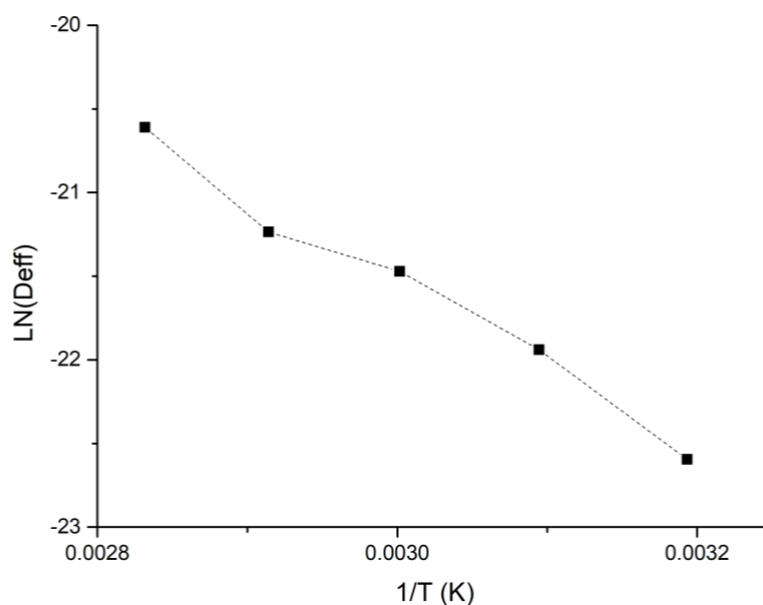


**Figure 4.15: Natural logarithm of effective diffusivity vs inverse of temperature in kelvin for determination of activation energy**

**Table 4.8: Effective moisture diffusivity ($D_{eff}$) and activation energy ($E_a$) for drying of GP**

| Temperature | Effective moisture diffusivity ($D_{eff}$) (m$^2$.s$^{-1}$) | $R^2$ | $E_a$ (kJ.mol$^{-1}$) |
|---|---|---|---|
| 40 | $1.54 \times 10^{-10}$ | 0.9968 | 42.79 |
| 50 | $2.96 \times 10^{-10}$ | 0.9699 | |
| 60 | $4.73 \times 10^{-10}$ | 0.9850 | |
| 70 | $5.99 \times 10^{-10}$ | 0.8760 | |
| 80 | $1.12 \times 10^{-09}$ | 0.9018 | |

**4.4.5 Effect of drying temperature on TPC, TFC, TAC and AA during drying of GP**

GP is the rich source of different phenols, flavonoids and anthocyanins and presence of these compounds in GP provides many health benefitting characteristics (Antonić et al., 2020; Bordiga et al., 2019; Muñoz-Bernal et al., 2021; Šelo et al., 2023). These compounds, which provide significant health benefits, are considered valuable quality components in GP. However, they are highly sensitive to various external environmental factors that can trigger their degradation. Temperature, in particular, is a major factor during the drying process, having a substantial impact on these quality parameters. The changes in content of TPC, TFC, TAC and AA during drying at temperature 40, 50, 60, 70 and 80 °C are as shown in fig. 4.16, 4.17, 4.18, 4.19. The concentration of all parameters is decreasing with increase in drying time. The values for $k$, $R^2$ and $E_a$ are presented in table 4.9. It can be observed that values of $k$ are increasing with increase in drying temperature for TPC, TFC, TAC and AA. From the values for $k$ it can be clearly observed that degradation was increased with temperature. However, the rate of degradation of TFC is faster than TPC. Further, the rate of degradation of AA is mainly dependant on TPC, TFC and TAC but the higher rate of degradation for AA could be due to cumulative effect of other factors along with TPC, TFC and TAC. Similarly, the half-life ($t_{1/2}$) and $D$ for all parameters showed decreasing trend with increase in drying temperature. The AA found to have lowest half-life at all temperatures indicating contribution of TPC, TFC and TAC. The highest $t_{1/2}$ at 40 °C was observed for TFC (6.82 hrs.) followed by TAC. The data on $t_{1/2}$ at 70 °C indicates that both AA ($t_{1/2} = 0.74$ hrs.) and TAC ($t_{1/2} = 0.77$ hrs.) with similar $t_{1/2}$ confirming highest contribution to AA degradation by degradation of TAC. The $E_a$ calculated for degradation of TPC, TFC, TAC and AA are shown in table 4.9. Higer value of $E_a$ suggests the temperature dependency on the degradation of phytochemicals (Vardin & Yilmaz, 2018). The highest value for $E_a$ was observed for TAC (48.019 kJ.mol$^{-1}$) followed by TPC and TFC at 43.133 and 45.607 kJ.mol$^{-1}$, respectively. The highest $E_a$ of TAC suggests that the comparative higher temperature dependency on degradation of TAC compared to TPC and TFC. The lowest value of $E_a$ was observed for AA (40.286 kJ.mol$^{-1}$) indicating that major factor responsible for degradation of AA during drying of GP is degradation of TAC followed by TFC and TPC but not limited to these parameters. Other factors such as system temperature, air

flow, light, oxygen, etc. may also be responsible. Our observation also in complementary to $E_a$ value reported under various drying temperatures for Terminalia fruits drying (Jha & Sit, 2020).

**Table 4.9: Parameters for degradation kinetics for TPC, TFC, TAC and AA in GP during drying at different temperature.**

| Parameters | Temperature (°C) | k | $t_{1/2}$ | D | $R^2$ | Ea (kJ.mol$^{-1}$) |
|---|---|---|---|---|---|---|
| **TPC** | 40°C | 0.1043 | 6.65 | 22.081 | 0.9399 | 43.133 |
| | 50°C | 0.1590 | 4.36 | 14.484 | 0.9612 | |
| | 60°C | 0.3518 | 1.97 | 6.5463 | 0.9460 | |
| | 70°C | 0.4515 | 1.54 | 5.1008 | 0.9518 | |
| | 80°C | 0.6407 | 1.08 | 3.5945 | 0.8819 | |
| **TFC** | 40°C | 0.1017 | 6.82 | 22.645 | 0.9793 | 45.607 |
| | 50°C | 0.1805 | 3.84 | 12.759 | 0.9563 | |
| | 60°C | 0.3080 | 2.25 | 7.4773 | 0.9272 | |
| | 70°C | 0.3478 | 1.99 | 6.6216 | 0.9319 | |
| | 80°C | 0.8452 | 0.79 | 2.6167 | 0.8801 | |
| **Anthocyanin** | 40°C | 0.1027 | 6.75 | 22.425 | 0.8575 | 48.019 |
| | 50°C | 0.2082 | 3.33 | 11.061 | 0.9603 | |
| | 60°C | 0.3924 | 1.77 | 5.869 | 0.9558 | |
| | 70°C | 0.4922 | 1.41 | 4.679 | 0.9574 | |
| | 80°C | 0.9028 | 0.77 | 2.551 | 0.9470 | |
| **AA** | 40°C | 0.1460 | 4.75 | 15.774 | 0.9816 | 40.286 |
| | 50°C | 0.2811 | 2.47 | 8.1928 | 0.9630 | |
| | 60°C | 0.4319 | 1.61 | 5.3323 | 0.9570 | |
| | 70°C | 0.5407 | 1.28 | 4.2593 | 0.8839 | |
| | 80°C | 0.9367 | 0.74 | 2.4586 | 0.9514 | |
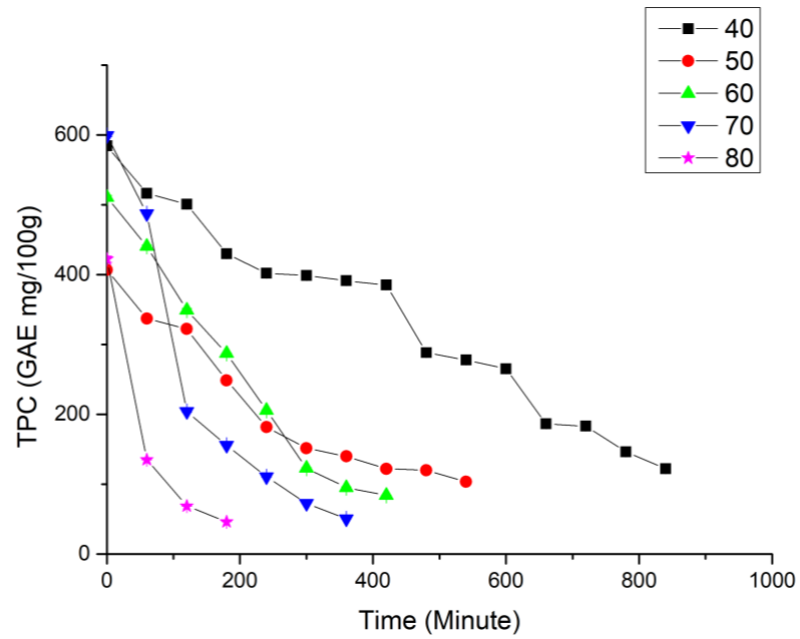
**Figure 4.16: Changes in total phenolic content in grape pomace drying**
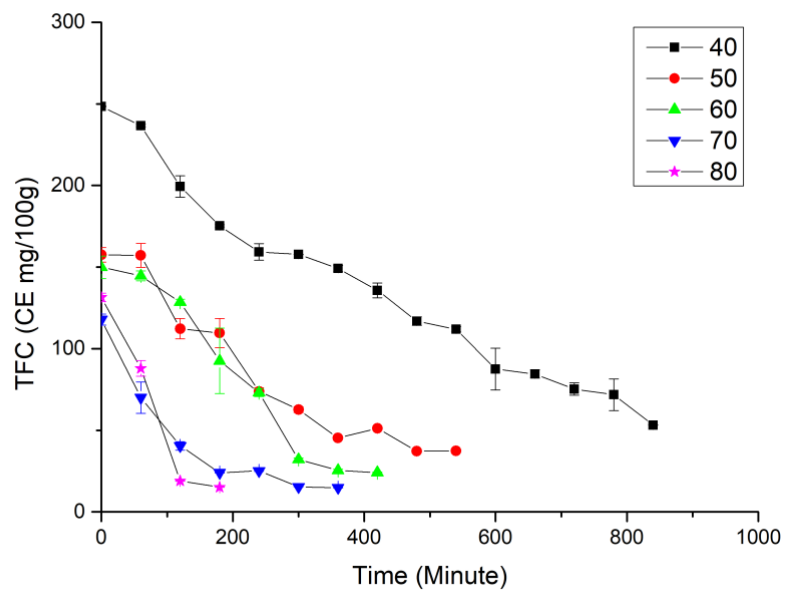


**Figure 4.17: Changes in total flavonoid content in grape pomace drying**
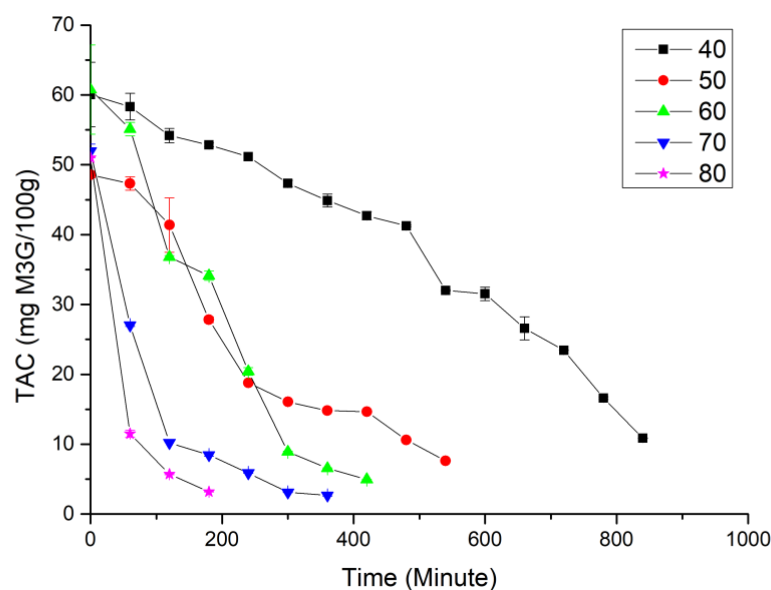
**Figure 4.18: Changes in total anthocyanin content in grape pomace drying**
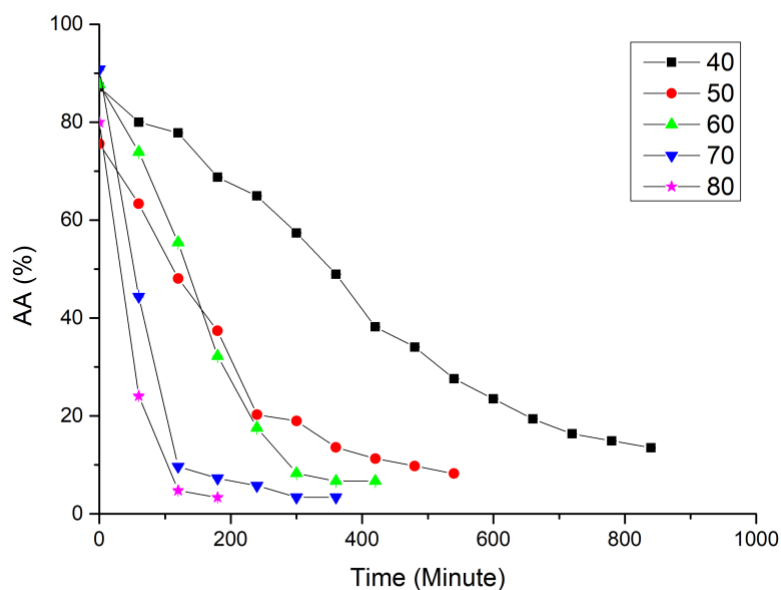


**Figure 4.19: Changes in antioxidant activity in grape pomace drying**

**4.4.6 Impact of temperature on anthocyanin profiles of grape pomace**

Anthocyanins are the natural colour pigments in the red grapes (Akbulut et al., 2024; Onache et al., 2022). The anthocyanin profiles were determined from the fresh GP and dried GP at different temperatures such as 40, 50, 60, 70 and 80 °C. As shown

in Table 4.10 there were 16 compounds were identified in both fresh GP and dried GP. The identified compounds were cyanidin, delphinidin, pelargonidin and glucosides of cyanidin, malvidin, delphinidin, pelargonidin, petunidin and peonidin. All these compounds were identified in all samples in fresh as well as dried. In the fresh GP, highest concentration was observed for malvidin-3-*O*-glucoside which accounted for 48.04 % of the total anthocyanin content identified where, it was 47.95, 49.64, 47.26, 49.50 and 47.52 % in dried GP at 40, 50, 60, 70 and 80 °C, respectively. Total anthocyanin content in fresh sample was found to be 32269.24 mg.kg$^{-1}$ C3GE DW which degraded to 16120.23, 24604.20, 22452.34, 10381.87 and 9336.8 mg.kg$^{-1}$ C3GE DW after drying at 40, 50, 60, 70 and 80 °C, respectively (Fig. 4.20). In comparison to fresh GP, the percent degradation of total anthocyanin was 23.75 and 30.42 % for GP dried at 50 and 60 °C, respectively. However, GP dried at 40 °C showed 50.04% degradation and at higher temperature 70 and 80°C showed a degradation of 67.83 and 71.07 %, respectively. This data clearly indicates the dependency of temperature and drying time on degradation of anthocyanin in GP. The higher degradation of anthocyanin at lower temperature 40 $^{0}$C compared to 50 and 60 $^{0}$C could be due to longer drying time at 40 $^{0}$C. Similarly, the higher degradation at 70 and 80 $^{0}$C compared to lower temperature could be due to degradation of anthocyanin influenced by temperature. The literature also reports higher temperature induced degradation of anthocyanins in blueberry ( Martín-Gómez et al., 2020) and degradation of strawberry anthocyanin during drying (Méndez-Lagunas et al., 2017). In the degradation kinetics study carried out in this current study also showed same behaviour in degradation of total anthocyanin contents with increase in drying temperature during drying of GP. Higher percentage of degradation at 40°C might be due to extended period of drying where oxidation of the anthocyanins occurred due to presence of polyphenol oxidase. Hence, drying of GP between 50 to 60 °C will be the optimal temperature and minimal drying time to preserve the anthocyanin in dried GP.
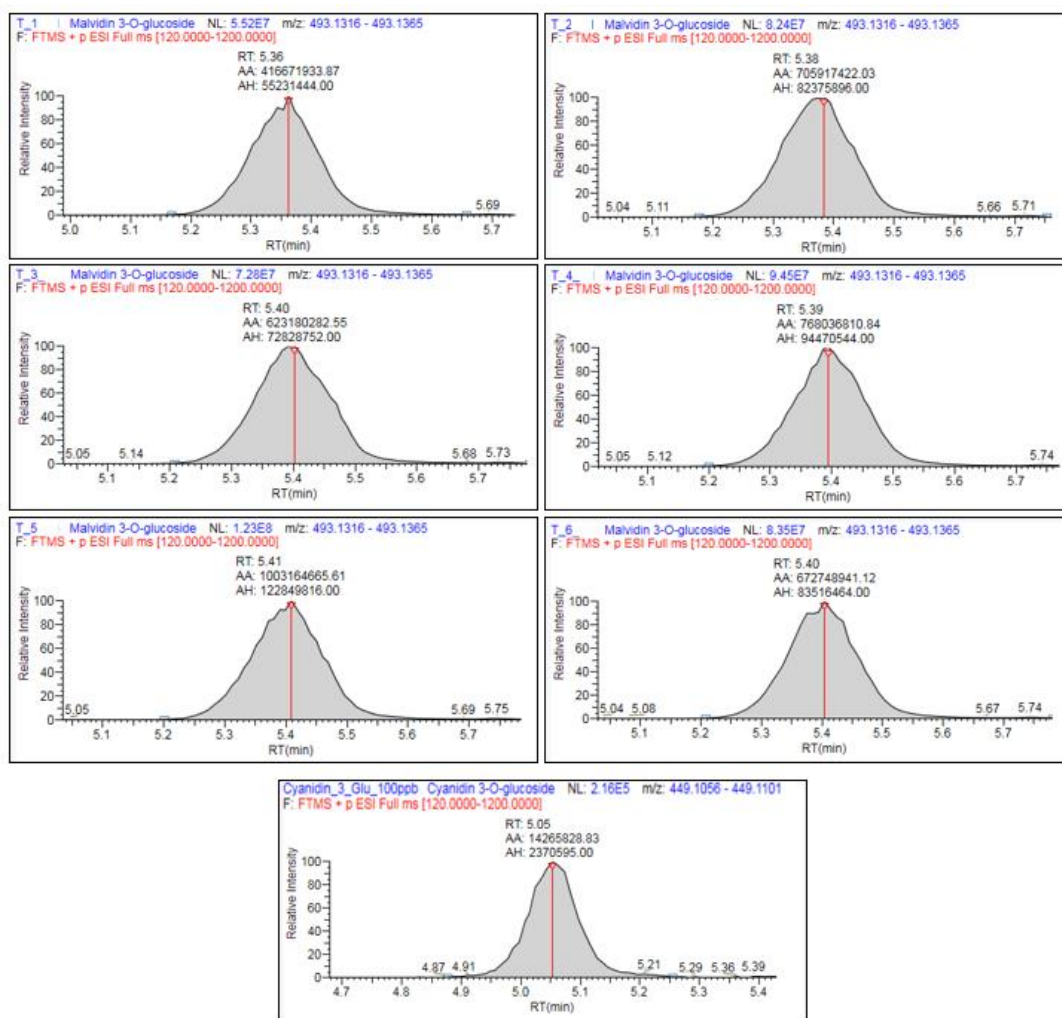
**Figure 4.20: XIC for standard (100 PPB) Cyanidin-3-*O*-glucoside and Malvidin-3-*O*-glucoside in GP (T_1: Fresh GP, T_2: DGP 40°C, T_3: DGP 50°C, T_4: DGP 60°C, T_5: DGP 70°C and T_6: DGP 80°C).**

**Table 4.10: Anthocyanin profiles with m/z value, RT measured value and relative concentration of fresh GP and Dried GP at different temperature.**

| Compound Name | m/z (Apex) | RT (Measured) | Fresh GP (mg/kg C3GE) | DGP 40°C (mg/kg C3GE) | DGP 50°C (mg/kg C3GE) | DGP 60°C (mg/kg C3GE) | DGP 70°C (mg/kg C3GE) | DGP 80°C (mg/kg C3GE |
|---|---|---|---|---|---|---|---|---|
| Cyanidin 3-(6-p-caffeoyl)glucoside | 611.1378 | 5.96 | 357.77 | 98.25 | 266.07 | 306.67 | 70.01 | 92.61 |
| Cyanidin 3,5-O-diglucoside | 611.1635 | 6.29 | 3.53 | 1.44 | 2.36 | 1.58 | 1.01 | 2.00 |
| Cyanidin 3-O-(6-O-p-coumaroyl) glucoside | 595.1428 | 6.13 | 205.10 | 75.34 | 151.49 | 167.64 | 58.35 | 58.92 |
| Cyanidin 3-O-glucoside | 449.1067 | 5.05 | 844.13 | 259.70 | 552.10 | 639.45 | 177.63 | 175.24 |
| Cyanidin | 287.0563 | 0.89 | 54.46 | 24.83 | 45.24 | 59.17 | 5.93 | 25.76 |
| Delphinidin 3,5-diglucoside | 627.1583 | 6.16 | 7.75 | 1.64 | 1.88 | 1.74 | 1.05 | 4.17 |
| Delphinidin 3-O-(6-caffeoyl-beta-D-glucoside) | 627.1314 | 5.7 | 10.34 | 3.87 | 11.82 | 10.27 | 2.30 | 1.10 |
| Delphinidin 3-O-glucoside | 465.1015 | 4.84 | 988.99 | 240.17 | 776.21 | 867.22 | 119.42 | 232.52 |
| Delphinidin 3-O-sophoroside | 627.1583 | 6.16 | 7.75 | 1.64 | 1.88 | 1.74 | 1.05 | 4.17 |
| Delphinidin | 303.0495 | 6.02 | 261.32 | 100.38 | 199.77 | 193.49 | 47.44 | 131.47 |
| Malvidin 3-O-glucoside | 493.1335 | 5.36 | 15502.84 | 7728.92 | 12212.80 | 10611.19 | 5138.77 | 4436.88 |
| Pelargonidin 3-(6-p-coumaroyl)glucoside | 579.148 | 5.25 | 539.46 | 394.34 | 165.95 | 1.43 | 10.55 | 85.71 |
| Pelargonidin 3-O-glucoside | 433.1121 | 5.24 | 106.47 | 49.10 | 76.21 | 73.46 | 32.18 | 26.77 |
| Pelargonidin | 271.0591 | 5.22 | 16.06 | 10.97 | 6.55 | 8.70 | 1.62 | 2.59 |
| Peonidin 3-O-glucoside | 463.1231 | 5.32 | 11321.18 | 6463.55 | 8500.66 | 7899.96 | 4300.40 | 3573.61 |
| Petunidin 3-O-glucoside | 479.1172 | 5.12 | 2042.11 | 666.09 | 1633.21 | 1608.63 | 414.15 | 483.29 |
| Total | - | - | 32269.24 | 16120.23 | 24604.2 | 22452.34 | 10381.87 | 9336.826 |

## 4.5 Extraction of bioactive compounds of banana peel

### 4.5.1 Fitting of models

The optimization of sonication time, solid to liquid ratio, sonication power and solvent concentration was carried out using RSM to get optimal recovery of total phenolic content, dopamine content, L-dopa content and L-tyrosine content from the banana peel powder (table 4.11). The analysis of variance of experimental data on the optimal recoveries shows the quadratic model as best fit (table 4.12, 4.13, 4.14 and 4.15). The coefficients of in terms of coded variables of total phenolic contents, dopamine content, L-dopa content and L-tyrosine content for the predicted models are given in equations

$$y_{TPC} = 73.84 + 4.43_A - 8.78_B + 2.49_C - 23.06_D - 0.5325_{AB} + 1.14_{AC} - 1.24_{AD} + 4.07_{BC} - 0.1212_{BD} - 2.39_{CD} - 4.86_{A^2} + 9.37_{B^2} - 1.53_{C^2} - 18.04_{D^2} \qquad (4.1)$$

$$y_{DC} = 7.21 + 0.0922_A + 4.83_B + 0.8533_C - 1.17_D - 0.0050_{AB} - 0.2812_{AC} + 0.0400_{AD} + 0.8650_{BC} - 0.9887_{BD} + 0.2700_{CD} - 1.40_{A^2} - 0.2779_{B^2} - 0.2529_{C^2} + 2.07_{D^2} (4.2)$$

$$y_{LDC} = 18.63 - 0.4654_A + 1.76_B + 0.1424_C - 7.23_D + 0.2542_{AB} - 0.2067_{AC} - 0.2492_{AD} - 0.3183_{BC} - 2.04_{BD} + 0.8783_{CD} - 0.2787_{A^2} + 2.87_{B^2} - 0.2587_{C^2} - 10.16_{D^2}$$
$$(4.3)$$

$$y_{LTC} = 11.16 - 0.1794_A + 1.39_B + 0.7011_C - 2.25_D + 0.2361_{AB} + 1.41_{AC} - 1.24_{AD} + 0.3019_{BC} - 0.8644_{BD} + 0.0244_{CD} - 1.01_{A^2} - 2.13_{B^2} + 2.01_{C^2} - 1.19_{D^2} \qquad (4.4)$$

Where the A, B, C and D corresponds to the coded variables sonication time, solid to liquid ratio, Sonication power and solvent concentration, respectively.

The model's fit was assessed using the lack of fit test, where a p-value greater than 0.05 indicates non-significance. Specifically, the lack of fit values for total phenolic content (TPC) at 0.3905, dopamine content at 0.5700, L-DOPA content at 0.7635 and L-tyrosine content at 0.8014 were all non-significant, demonstrating that

the models accurately describe the data (table 4.12, 4.13, 4.14 and 4.15). This implies that the lack of fit does not account for a significant portion of the error, confirming that the experimental data are well-represented by the models. In addition to the lack of fit test, the models were further validated by their p-values, which demonstrate that the models are well-suited for predicting the variability in the data. A key parameter used to evaluate model performance is the $R^2$. For TPC, the $R^2$ was 0.9907, for dopamine content it was 0.9906, for L-DOPA content it was 0.9380, and for L-tyrosine content it was 0.9265 (table 4.12, 4.13, 4.14 and 4.15). These high $R^2$ values indicate that over 90% of the variability in the responses is explained by the models. However, as noted by Dahmoune et al. (2015), a high $R^2$ value alone is not a definitive indicator of a sound model. To ensure the robustness of the model, it is important that the $R^2$ value is close to the adjusted $R^2$ value. In this case, the difference between $R^2$ and adjusted $R^2$ was less than 0.2 for all the response variables, further confirming the statistical reliability of the models.

Moreover, the models were evaluated for adequacy by examining the predicted $R^2$, adjusted $R^2$, and overall $R^2$, all of which exceeded 90%. This high level of congruence among these statistical parameters indicates that the models are not only well-fitted to the data but also have strong predictive capabilities. The significance of this fit was established at a probability level of 0.0001%, providing strong evidence that the models are highly reliable. The CV is a measure of the extent of variability relative to the mean of the data. Lower CV values indicate that the data points are closely clustered around the mean, signifying greater consistency and reproducibility of the experimental results. In this case, the CV values for TPC, dopamine content, L-DOPA content and L-tyrosine content were all low, reinforcing the high reproducibility of the experimental findings. According to Liyana-Pathirana and Shahidi (2005), low CV values are indicative of reliable and stable models, which further supports the robustness of the fitted models in this study.

Thus, the combined metrics—lack of fit, $R^2$, adjusted $R^2$, predicted $R^2$ and CV all validate the quality and reliability of the models used to describe the effects on TPC, dopamine, L-DOPA and L-tyrosine content in banana peel extracts. These results suggest that the models are highly capable of accurately predicting outcomes in similar experimental setups.

**Table 4.11: Face centred central composite design and recorded responses**

| Std. run | A:Time (Minutes) | B:Solit to liquid ratio (mg/100g) | C:Power (W) | D:Solvent concentration (%) | TPC (mg GAE/100g) | Dopamine Content (mg/100g) | L-dopa Content (mg/100g) | L-tyrosine Content (mg/100g) |
|---|---|---|---|---|---|---|---|---|
| 1 | 5 | 2 | 200 | 50 | 82.24 | 2.74 | 13.15 | 9.34 |
| 2 | 15 | 2 | 200 | 50 | 94.09 | 2.62 | 13.97 | 6.64 |
| 3 | 5 | 8 | 200 | 50 | 61.92 | 12.55 | 24.2 | 13.01 |
| 4 | 15 | 8 | 200 | 50 | 69.93 | 13.59 | 21.8 | 12.04 |
| 5 | 5 | 2 | 400 | 50 | 85.31 | 2.97 | 14.64 | 7.88 |
| 6 | 15 | 2 | 400 | 50 | 97.29 | 2.23 | 12.15 | 11.49 |
| 7 | 5 | 8 | 400 | 50 | 74.04 | 15.75 | 19.5 | 11.83 |
| 8 | 15 | 8 | 400 | 50 | 87.44 | 15.73 | 21.53 | 15.56 |
| 9 | 5 | 2 | 200 | 100 | 47.76 | 1.6 | 2.63 | 9.12 |
| 10 | 15 | 2 | 200 | 100 | 52.23 | 2.68 | 2.11 | 3.38 |
| 11 | 5 | 8 | 200 | 100 | 21.74 | 7.5 | 2.73 | 7.15 |
| 12 | 15 | 8 | 200 | 100 | 23.57 | 8.23 | 2.45 | 4.04 |
| 13 | 5 | 2 | 400 | 100 | 33.32 | 2.28 | 6.61 | 5.56 |
| 14 | 15 | 2 | 400 | 100 | 44.59 | 2.58 | 2.733 | 7.06 |
| 15 | 5 | 8 | 400 | 100 | 28.62 | 12.98 | 5.34 | 7.98 |
| 16 | 15 | 8 | 400 | 100 | 36.43 | 11.67 | 3.99 | 9.21 |
| 17 | 5 | 5 | 300 | 75 | 64.34 | 5.43 | 20.11 | 10.55 |
| 18 | 15 | 5 | 300 | 75 | 73.54 | 6.13 | 19.8 | 9.77 |
| 19 | 10 | 2 | 300 | 75 | 95.63 | 2.6 | 24 | 6.71 |
| 20 | 10 | 8 | 300 | 75 | 70.72 | 11.21 | 22.2 | 11.38 |
| 21 | 10 | 5 | 200 | 75 | 66.66 | 6.59 | 20.42 | 12.8 |
| 22 | 10 | 5 | 400 | 75 | 77.88 | 7.27 | 19.53 | 13.57 |
| 23 | 10 | 5 | 300 | 50 | 81.27 | 10.47 | 18.93 | 13.04 |
| 24 | 10 | 5 | 300 | 100 | 30.25 | 8.04 | 1.21 | 6.92 |
| 25 | 10 | 5 | 300 | 75 | 76.65 | 7.64 | 14.91 | 11.21 |
| 26 | 10 | 5 | 300 | 75 | 71.3 | 6.37 | 22.6 | 12.36 |
| 27 | 10 | 5 | 300 | 75 | 72.49 | 7.47 | 12.65 | 11.8 |
| 28 | 10 | 5 | 300 | 75 | 77.75 | 7.66 | 17.1 | 8.83 |
| 29 | 10 | 5 | 300 | 75 | 72.09 | 6.66 | 18.68 | 11.58 |
| 30 | 10 | 5 | 300 | 75 | 73 | 7.67 | 16.23 | 11.11 |

## 4.5.2 Effect of extraction parameters on the total phenolic contents in banana peel extract

The extraction variables, sonication time, solid-to-liquid ratio, sonication power and solvent concentration were systematically examined to identify the optimal conditions for maximum TPC recovery. The study revealed that sonication time,

solid-to-liquid ratio, and solvent concentration had the most significant influence on the TPC yield (p< 0.0001), indicating a highly significant impact on phenolic compound recovery (table 4.12). These findings are consistent with previous research, where these factors were found to be critical in the extraction of phenolics and other bioactive compounds from plant matrices (Chemat et al., 2017). Sonication time enhances the recovery of bioactive compounds by promoting greater disruption of plant cell walls and increased penetration of the solvent into plant tissues. In this study, prolonged sonication times resulted in higher phenolic recovery, which suggests that the increased exposure to ultrasonic waves facilitated the release of more phenolic compounds from the banana peel. However, care must be taken not to exceed the optimal sonication time, as excessively long times may cause degradation of sensitive phenolic compounds (Wang & Weller, 2006). Higher solid concentrations provide more bioactive material for extraction, but excessive solid content can lead to saturation of the solvent, reducing extraction efficiency (Lefebvre et al., 2021). In this study, increasing the solid-to-liquid ratio up to an optimal point resulted in higher TPC recovery.

Solvent concentration, particularly the ethanol-to-water ratio, had the most profound effect on TPC extraction. Ethanol-water mixtures are frequently used in phenolic compound extraction due to their ability to adjust solvent polarity, thereby enhancing the solubility of phenolic compounds (Azmir et al., 2013). In this study, ethanol concentrations ranging from 50% to 100% v/v were tested, and the highest TPC yield of 89.3 mg GAE/100g dry weight was achieved at 50% ethanol concentration. This result suggests that a balanced ethanol-water mixture is ideal for solubilizing phenolic compounds, as the addition of water to ethanol increases solvent polarity, which enhances its ability to penetrate the plant matrix and solubilize phenolics (Sulaiman et al., 2011). These findings align with other studies that have reported similar results, highlighting that ethanol-water mixtures are more effective in extracting phenolic compounds than using ethanol or water alone (Rodríguez De Luna et al., 2020). Sonication power was also a significant factor, though its impact was less pronounced compared to the other variables (p< 0.05). The application of ultrasonic power causes cavitation, leading to the formation of microbubbles in the solvent. When these bubbles collapse, they create localized high temperatures and pressures, which rupture plant cells and enhance the release of intracellular

compounds such as phenolics. In this study, a sonication power of 400 W was found to be optimal for TPC recovery, as higher power levels increased the mechanical forces applied to the plant material, leading to greater cell wall disruption and enhanced extraction of phenolics. However, while higher sonication power improves extraction efficiency, it is important to control the power level to avoid excessive cavitation, affecting phenols (Chemat et al., 2017). This is supported by findings from Žlabur et al. (2021), which emphasize that higher sonication power levels can be beneficial, but only up to a certain threshold, beyond which compound degradation may occur.

In addition to the direct effects of sonication time, solid-to-liquid ratio, sonication power, and solvent concentration, quadratic terms for these parameters were found to be statistically significant, with p-values of less than 0.0001 for sonication time, solid-to-liquid ratio, and solvent concentration, and $p < 0.05$ for sonication power (table 4.12). The significance of these quadratic effects implies that moderate levels of these variables yield the best results and deviation from the optimal range could either decrease the extraction efficiency or degrade the phenolic compounds (Azmir et al., 2013). As shown in Table 4.12, interactions between independent variables were also critical for the recovery of TPC. For instance, the interaction between solid-to-liquid ratio and solvent concentration significantly influenced TPC recovery, as the combination of optimal levels of both factors allowed for greater solubilization and extraction of phenolics (fig. 4.21). Similarly, the interaction between sonication time and sonication power had a significant impact, indicating that higher power levels combined with optimal sonication time produced superior TPC yields. These results demonstrate the complex nature of the extraction process, where the combined effects of multiple variables play a crucial role in determining the final yield of bioactive compounds (Rodríguez De Luna et al., 2020).

The optimal conditions for TPC extraction were identified as 400 W sonication power, a solid-to-liquid ratio of 8 mg/100 mL, a sonication time of 13.8 minutes, and a solvent concentration of 50% ethanol. Under these conditions, the maximum TPC yield of 89.3 mg GAE/100g dry weight was achieved, demonstrating the efficacy of UAE in recovering phenolic compounds from banana peel. The findings suggest that optimizing extraction parameters is essential to maximize

phenolic recovery and that UAE is a highly effective method for extracting bioactive compounds (Chemat et al., 2017).



**Figure 4.21: Impact of different extraction parameters on total phenol content in banana peel extract**

**Table 4.12: Data of analysis of variance for total phenol content in banana peel extract**

| Source | Sum of Squares | df | Mean Square | F-value | p-value |
|---|---|---|---|---|---|
| Model | 13888.01 | 14 | 992.00 | 114.34 | < 0.0001 |
| A-Sonication time | 353.96 | 1 | 353.96 | 40.80 | < 0.0001 |
| B-Solid to liquid ratio | 1387.77 | 1 | 1387.77 | 159.96 | < 0.0001 |
| C-Sonication power | 111.40 | 1 | 111.40 | 12.84 | 0.0027 |
| D-Solvent concentration | 9568.98 | 1 | 9568.98 | 1102.96 | < 0.0001 |
| AB | 4.54 | 1 | 4.54 | 0.5229 | 0.4807 |
| AC | 20.93 | 1 | 20.93 | 2.41 | 0.1412 |
| AD | 24.65 | 1 | 24.65 | 2.84 | 0.1125 |
| BC | 265.53 | 1 | 265.53 | 30.61 | < 0.0001 |
| BD | 0.2352 | 1 | 0.2352 | 0.0271 | 0.8714 |
| CD | 91.39 | 1 | 91.39 | 10.53 | 0.0054 |
| A² | 61.25 | 1 | 61.25 | 7.06 | 0.0179 |
| B² | 227.61 | 1 | 227.61 | 26.24 | 0.0001 |
| C² | 6.08 | 1 | 6.08 | 0.7010 | 0.4156 |
| D² | 843.39 | 1 | 843.39 | 97.21 | < 0.0001 |
| Residual | 130.14 | 15 | 8.68 | | |
| Lack of Fit | 94.92 | 10 | 9.49 | 1.35 | 0.3905 |
| Pure Error | 35.22 | 5 | 7.04 | | |
| Cor Total | 14018.14 | 29 | | | |
| C.V. % | 4.55 | | | | |
| R² | 0.9907 | | | | |
| Adjusted R² | 0.9821 | | | | |
| Predicted R² | 0.9589 | | | | |
| Adeq Precision | 37.2194 | | | | |
| PRESS | 575.98 | | | | |

### 4.5.3 Effect of extraction parameters on dopamine in banana peel extract

The impact of various parameters of ultrasound-assisted extraction (UAE) on the yield of dopamine from BP was evaluated, and the findings are illustrated in Figure 4.22. The mathematical models used for dopamine yield were statistically significant (p < 0.0001), indicating a strong relationship between the extraction parameters and the recovery of dopamine content. Among the parameters studied, the solid-to-liquid ratio, sonication power, and concentration of solvent were having significant influence on dopamine yield (p < 0.0001), as shown in Table 4.13. Similar trends have been observed in studies on bioactive compound extraction using UAE,

which highlight the importance of these parameters in enhancing yield (Chemat et al., 2017; Zhou et al., 2017).

The extraction process revealed that an increase in the solids (BP) content in the solvent led to a corresponding increase in dopamine yield. This is likely due to a higher concentration of bioactive compounds available for extraction when more solid material is present in the solvent, as supported by findings in other plant-based extraction studies (Azmir et al., 2013). Additionally, increasing the sonication power from 200W to 400W also resulted in higher dopamine yields. The increased power likely generates greater shear forces, causing more disruption of the banana peel cell walls, which leads to the release of more intracellular compounds, including dopamine. Similar results have been documented in the extraction of phenolic compounds, where higher sonication power enhanced cell wall disruption and bioactive release (Ghafoor et al., 2009).

In terms of solvent concentration, a lower ethanol concentration facilitated a higher recovery of dopamine. Unlike the other parameters, sonication time did not significantly impact dopamine yield, suggesting that the time factor alone may not be critical within the studied range for extracting dopamine from banana peel. These findings are consistent with previous research indicating that sonication time has less influence on bioactive extraction compared to other parameters like sonication power and solvent composition (Chemat et al., 2017).

Significant interactions were also observed between the extraction parameters. Specifically, the interaction between solid-to-liquid ratio and sonication power, as well as solid-to-liquid ratio and solvent concentration, had a highly significant effect ($p < 0.0001$) on dopamine yield. These interactions were followed by the sonication time and sonication power combination, as well as the interaction between sonication power and solvent concentration, both of which were also significant ($p < 0.05$), indicating the complex nature of UAE processes (Chemat et al., 2017). These results underscore the importance of the combined effects of these variables in optimizing dopamine extraction. The range of extraction conditions studied included a solid-to-liquid ratio of 2 to 8 mg/100mL, sonication times between 5 and 15 minutes, sonication powers from 200W to 400W and solvent concentrations from 50% to

100%. Across all variables, dopamine yield generally increased; however, extended sonication time beyond optimal levels resulted in a noticeable decline in yield.

The optimal conditions for maximum dopamine (15.03 mg/100g) recovery were found to be 13.8 minutes of sonication time, a solid-to-liquid ratio of 8 mg/100mL, sonication power of 400W, and a solvent concentration of 50% ethanol. These results demonstrate that the choice of extraction conditions significantly affects dopamine recovery, with a strong dependence on factors such as sonication power, solvent concentration and the interaction between variables. Optimizing these parameters is crucial for achieving the highest possible yields of dopamine and other bioactive compounds from banana peel, which has potential applications in food, pharmaceutical and nutraceutical industries due to its bioactive properties (Chemat et al., 2017; Zhou et al., 2017; Azmir et al., 2013)

**Table 4.13:  Data on the analysis of variance for dopamine content in banana peel extract**

| Source | Sum of Squares | df | Mean Square | F-value | p-value |
|---|---|---|---|---|---|
| Model | 500.58 | 14 | 35.76 | 112.36 | < 0.0001 |
| A-Sonication time | 0.1531 | 1 | 0.1531 | 0.4811 | 0.4985 |
| B-Solid to liquid ratio | 419.63 | 1 | 419.63 | 1318.62 | < 0.0001 |
| C-Sonication power | 13.11 | 1 | 13.11 | 41.19 | < 0.0001 |
| D-Solvent concentration | 24.71 | 1 | 24.71 | 77.65 | < 0.0001 |
| AB | 0.0004 | 1 | 0.0004 | 0.0013 | 0.9722 |
| AC | 1.27 | 1 | 1.27 | 3.98 | 0.0646 |
| AD | 0.0256 | 1 | 0.0256 | 0.0804 | 0.7806 |
| BC | 11.97 | 1 | 11.97 | 37.62 | < 0.0001 |
| BD | 15.64 | 1 | 15.64 | 49.15 | < 0.0001 |
| CD | 1.17 | 1 | 1.17 | 3.67 | 0.0748 |
| $A^2$ | 5.10 | 1 | 5.10 | 16.02 | 0.0012 |
| $B^2$ | 0.2001 | 1 | 0.2001 | 0.6287 | 0.4402 |
| $C^2$ | 0.1657 | 1 | 0.1657 | 0.5207 | 0.4816 |
| $D^2$ | 11.12 | 1 | 11.12 | 34.96 | < 0.0001 |
| Residual | 4.77 | 15 | 0.3182 | | |
| Lack of Fit | 3.11 | 10 | 0.3106 | 0.9315 | 0.5700 |
| Pure Error | 1.67 | 5 | 0.3335 | | |
| Cor Total | 505.35 | 29 | | | |
| C.V. % | 7.73 | | | | |
| $R^2$ | 0.9906 | | | | |
| Adjusted $R^2$ | 0.9817 | | | | |
| Predicted $R^2$ | 0.9549 | | | | |
| Adeq Precision | 35.9973 | | | | |
| PRESS | 22.80 | | | | |

**Figure 4.22: Impact of different extraction parameters on dopamine content in banana peel extract**
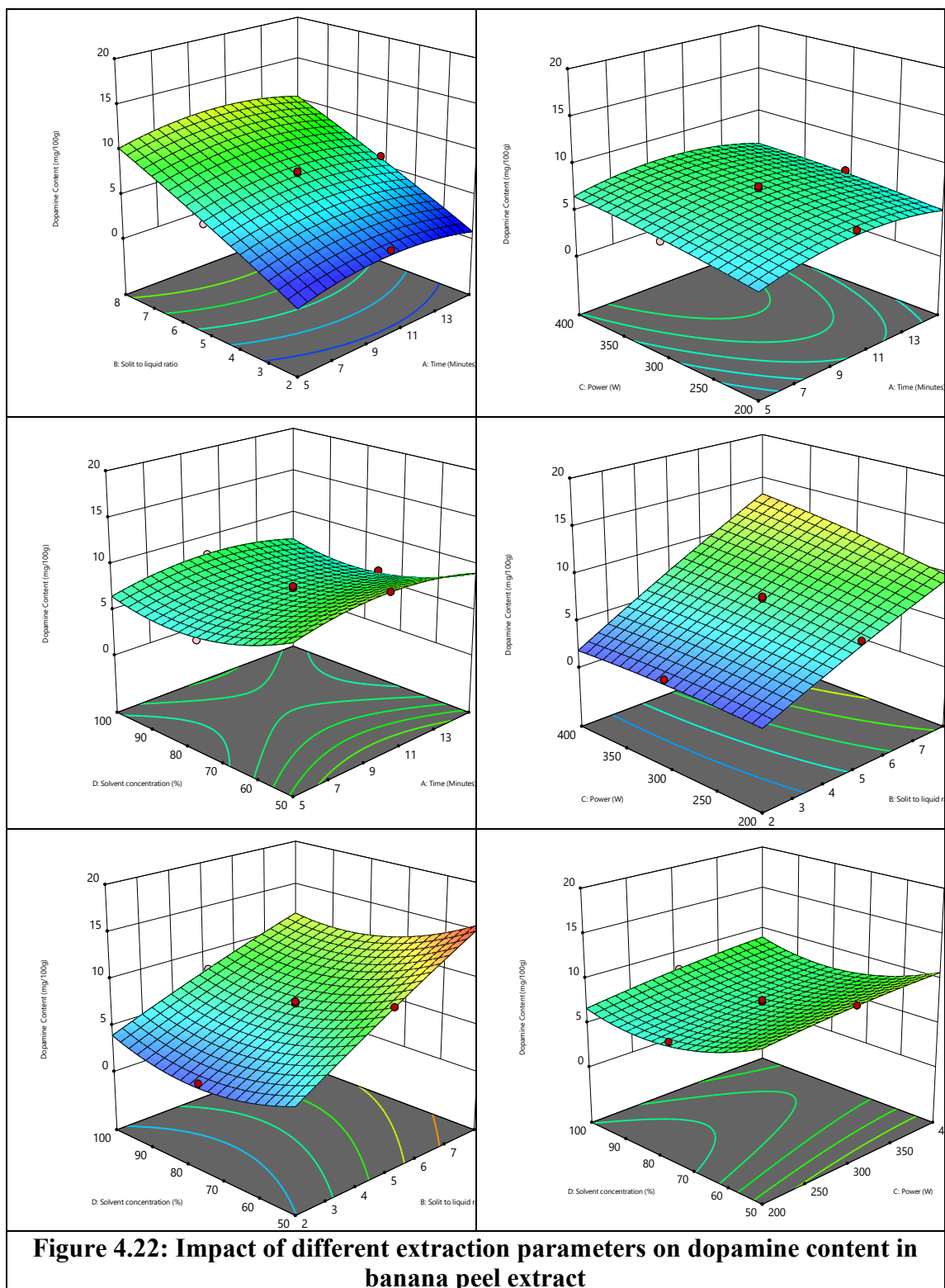
## 4.5.4 Effect of extraction parameters on L-dopa content in banana peel extract

Effect of different extraction parameters on the yield of L-dopa content illustrated in figure 4.23. The recovery of L-dopa from banana peel powder is strongly influenced by solvent concentration, with statistical analysis showing a highly significant effect ($p < 0.0001$) (table 4.14). This is in line with well-established principles of solvent extraction, where solvent polarity plays a crucial role in determining the efficiency of compound recovery. L-dopa, being a hydrophilic compound, is more effectively solubilized in ethanol-water mixtures with a higher water content. This is because water enhances the swelling of plant tissues, promoting better penetration of the solvent into the matrix and facilitating the release of intracellular bioactive compounds, including L-dopa (Li et al., 2020). This aligns with studies showing that ethanol concentrations around 50% v/v are particularly effective for polyphenol and amino acid extractions due to their balance between solubilizing both polar and non-polar compounds (Chemat et al., 2020). The solid-to-liquid ratio also showed a significant role in L-dopa yield ($p < 0.05$) (Table 4.14), which is expected as higher amounts of solid material increase the concentration of bioactive compounds available for extraction. However, there is a limit beyond which additional solid material does not contribute to increased recovery, as the solvent reaches its saturation point (Dahmoune et al., 2015). In this study, the optimal solid-to-liquid ratio was found to be 8 mg/100mL, which provided a balance between sufficient solid material and enough solvent to maintain high extraction efficiency. Interestingly, neither sonication time nor sonication power significantly affected L-dopa recovery, indicating that these parameters may not play as critical a role in the extraction of this particular compound from banana peel. This contrasts with findings for other bioactive compounds like total phenolic content, where sonication power often contributes to greater cell wall disruption and enhanced extraction (Rodrigues et al., 2020). It is possible that L-dopa, being a relatively small and easily solubilized molecule, does not require prolonged or intense sonication for effective extraction.

The interaction between the solid-to-liquid ratio and solvent concentration was found to have a significant effect ($p < 0.05$) on L-dopa yield, further underscoring the importance of optimizing these variables together. A well-balanced combination of a high solid-to-liquid ratio and an optimal solvent concentration maximizes the solubilization and recovery of L-dopa. However, other interaction terms, such as sonication time with sonication power or solvent concentration, did not show any

significant effects, suggesting that these variables are less critical for the extraction of L-dopa under the tested conditions. Under the optimal conditions of a solid-to-liquid ratio of 8 mg/100mL and a solvent concentration of 50% ethanol, the highest recovery of L-dopa from BP powder was 21.64 mg/100g dry weight.
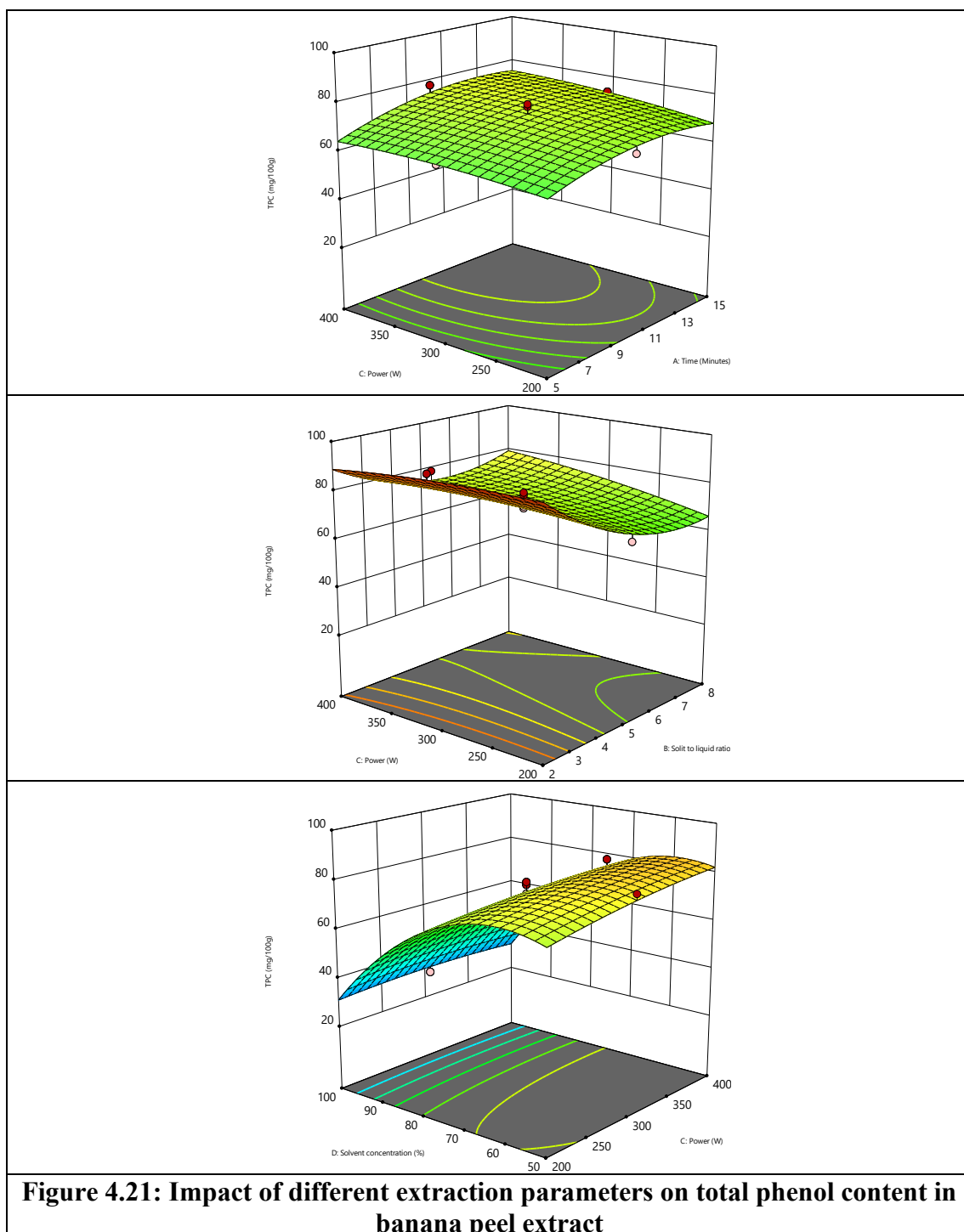
**Table 4.14: Data on analysis of variance for L-dopa content banana peel extract**

| Source | Sum of Squares | df | Mean Square | F-value | p-value |
|---|---|---|---|---|---|
| **Model** | 1626.12 | 14 | 116.15 | 13.51 | < 0.0001 |
| A-Sonication time | 3.90 | 1 | 3.90 | 0.4535 | 0.5109 |
| B-Solid to liquid ratio | 55.99 | 1 | 55.99 | 6.51 | 0.0221 |
| C-Sonication power | 0.3649 | 1 | 0.3649 | 0.0425 | 0.8395 |
| D-Solvent concentration | 939.86 | 1 | 939.86 | 109.34 | < 0.0001 |
| AB | 1.03 | 1 | 1.03 | 0.1203 | 0.7336 |
| AC | 0.6835 | 1 | 0.6835 | 0.0795 | 0.7818 |
| AD | 0.9935 | 1 | 0.9935 | 0.1156 | 0.7386 |
| BC | 1.62 | 1 | 1.62 | 0.1886 | 0.6703 |
| BD | 66.80 | 1 | 66.80 | 7.77 | 0.0138 |
| CD | 12.34 | 1 | 12.34 | 1.44 | 0.2494 |
| $A^2$ | 0.2013 | 1 | 0.2013 | 0.0234 | 0.8804 |
| $B^2$ | 21.29 | 1 | 21.29 | 2.48 | 0.1364 |
| $C^2$ | 0.1734 | 1 | 0.1734 | 0.0202 | 0.8889 |
| $D^2$ | 267.64 | 1 | 267.64 | 31.14 | < 0.0001 |
| Residual | 128.94 | 15 | 8.60 | | |
| Lack of Fit | 70.86 | 10 | 7.09 | 0.6101 | 0.7635 |
| Pure Error | 58.07 | 5 | 11.61 | | |
| Cor Total | 1755.05 | 29 | | | |
| C.V. % | 21.05 | | | | |
| $R^2$ | 0.9265 | | | | |
| Adjusted $R^2$ | 0.8580 | | | | |
| Predicted $R^2$ | 0.7897 | | | | |
| Adeq Precision | 10.6215 | | | | |
| PRESS | 369.02 | | | | |
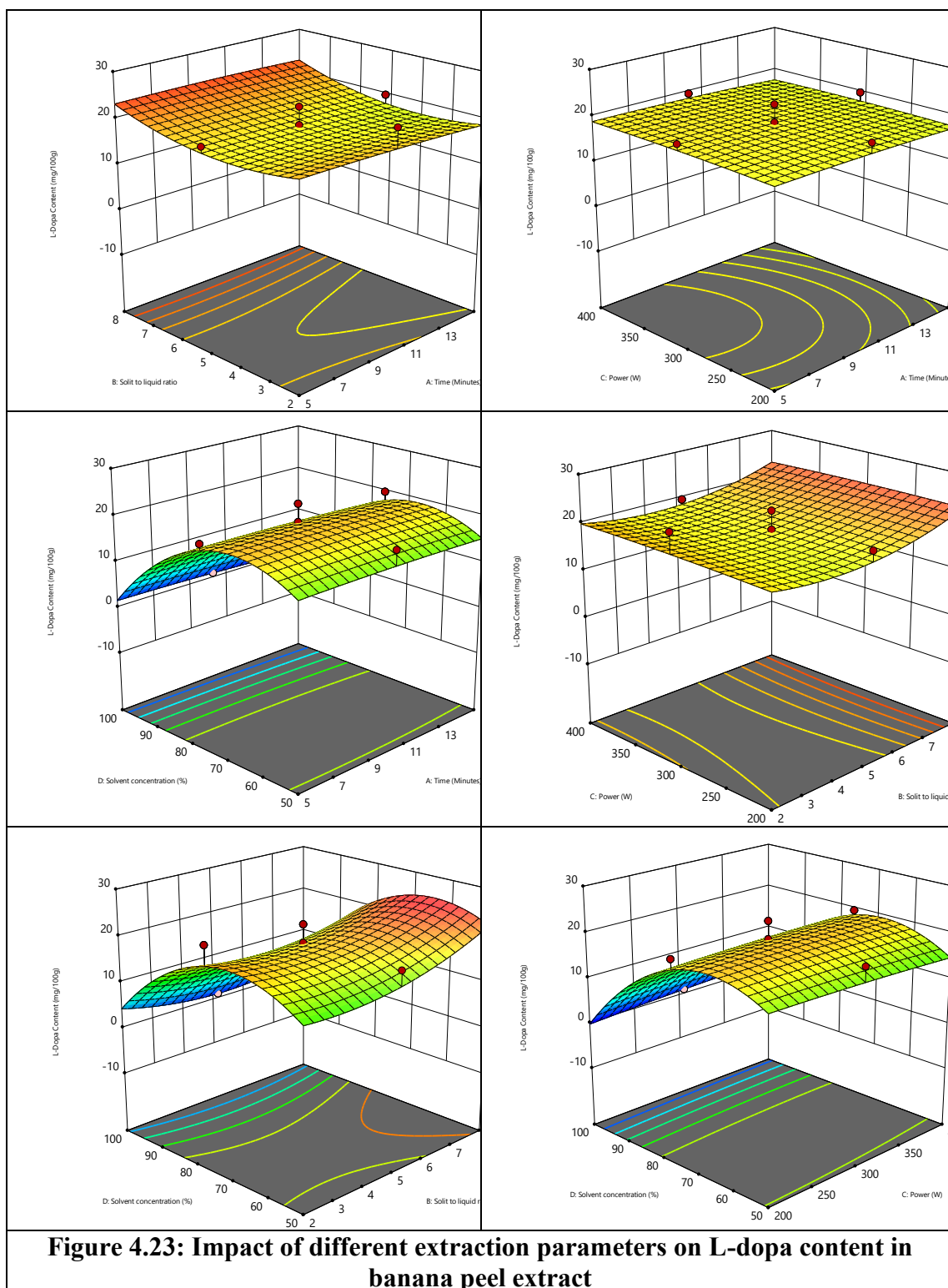
**Figure 4.23: Impact of different extraction parameters on L-dopa content in banana peel extract**

## 4.5.5 Effect of extraction parameters on L-tyrosine content in banana peel extract

The yield of L-tyrosine was significantly influenced by the solid-to-liquid ratio and solvent concentration, both of which were highly significant factors ($p < 0.0001$) (table 4.15). These two parameters demonstrated the greatest impact on the efficiency

of L-tyrosine extraction, suggesting that their optimization is crucial for maximizing yield. The solid-to-liquid ratio was shown to have a pronounced influence on L-tyrosine recovery ($p< 0.0001$). Increasing the solid-to-liquid ratio resulted in a higher concentration of plant material in the solvent, which enhanced the availability of L-tyrosine for extraction. However, as observed in other studies, maintaining an optimal balance is important to avoid saturation of the solvent and the associated decrease in extraction efficiency (Chemat et al., 2017). Solvent concentration, particularly the ethanol-to-water ratio, also played a critical role in L-tyrosine recovery. Ethanol is commonly used in phenolic compound extraction due to its polarity, which allows for greater solubilisation of both polar and non-polar compounds (Azmir et al., 2013). In this study, lower ethanol concentrations, particularly mixtures with higher water content, were more effective in extracting L-tyrosine, possibly due to the enhanced solubility of L-tyrosine in polar solvents (Sulaiman et al., 2011). The results are consistent with previous reports indicating that solvent polarity and composition can significantly influence the extraction efficiency of amino acids and phenolic compounds from plant matrices (Zhang et al., 2018). Sonication power, which generates ultrasonic waves that create cavitational forces within the solvent, was found to have a significant effect on the extraction of L-tyrosine ($p< 0.05$). Higher sonication power increases mechanical forces that rupture plant cell walls, leading to a more efficient release of intracellular compounds such as L-tyrosine (Altemimi et al., 2016). In this study, the application of higher sonication power (400 W) improved L-tyrosine recovery, likely due to the increased disruption of the banana peel matrix. Contrary to other parameters, sonication time did not have a significant independent effect on L-tyrosine extraction. This suggests that within the time range studied (5 to 15 minutes), the majority of L-tyrosine may have been released early in the process, and prolonged sonication did not substantially enhance recovery (Rodsamran and Sothornvit, 2019). Similar trends have been reported in previous studies on bioactive compound extraction, where extraction time was less critical than other factors such as power and solvent composition (Fatemeh et al., 2012).

Interactions between various extraction parameters were also analysed and significant interactions were observed (fig. 4.24). While sonication time alone did not show significant results, its interaction with sonication power revealed that the combination of higher power and optimal time improved extraction efficiency. This

may be due to the synergistic effect of prolonged exposure to ultrasonic waves combined with increased cavitation energy, which leads to more effective cell wall disruption and compound release (Pollini et al., 2020). Furthermore, the interaction between the solid-to-liquid ratio and solvent concentration also significantly influenced L-tyrosine recovery ($p < 0.05$). The optimal combination of these factors allowed for enhanced solubilization of L-tyrosine from the banana peel matrix, corroborating findings from previous studies that emphasize the importance of solvent composition in ultrasound-assisted extractions (Altemimi et al., 2016).

Under the optimal extraction conditions, which were determined to be a sonication time of 15 min., solid-to-liquid ratio of 8 mg/100 mL, sonication power of 400 W and a solvent concentration of 50% ethanol, the highest recovery of L-tyrosine was 21.64 mg/100 g dry weight from the banana peel powder.

**Table 4.15: Data on analysis of variance for L-tyrosine content in banana peel extract**

| L-tyrosine content | | | | | |
|---|---|---|---|---|---|
| **Source** | **Sum of Squares** | **df** | **Mean Square** | **F-value** | **p-value** |
| **Model** | 237.62 | 14 | 16.97 | 16.21 | < 0.0001 |
| A-Sonication time | 0.5796 | 1 | 0.5796 | 0.5536 | 0.4683 |
| B-Solid to liquid ratio | 34.78 | 1 | 34.78 | 33.22 | < 0.0001 |
| C-Sonication power | 8.85 | 1 | 8.85 | 8.45 | 0.0108 |
| D-Solvent concentration | 90.72 | 1 | 90.72 | 86.66 | < 0.0001 |
| AB | 1.11 | 1 | 1.11 | 1.06 | 0.3199 |
| AC | 31.89 | 1 | 31.89 | 30.47 | < 0.0001 |
| AD | 5.99 | 1 | 5.99 | 5.72 | 0.0303 |
| BC | 1.46 | 1 | 1.46 | 1.39 | 0.2563 |
| BD | 11.95 | 1 | 11.95 | 11.42 | 0.0041 |
| CD | 0.0095 | 1 | 0.0095 | 0.0091 | 0.9253 |
| $A^2$ | 2.67 | 1 | 2.67 | 2.55 | 0.1312 |
| $B^2$ | 11.75 | 1 | 11.75 | 11.23 | 0.0044 |
| $C^2$ | 10.47 | 1 | 10.47 | 10.00 | 0.0064 |
| $D^2$ | 3.70 | 1 | 3.70 | 3.53 | 0.0797 |
| Residual | 15.70 | 15 | 1.05 | | |
| Lack of Fit | 8.24 | 10 | 0.8244 | 0.5526 | 0.8014 |
| Pure Error | 7.46 | 5 | 1.49 | | |
| Cor Total | 253.33 | 29 | | | |
| C.V. % | 10.48 | | | | |
| $R^2$ | 0.9380 | | | | |
| Adjusted $R^2$ | 0.8802 | | | | |
| Predicted $R^2$ | 0.7493 | | | | |
| Adeq Precision | 18.3083 | | | | |

| PRESS | 63.52 | | | | |
|---|---|---|---|---|---|



**Figure 4.24: Impact of different extraction parameters on L-tyrosine content in banana peel extract**
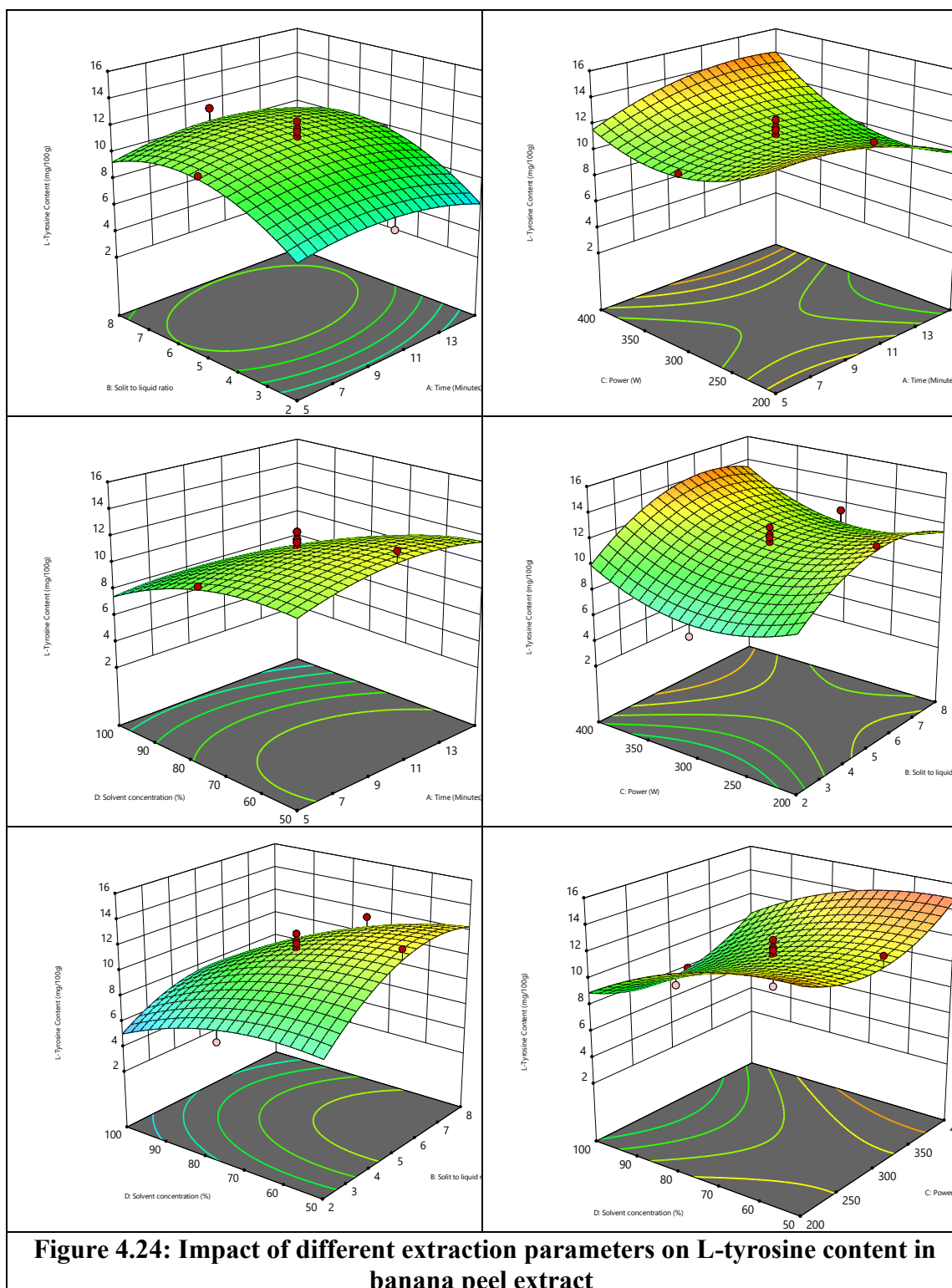
## 4.5.6 Optimization and validation of the models

The ideal extraction conditions were found to be a sonication time of 13.8 minutes, a solid-to-liquid ratio of 8 mg/100 mL, an ultrasonic power of 400W and a solvent concentration of 50% ethanol. The predicted and actual extraction yields, presented in Table 4.16, showed no statistically significant differences, validating the RSM models and extraction parameters.

Under these optimal conditions, the banana peel yielded 88.95 mg GAE/100g of total phenolics, 16.20 mg/100g of dopamine, 20.76 mg/100g of L-DOPA and 16.34 mg/100g of L-tyrosine. The extracted phenolic content falls within the range reported by previous studies, such as those by Sulaiman et al. (2011) and Fatemeh et al. (2012), who found TPC levels ranging from 0.78 to 76.37 mg GAE/g DW. While the TPC from banana peel was slightly lower than that reported for pomegranate peel (91.98 mg GAE/g DW) and pear pomace (41 mg GAE/g DW), it still demonstrates banana peel's effectiveness as a competitive source of phenolic compounds.
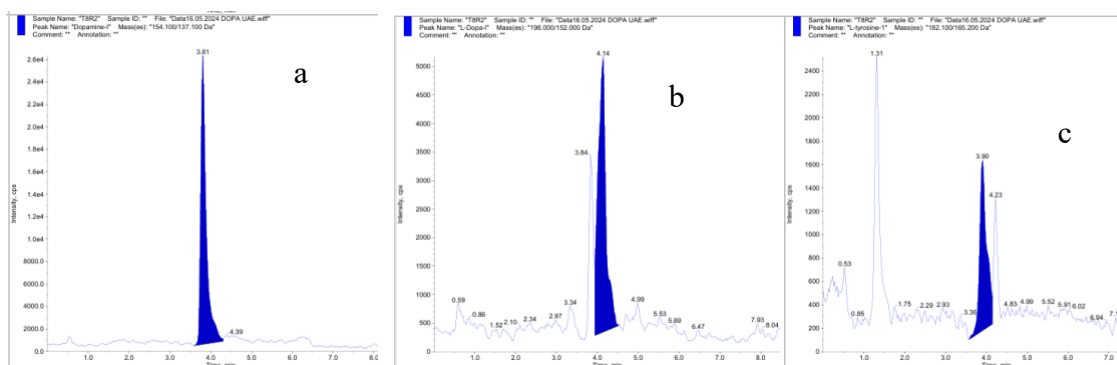


**Figure 4.25: XIC of dopamine (a), L-dopa (b) and L-tyrosine (c) in banana peel extract of optimal conditions**

**Table 4.16: Validation of the predicted values for TPC, dopamine content, L-dopa content and L-tyrosine content in banana peel extract**

| Responses | Predicted value | Actual value |
|---|---|---|
| TPC (mg GAE/100g) | 88.96±2.95 | 89.3±0.77 |
| Dopamine content (mg/100g) | 16.20±0.56 | 15.60±0.06 |
| L-dopa content (mg/100g) | 20.76±2.85 | 21.84±0.32 |
| L-tyrosine content (mg/100g) | 16.34±1.02 | 14.81±0.66 |

## 4.6 Encapsulation of banana peel extract with grape pomace

### 4.6.1 Model Fitting and Optimization

As presented in table 4.17 the responses were recorded for all treatments developed for optimisation using face centred central composite design. The quadratic model for encapsulation efficiency showed a high coefficient of determination ($R^2$=0.9674), indicating that 96.74% of the variation in encapsulation efficiency could be explained by the model. The adjusted $R^2$ value of 0.9370 confirmed the robustness of the model, accounting for the number of predictors used. The predicted $R^2$ of 0.8699 demonstrated good predictive ability, meaning the model was reliable for optimizing encapsulation efficiency under different conditions (table 4.18). The adequate precision value of 25.2963 was well above the threshold of 4, indicating a strong signal-to-noise ratio. The quadratic model for yield was similarly robust, with an $R^2$ of 0.9639 and an adjusted $R^2$ of 0.9301 (4.19). The adequate precision of 21.5834 further validated the model's strong signal, while the predicted $R^2$ of 0.8239 confirmed its predictive capability. These results suggest that the model provides a reliable basis for optimizing yield by adjusting the spray drying parameters (Bhandari et al., 1997). The moisture content model had an $R^2$ value of 0.9767 and an adjusted $R^2$ of 0.9550, showing that 97.67% of the variability in moisture content was explained by the model (table 4.20). The adequate precision value of 29.5285 indicated that the model provided a strong and reliable signal for optimization. A predicted $R^2$ of 0.8674 demonstrated good predictive performance, meaning the model can accurately forecast moisture levels based on different drying conditions (Tonon et al., 2008).

The model for dopamine content had an $R^2$ of 0.9190 and an adjusted $R^2$ of 0.8433, indicating that 91.9% of the variability could be explained by the model (table 4.21). The adequate precision value of 13.9122 suggested a good signal-to-noise ratio, and the predicted $R^2$ of 0.7140 indicated reasonable predictive accuracy. The model for L-dopa content showed a high $R^2$ of 0.9638 and an adjusted $R^2$ of 0.9300, confirming that 96.38% of the variation in L-dopa retention was captured by the model (table 4.22). The adequate precision value of 20.1707 indicated that the model provided a strong basis for optimization, while the predicted $R^2$ of 0.8103 showed good forecasting power. The model for L-tyrosine content had an $R^2$ value of 0.9264 and an adjusted $R^2$ of 0.8577. With an adequate precision of 17.5550 and a predicted $R^2$ of 0.6958, the model was reliable for optimizing the conditions to retain L-tyrosine during spray drying (table 4.23).

**Table 4.17: Face centred central composite design and recorded responses**

| Std | A: Inlet air temperature (°C) | B: Pomace to maltodextrin ratio | C: Wall to core material ratio | D: Aspirator flow rate (Nm³/hr) | Encapsulation efficiency (%) | Yield (%) | Moisture (%) | Dopamine content (mg/100g) | L-dopa content (mg/100g) | L-tyrosine content (mg/100g) |
|---|---|---|---|---|---|---|---|---|---|---|
| 1 | 180 | 5 | 1 | 80 | 27.23 | 39.97 | 8.37 | 90.46 | 589.0 | 1510.0 |
| 2 | 220 | 5 | 1 | 80 | 31.14 | 43.25 | 10.28 | 83.95 | 437.0 | 1150.0 |
| 3 | 180 | 30 | 1 | 80 | 32.69 | 35.77 | 10.90 | 58.40 | 336.5 | 1855.0 |
| 4 | 220 | 30 | 1 | 80 | 28.99 | 32.00 | 9.90 | 78.90 | 274.0 | 1275.0 |
| 5 | 180 | 5 | 5 | 80 | 18.92 | 44.03 | 8.68 | 32.56 | 261.0 | 761.5 |
| 6 | 220 | 5 | 5 | 80 | 21.59 | 44.82 | 10.00 | 26.05 | 273.0 | 1270.0 |
| 7 | 180 | 30 | 5 | 80 | 33.67 | 39.82 | 10.03 | 14.45 | 197.5 | 1285.0 |
| 8 | 220 | 30 | 5 | 80 | 21.01 | 28.62 | 9.33 | 64.30 | 218.0 | 1420.0 |
| 9 | 180 | 5 | 1 | 100 | 6.416 | 31.43 | 7.06 | 66.05 | 529.5 | 1180.0 |
| 10 | 220 | 5 | 1 | 100 | 19.47 | 43.69 | 10.78 | 22.10 | 487.0 | 1315.0 |
| 11 | 180 | 30 | 1 | 100 | 18.45 | 35.58 | 9.64 | 45.05 | 362.5 | 1373.0 |
| 12 | 220 | 30 | 1 | 100 | 17.62 | 33.46 | 9.77 | 25.90 | 318.0 | 1455.0 |
| 13 | 180 | 5 | 5 | 100 | 18.13 | 41.75 | 6.96 | 63.25 | 252.5 | 997.5 |
| 14 | 220 | 5 | 5 | 100 | 25.35 | 50.78 | 8.90 | 20.65 | 303.0 | 1475.0 |
| 15 | 180 | 30 | 5 | 100 | 32.26 | 43.85 | 8.29 | 54.85 | 203.0 | 1310.0 |
| 16 | 220 | 30 | 5 | 100 | 30.1 | 37.92 | 7.44 | 65.29 | 209.5 | 1564.5 |
| 17 | 180 | 17.5 | 3 | 90 | 22.14 | 44.33 | 10.26 | 40.40 | 276.5 | 1045.0 |
| 18 | 220 | 17.5 | 3 | 90 | 22.17 | 45.72 | 11.06 | 38.85 | 266.5 | 1325.0 |
| 19 | 200 | 5 | 3 | 90 | 22.19 | 43.45 | 8.12 | 66.80 | 302.0 | 2295.0 |
| 20 | 200 | 30 | 3 | 90 | 27.20 | 38.30 | 8.39 | 67.65 | 258.0 | 2655.0 |
| 21 | 200 | 17.5 | 1 | 90 | 28.16 | 43.10 | 9.19 | 66.90 | 376.0 | 818.0 |
| 22 | 200 | 17.5 | 5 | 90 | 31.60 | 44.45 | 8.35 | 47.95 | 222.0 | 799.5 |
| 23 | 200 | 17.5 | 3 | 80 | 21.15 | 31.32 | 12.55 | 53.85 | 274.5 | 1008.0 |
| 24 | 200 | 17.5 | 3 | 100 | 14.94 | 34.18 | 11.75 | 23.40 | 264.0 | 1210.0 |
| 25 | 200 | 17.5 | 3 | 90 | 26.11 | 40.37 | 10.23 | 58.15 | 243.0 | 1095.0 |
| 26 | 200 | 17.5 | 3 | 90 | 26.53 | 43.52 | 10.82 | 48.80 | 265.0 | 1292.0 |
| 27 | 200 | 17.5 | 3 | 90 | 26.07 | 42.12 | 10.00 | 30.25 | 292.0 | 1189.0 |
| 28 | 200 | 17.5 | 3 | 90 | 25.96 | 43.37 | 10.34 | 49.10 | 247.5 | 1243.0 |
| 29 | 200 | 17.5 | 3 | 90 | 21.85 | 42.73 | 10.10 | 51.10 | 254.5 | 1007.5 |
| 30 | 200 | 17.5 | 3 | 90 | 25.07 | 42.66 | 10.12 | 58.00 | 289.5 | 1325.0 |

## 4.6.2 Encapsulation efficiency

Table 4.18 gives detailed insights on the effect of different encapsulation parameters on the encapsulation efficiency of encapsulated powder. Encapsulation efficiency was significantly influenced by the, wall-to-core material ratio, pomace-to-maltodextrin ratio and aspirator flow rate, all with p-values < 0.0001. The quadratic

effects of these variables were also significant, demonstrating that precise control over these parameters is crucial for maximizing encapsulation efficiency. The highest encapsulation efficiency (33.67%) was obtained at a pomace-to-maltodextrin ratio of 30:1, 180°C inlet air temperature, and a 5:1 wall-to-core material ratio. These results are consistent with previous studies showing that higher maltodextrin concentrations enhance encapsulation by providing a larger surface area for wall material formation (Gharsallaoui et al., 2007). The aspirator flow rate played a particularly important role, as higher flow rates ensured better atomization of the feed mixture, leading to more uniform particle formation and improved encapsulation efficiency. This observation is in line with studies demonstrating that higher aspirator rates improve the encapsulation of heat-sensitive bioactive compounds, such as phenolics and flavonoids, during spray drying (Caliskan & Dirim, 2016).

Significant interactions between the parameters were observed for encapsulation efficiency as shown in figure 4.26. The interaction between aspirator flow rate and inlet air temperature (p < 0.0001) had a major effect on encapsulation efficiency, indicating that higher temperatures combined with an optimal aspirator flow rate enhance atomization and encapsulation. Higher inlet air temperatures speed up drying, while the aspirator flow rate ensures uniform droplet formation, leading to better encapsulation. These results align with studies that suggest faster drying and uniform particle formation improve the efficiency of spray-dried powders (Tonon et al., 2008). The interaction between pomace-to-maltodextrin ratio and wall material ratio (p < 0.0001) also significantly impacted encapsulation efficiency. Increasing the wall material (maltodextrin) relative to the core material (grape pomace) improves the protective coating around bioactive compounds, enhancing encapsulation. Similar findings by Fernandes et al. (2017) suggest that higher concentrations of wall material improve microencapsulation by forming a robust matrix that reduces bioactive compound degradation.

**Table 4.18: Data on analysis of variance for encapsulation efficiency of TPC**

| Source | Sum of Squares | df | Mean Square | F-value | p-value |
|---|---|---|---|---|---|
| **Model** | 1015.07 | 14 | 72.51 | 31.83 | < 0.0001 |
| A-Inlet air temperature | 3.21 | 1 | 3.21 | 1.41 | 0.2540 |

| | | | | | |
|---|---|---|---|---|---|
| B-Pomace to maltodextrin ratio | 148.11 | 1 | 148.11 | 65.02 | < 0.0001 |
| C-wall to core material ratio | 28.17 | 1 | 28.17 | 12.37 | 0.0031 |
| D-aspirator flow rate | 159.68 | 1 | 159.68 | 70.10 | < 0.0001 |
| AB | 133.09 | 1 | 133.09 | 58.42 | < 0.0001 |
| AC | 18.72 | 1 | 18.72 | 8.22 | 0.0118 |
| AD | 45.91 | 1 | 45.91 | 20.15 | 0.0004 |
| BC | 24.02 | 1 | 24.02 | 10.55 | 0.0054 |
| BD | 8.50 | 1 | 8.50 | 3.73 | 0.0725 |
| CD | 295.69 | 1 | 295.69 | 129.81 | < 0.0001 |
| A² | 7.61 | 1 | 7.61 | 3.34 | 0.0875 |
| B² | 1.75 | 1 | 1.75 | 0.7689 | 0.3944 |
| C² | 93.53 | 1 | 93.53 | 41.06 | < 0.0001 |
| D² | 87.98 | 1 | 87.98 | 38.62 | < 0.0001 |
| Residual | 34.17 | 15 | 2.28 | | |
| Lack of Fit | 19.04 | 10 | 1.90 | 0.6289 | 0.7512 |
| Pure Error | 15.13 | 5 | 3.03 | | |
| Cor Total | 1049.24 | 29 | | | |
| Std. Dev. | 1.51 | | | | |
| Mean | 24.14 | | | | |
| C.V. % | 6.25 | | | | |
| R² | 0.9674 | | | | |
| Adjusted R² | 0.9370 | | | | |
| Predicted R² | 0.8699 | | | | |
| Adeq Precision | 25.2963 | | | | |

**Figure 4.26: Effect of interaction between different encapsulation variables on encapsulation efficiency of TPC**
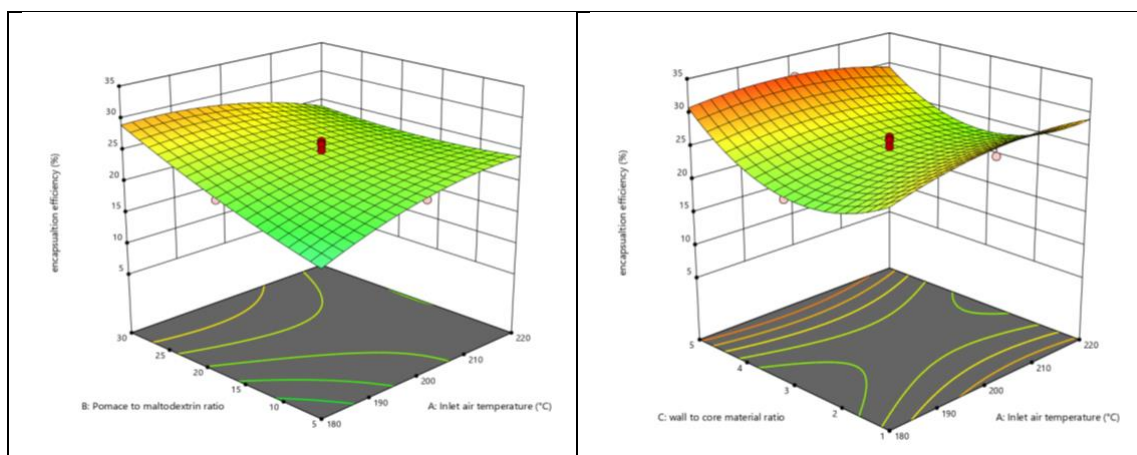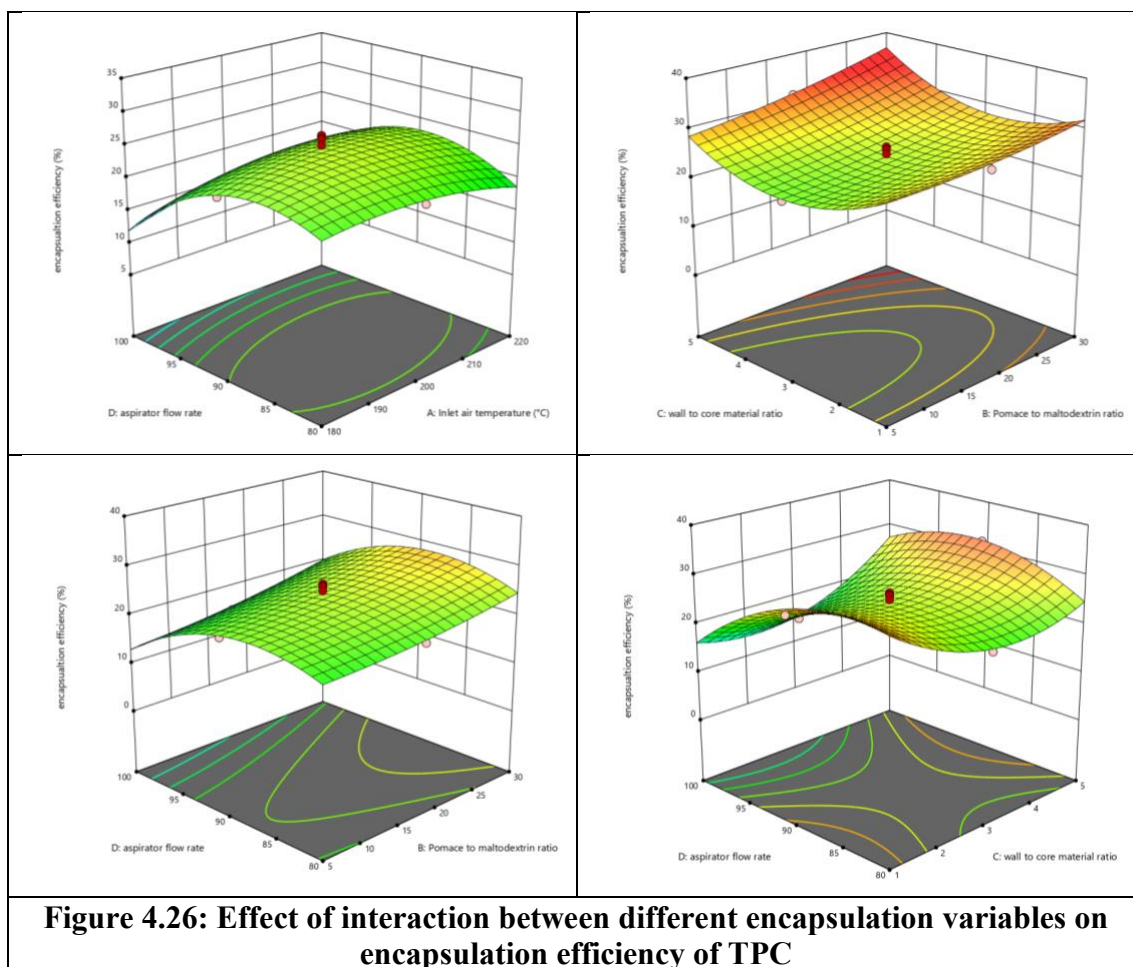
### 4.6.3 Encapsulation yield

Table 4.19 gives detailed insights on the effect different encapsulation parameters on the encapsulation yield in encapsulated powder. The yield of the encapsulated powder was strongly affected by the wall-to-core material ratio, pomace-to-maltodextrin ratio and aspirator flow rate. The highest yield (50.78%) was observed at a 5:1 wall-to-core material ratio and 220°C inlet air temperature. The aspirator flow rate, although statistically significant, showed a less pronounced effect on yield compared to the wall-to-core ratio and pomace-to-maltodextrin ratio, indicating that the overall powder recovery is more influenced by the composition of the feed rather than the drying conditions (Jafari et al., 2017).

Significant interactions between the parameters were observed for encapsulation yield as shown in figure 4.27. The yield of powder was significantly influenced by the interaction between pomace-to-maltodextrin ratio and wall material ratio. The yield increased with a higher maltodextrin concentration, which facilitated

the formation of a stable wall structure, improving powder recovery. The interaction between inlet air temperature and aspirator flow rate also significantly affected the yield, with higher air temperatures coupled with optimized aspirator flow rates increasing the drying rate and reducing powder loss, in agreement with the findings of Jafari et al. (2017).

**Table 4.19: Data on analysis of variance for encapsulation yield**

| Source | Sum of Squares | df | Mean Square | F-value | p-value |
|---|---|---|---|---|---|
| **Model** | 767.05 | 14 | 54.79 | 28.58 | < 0.0001 |
| A-Inlet air temperature | 0.7710 | 1 | 0.7710 | 0.4021 | 0.5355 |
| B-Pomace to maltodextrin ratio | 185.98 | 1 | 185.98 | 97.01 | < 0.0001 |
| C-wall to core material ratio | 79.28 | 1 | 79.28 | 41.35 | < 0.0001 |
| D-aspirator flow rate | 9.50 | 1 | 9.50 | 4.95 | 0.0418 |
| AB | 146.26 | 1 | 146.26 | 76.29 | < 0.0001 |
| AC | 18.01 | 1 | 18.01 | 9.39 | 0.0079 |
| AD | 36.43 | 1 | 36.43 | 19.00 | 0.0006 |
| BC | 5.83 | 1 | 5.83 | 3.04 | 0.1016 |
| BD | 22.62 | 1 | 22.62 | 11.80 | 0.0037 |
| CD | 35.48 | 1 | 35.48 | 18.51 | 0.0006 |
| A² | 35.91 | 1 | 35.91 | 18.73 | 0.0006 |
| B² | 0.4731 | 1 | 0.4731 | 0.2468 | 0.6265 |
| C² | 15.84 | 1 | 15.84 | 8.26 | 0.0116 |
| D² | 189.51 | 1 | 189.51 | 98.85 | < 0.0001 |
| Residual | 28.76 | 15 | 1.92 | | |
| Lack of Fit | 22.19 | 10 | 2.22 | 1.69 | 0.2925 |
| Pure Error | 6.56 | 5 | 1.31 | | |
| Cor Total | 795.81 | 29 | | | |
| Std. Dev. | 1.38 | | | | |
| Mean | 40.21 | | | | |
| C.V. % | 3.44 | | | | |
| R² | 0.9639 | | | | |
| Adjusted R² | 0.9301 | | | | |
| Predicted R² | 0.8239 | | | | |
| Adeq Precision | 21.5834 | | | | |
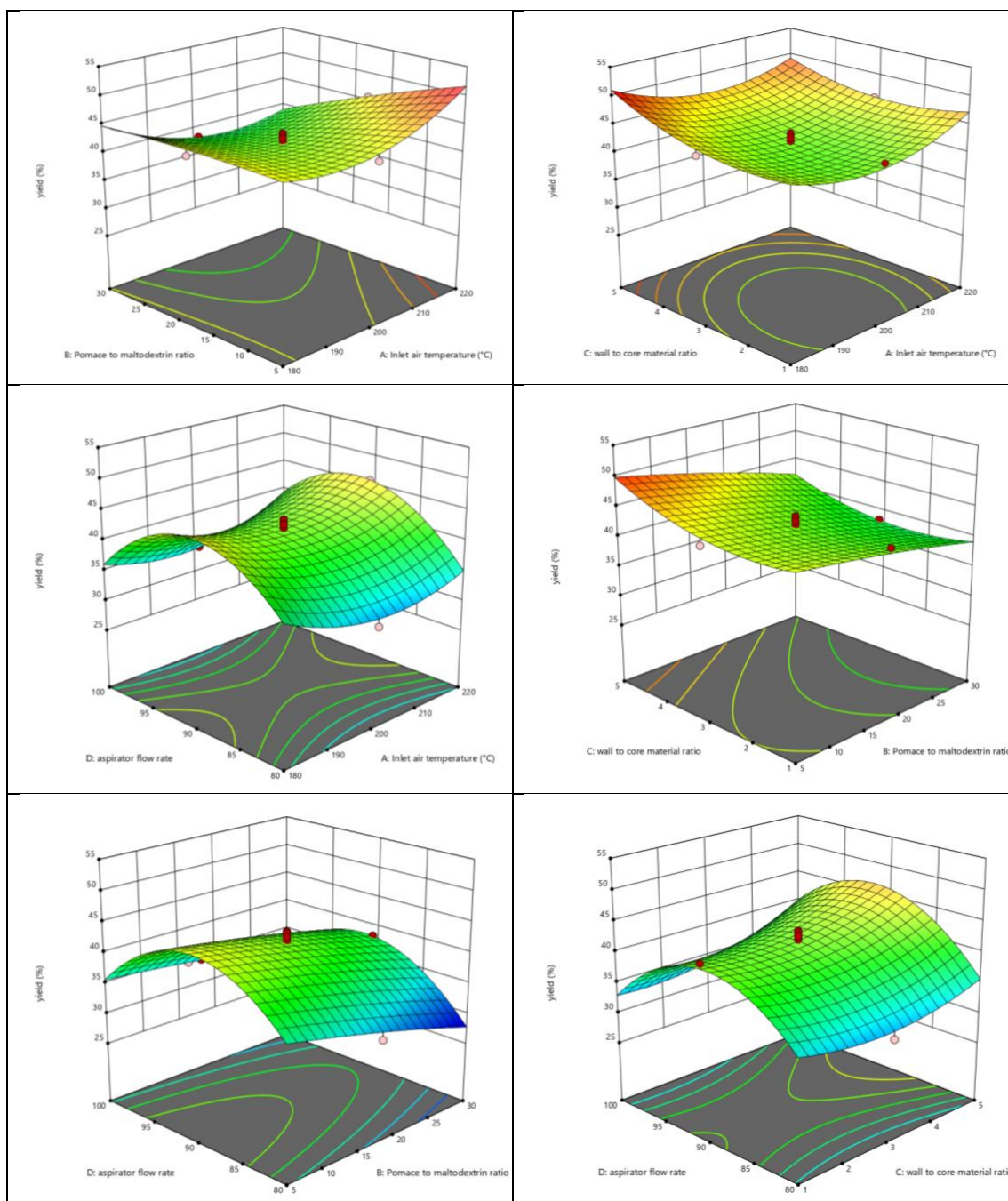
**Figure 4.27: Effect of interaction between different encapsulation variables on encapsulation yield**

## 4.6.4 Moisture of encapsulated powder

Table 4.20 gives detailed insights on the effect different encapsulation parameters on the moisture in encapsulated powder. Powder moisture was between 6.96% to 12.55%, with inlet air temperature (p < 0.0001), pomace-to-maltodextrin ratio (p = 0.0018) and aspirator flow rate (p < 0.0001) being significant factors. The lowest moisture content (6.96%) was recorded at a 5:1 pomace-to-maltodextrin ratio

and 100 Nm³/hr aspirator flow rate. Lower moisture content is desirable for increased shelf life and stability of the encapsulated powder, as it minimizes microbial growth and oxidation of bioactive compounds (Bhandari et al., 1997).  Higher temperatures and aspirator flow rates resulted in more effective water evaporation, leading to lower moisture content, a finding that aligns with previous studies showing that optimal drying parameters improve the drying efficiency in spray-dried powders (Tonon et al., 2008). This finding is consistent with research showing that a higher air temperature increases the rate of drying, which reduces moisture content and leads to more stable powders (Bhandari et al., 1997).

Significant interactions between the parameters were observed for moisture as shown in figure 4.28. The interaction between pomace-to-maltodextrin ratio and wall material ratio (p < 0.05) also played a significant role in moisture content, where a higher maltodextrin concentration decreased moisture levels due to the hygroscopic nature of maltodextrin, which absorbs water and reduces the residual moisture in the final powder.

**Table 4.20: Data on analysis of variance for moisture of encapsulated powder**

| Source | Sum of Squares | df | Mean Square | F-value | p-value |
|---|---|---|---|---|---|
| **Model** | 49.95 | 14 | 3.57 | 44.98 | < 0.0001 |
| A-Inlet air temperature | 2.94 | 1 | 2.94 | 37.07 | < 0.0001 |
| B-Pomace to maltodextrin ratio | 1.14 | 1 | 1.14 | 14.33 | 0.0018 |
| C-wall to core material ratio | 3.47 | 1 | 3.47 | 43.74 | < 0.0001 |
| D-aspirator flow rate | 4.95 | 1 | 4.95 | 62.47 | < 0.0001 |
| AB | 7.98 | 1 | 7.98 | 100.62 | < 0.0001 |
| AC | 0.5806 | 1 | 0.5806 | 7.32 | 0.0163 |
| AD | 0.7349 | 1 | 0.7349 | 9.27 | 0.0082 |
| BC | 0.6336 | 1 | 0.6336 | 7.99 | 0.0128 |
| BD | 0.1199 | 1 | 0.1199 | 1.51 | 0.2378 |
| CD | 1.13 | 1 | 1.13 | 14.29 | 0.0018 |
| A² | 0.4641 | 1 | 0.4641 | 5.85 | 0.0287 |
| B² | 10.16 | 1 | 10.16 | 128.10 | < 0.0001 |
| C² | 5.59 | 1 | 5.59 | 70.47 | < 0.0001 |
| D² | 9.51 | 1 | 9.51 | 119.89 | < 0.0001 |
| Residual | 1.19 | 15 | 0.0793 | | |
| Lack of Fit | 0.7652 | 10 | 0.0765 | 0.9014 | 0.5862 |
| Pure Error | 0.4245 | 5 | 0.0849 | | |

| Cor Total | 51.14 | 29 | | | |
|---|---|---|---|---|---|
| Std. Dev. | 0.2816 | | | | |
| Mean | 9.59 | | | | |
| C.V. % | 2.94 | | | | |
| R² | 0.9767 | | | | |
| Adjusted R² | 0.9550 | | | | |
| Predicted R² | 0.8674 | | | | |
| Adeq Precision | 29.5285 | | | | |
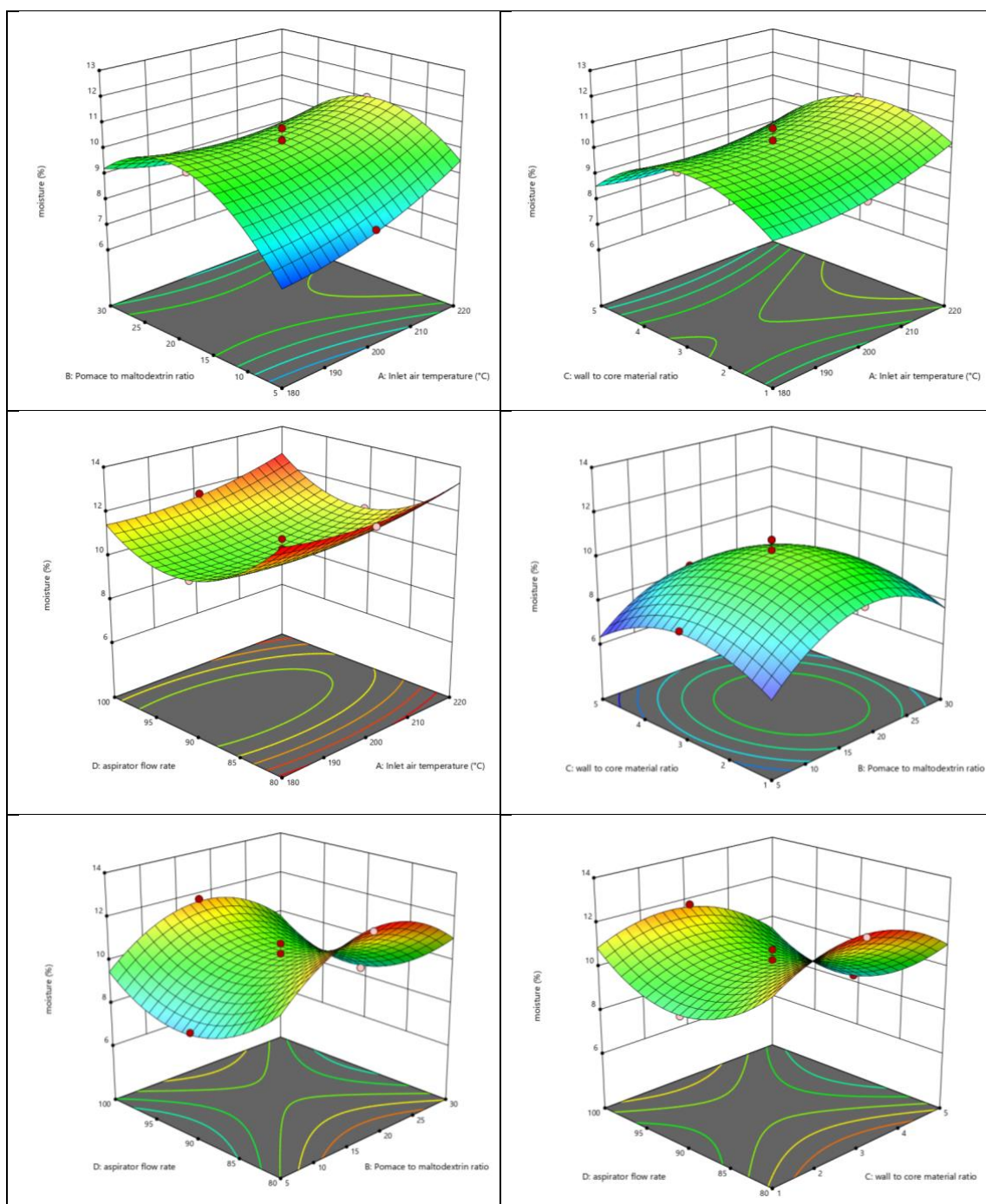


**Figure 4.28: Effect of interaction between different encapsulation variables on moisture in encapsulated powder**

### 4.6.5 Dopamine Content

Table 4.21 gives detailed insights on the effect different encapsulation parameters on the dopamine content in encapsulated powder. The dopamine content was significantly affected by the wall material ratio and aspirator flow rate. The interaction between the pomace-to-maltodextrin ratio and wall material ratio ($p < 0.0001$) was particularly impactful. This suggests that the grape pomace provided effective protection for dopamine during the spray drying process, as phenolic-rich materials are known to stabilize sensitive compounds (Caliskan & Dirim, 2016).

Significant interactions between the parameters were observed for dopamine content as shown in figure 4.29. The interaction between pomace-to-maltodextrin ratio and wall material ratio ($p < 0.0001$) significantly affected the retention of bioactive compounds such as dopamine, L-DOPA and L-tyrosine. Higher maltodextrin concentrations provided better protection against degradation during spray drying by forming a stronger encapsulation matrix, which was critical for stabilizing sensitive compounds like dopamine. The interaction between wall material and inlet air temperature ratio also impacted dopamine content ($p=0.0004$), with moderate temperatures (180-200°C) and higher maltodextrin concentrations preserving higher dopamine levels. Excessive temperatures, however, can degrade bioactive compounds, suggesting that moderate heat combined with an appropriate wall material is essential for stabilizing thermolabile compounds during spray drying (Gharsallaoui et al., 2007).

**Table 4.21: Data on analysis of variance for moisture of dopamine content in encapsulated powder**

| Source | Sum of Squares | df | Mean Square | F-value | p-value |
|---|---|---|---|---|---|
| **Model** | 10400.42 | 14 | 742.89 | 12.15 | < 0.0001 |
| A-Inlet air temperature | 86.59 | 1 | 86.59 | 1.42 | 0.2525 |
| B-Pomace to maltodextrin ratio | 0.4737 | 1 | 0.4737 | 0.0077 | 0.9310 |
| C-wall to core material ratio | 1222.82 | 1 | 1222.82 | 20.00 | 0.0004 |
| D-aspirator flow rate | 752.46 | 1 | 752.46 | 12.31 | 0.0032 |
| AB | 1624.29 | 1 | 1624.29 | 26.57 | 0.0001 |
| AC | 227.18 | 1 | 227.18 | 3.72 | 0.0730 |
| AD | 1455.23 | 1 | 1455.23 | 23.80 | 0.0002 |

| | | | | | |
|---|---|---|---|---|---|
| BC | 765.77 | 1 | 765.77 | 12.53 | 0.0030 |
| BD | 81.05 | 1 | 81.05 | 1.33 | 0.2676 |
| CD | 3005.51 | 1 | 3005.51 | 49.16 | < 0.0001 |
| A² | 305.22 | 1 | 305.22 | 4.99 | 0.0411 |
| B² | 726.58 | 1 | 726.58 | 11.88 | 0.0036 |
| C² | 125.01 | 1 | 125.01 | 2.04 | 0.1732 |
| D² | 364.05 | 1 | 364.05 | 5.95 | 0.0276 |
| Residual | 917.02 | 15 | 61.13 | | |
| Lack of Fit | 396.61 | 10 | 39.66 | 0.3810 | 0.9089 |
| Pure Error | 520.42 | 5 | 104.08 | | |
| Cor Total | 11317.44 | 29 | | | |
| Std. Dev. | 7.82 | | | | |
| Mean | 50.45 | | | | |
| C.V. % | 15.50 | | | | |
| R² | 0.9190 | | | | |
| Adjusted R² | 0.8433 | | | | |
| Predicted R² | 0.7140 | | | | |
| Adeq Precision | 13.9122 | | | | |

**Figure 4.29: Effect of interaction between different encapsulation variables on dopamine content in encapsulated powder**
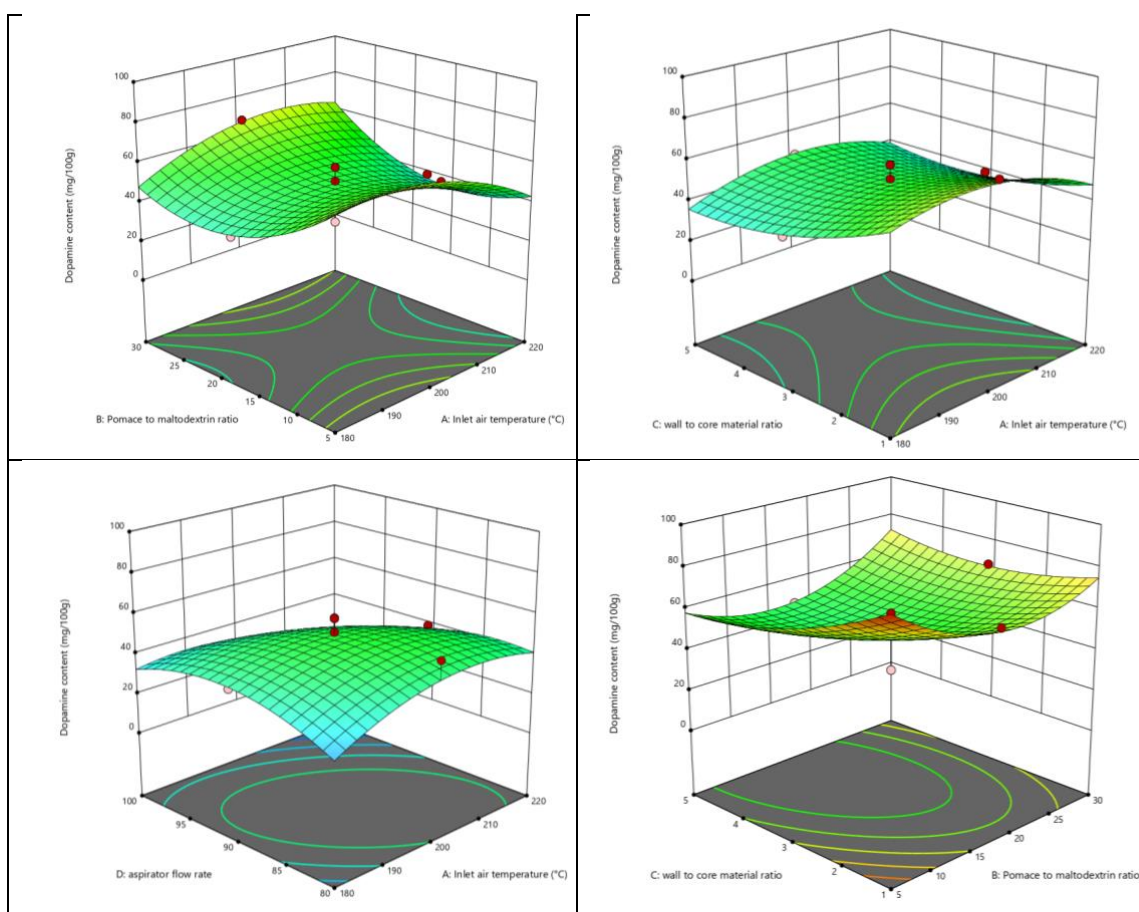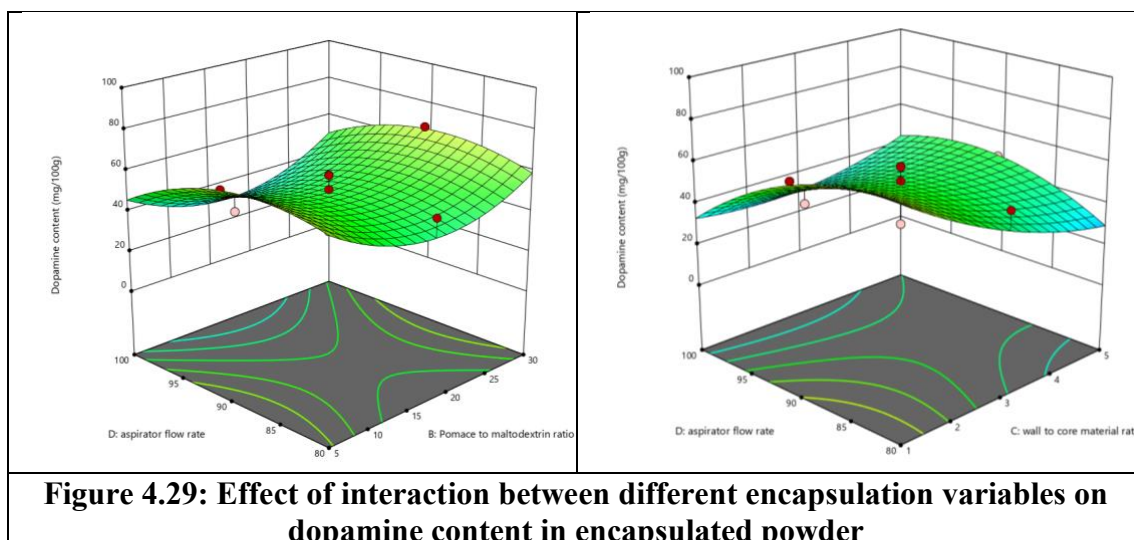
### 4.6.6 L-dopa Content

Table 4.22 gives detailed insights on the effect different encapsulation parameters on the L-dopa content in encapsulated powder. The L-dopa content varied significantly with changes in the wall material ratio and pomace-to-maltodextrin ratio. The highest L-DOPA concentration (2655 mg/100g) was obtained at temperature of 200°C, a pomace-to-maltodextrin ratio of 30:1 and a wall-to-core material ratio of 1:1 (figure 4.30). These findings are supported by studies indicating that plant-based wall materials, such as maltodextrin and grape pomace, protect bioactive compounds from degradation during spray drying by forming a stable matrix around the core compounds (Caliskan & Dirim, 2016).

**Table 4.22: Data on analysis of variance for L-dopa content in encapsulated powder**

| Source | Sum of Squares | df | Mean Square | F-value | p-value |
|---|---|---|---|---|---|
| **Model** | 2.525E+05 | 14 | 18037.65 | 28.53 | < 0.0001 |
| A-Inlet air temperature | 2738.00 | 1 | 2738.00 | 4.33 | 0.0550 |
| B-Pomace to maltodextrin ratio | 62069.39 | 1 | 62069.39 | 98.16 | < 0.0001 |
| C-wall to core material ratio | 1.369E+05 | 1 | 1.369E+05 | 216.57 | < 0.0001 |
| D-aspirator flow rate | 260.68 | 1 | 260.68 | 0.4123 | 0.5305 |
| AB | 169.00 | 1 | 169.00 | 0.2673 | 0.6127 |
| AC | 9555.06 | 1 | 9555.06 | 15.11 | 0.0015 |
| AD | 1444.00 | 1 | 1444.00 | 2.28 | 0.1515 |
| BC | 15006.25 | 1 | 15006.25 | 23.73 | 0.0002 |
| BD | 189.06 | 1 | 189.06 | 0.2990 | 0.5926 |

| | | | | | |
|---|---|---|---|---|---|
| CD | 110.25 | 1 | 110.25 | 0.1744 | 0.6822 |
| A² | 142.86 | 1 | 142.86 | 0.2259 | 0.6414 |
| B² | 657.11 | 1 | 657.11 | 1.04 | 0.3242 |
| C² | 3160.36 | 1 | 3160.36 | 5.00 | 0.0410 |
| D² | 69.40 | 1 | 69.40 | 0.1098 | 0.7450 |
| Residual | 9484.78 | 15 | 632.32 | | |
| Lack of Fit | 7255.40 | 10 | 725.54 | 1.63 | 0.3080 |
| Pure Error | 2229.38 | 5 | 445.88 | | |
| Cor Total | 2.620E+05 | 29 | | | |
| Std. Dev. | 25.15 | | | | |
| Mean | 302.73 | | | | |
| C.V. % | 8.31 | | | | |
| R² | 0.9638 | | | | |
| Adjusted R² | 0.9300 | | | | |
| Predicted R² | 0.8103 | | | | |
| Adeq Precision | 20.1707 | | | | |
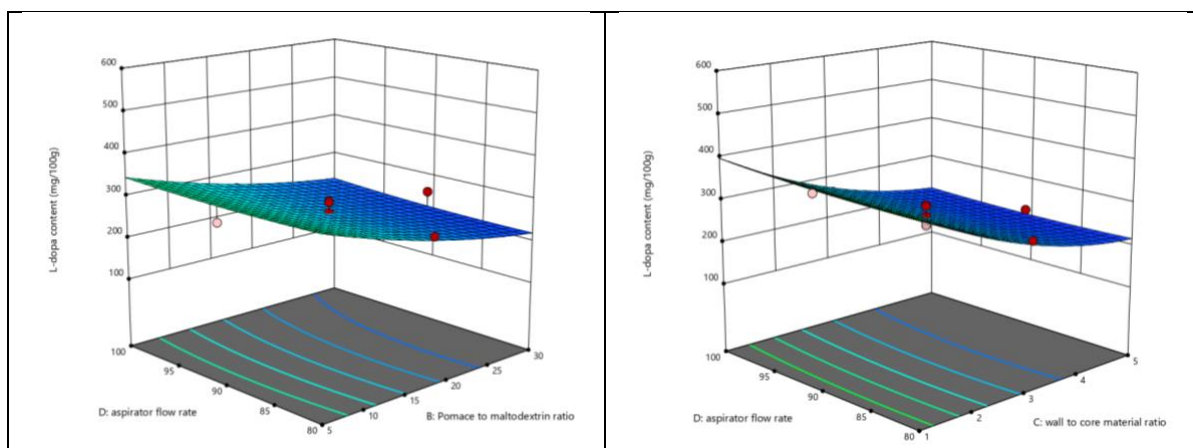
**Figure 4.30: Effect of interaction between different encapsulation variables on L-dopa content in encapsulated powder**

### 4.6.7 L-tyrosine content
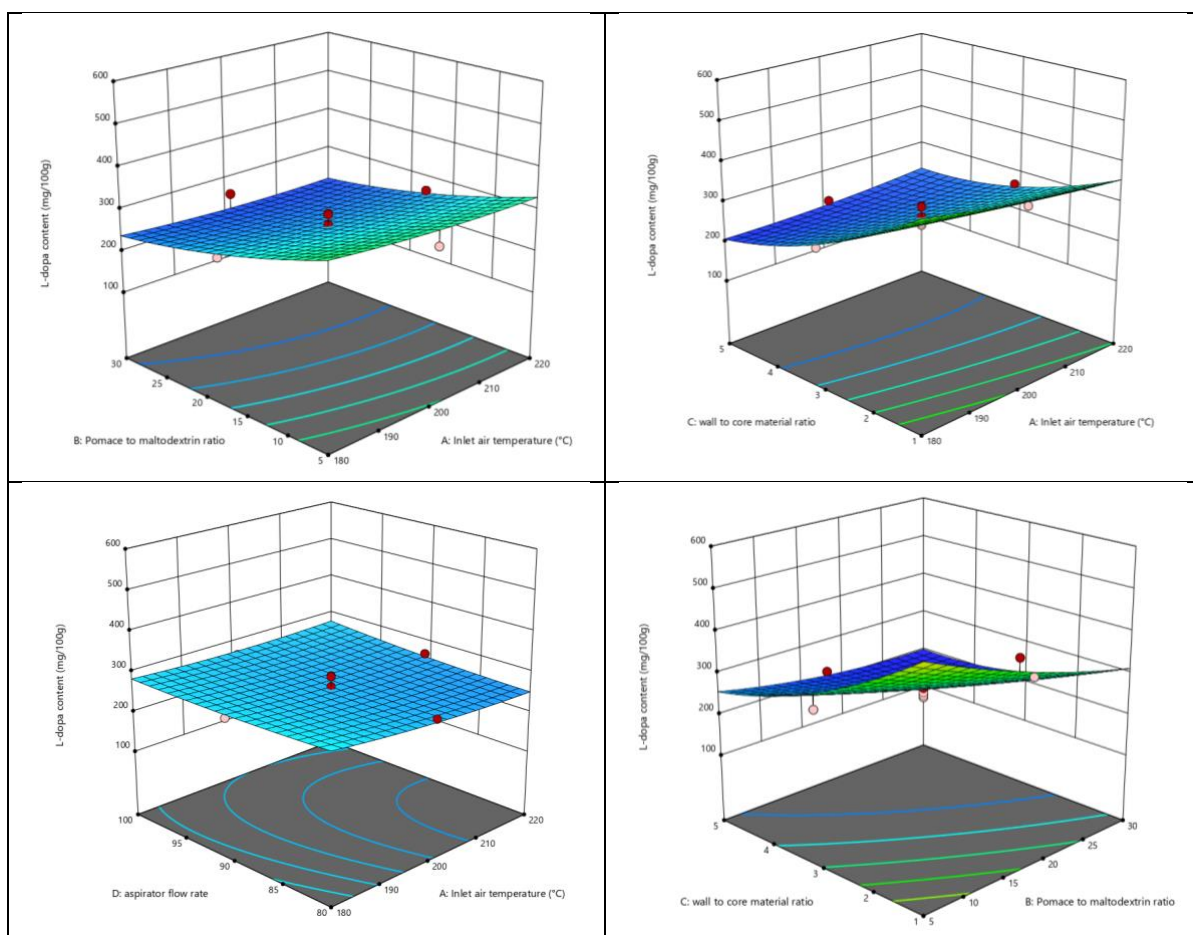
Table 4.19 gives detailed insights on the effect different encapsulation parameters on the L-tyrosine content in encapsulated powder. The L-tyrosine content was influenced by the pomace-to-maltodextrin ratio ($p = 0.0030$) and the quadratic effect of wall material ratio ($p < 0.0001$). The highest L-tyrosine concentration (2655 mg/100g) was observed under similar conditions to L-DOPA, with a 30:1 pomace-to-maltodextrin ratio and a 1:1 wall-to-core material ratio (figure 4.31). The use of grape pomace as an encapsulant likely contributed to the preservation of L-tyrosine due to its rich antioxidant content, which helps to stabilize amino acids during the drying process (Fernandes et al., 2017).

**Table 4.23: Data on analysis of variance for L-tyrosine content in encapsulated powder**

| Source | Sum of Squares | df | Mean Square | F-value | p-value |
|---|---|---|---|---|---|
| **Model** | 4.187E+06 | 14 | 2.991E+05 | 13.48 | < 0.0001 |
| A-Inlet air temperature | 48308.68 | 1 | 48308.68 | 2.18 | 0.1607 |
| B-Pomace to maltodextrin ratio | 2.784E+05 | 1 | 2.784E+05 | 12.55 | 0.0030 |
| C-wall to core material ratio | 61016.89 | 1 | 61016.89 | 2.75 | 0.1180 |
| D-aspirator flow rate | 6631.68 | 1 | 6631.68 | 0.2989 | 0.5926 |
| AB | 47251.89 | 1 | 47251.89 | 2.13 | 0.1651 |
| AC | 2.752E+05 | 1 | 2.752E+05 | 12.41 | 0.0031 |
| AD | 96954.39 | 1 | 96954.39 | 4.37 | 0.0540 |
| BC | 4641.02 | 1 | 4641.02 | 0.2092 | 0.6539 |
| BD | 10429.52 | 1 | 10429.52 | 0.4702 | 0.5034 |
| CD | 72562.89 | 1 | 72562.89 | 3.27 | 0.0906 |
| A² | 1.006E+05 | 1 | 1.006E+05 | 4.53 | 0.0502 |

| | | | | | |
|---|---|---|---|---|---|
| B² | 3.095E+06 | 1 | 3.095E+06 | 139.53 | < 0.0001 |
| C² | 8.515E+05 | 1 | 8.515E+05 | 38.38 | < 0.0001 |
| D² | 1.931E+05 | 1 | 1.931E+05 | 8.71 | 0.0099 |
| Residual | 3.327E+05 | 15 | 22183.30 | | |
| Lack of Fit | 2.590E+05 | 10 | 25900.13 | 1.76 | 0.2776 |
| Pure Error | 73748.21 | 5 | 14749.64 | | |
| Cor Total | 4.520E+06 | 29 | | | |
| Std. Dev. | 148.94 | | | | |
| Mean | 1316.78 | | | | |
| C.V. % | 11.31 | | | | |
| R² | 0.9264 | | | | |
| Adjusted R² | 0.8577 | | | | |
| Predicted R² | 0.6958 | | | | |
| Adeq Precision | 17.5550 | | | | |
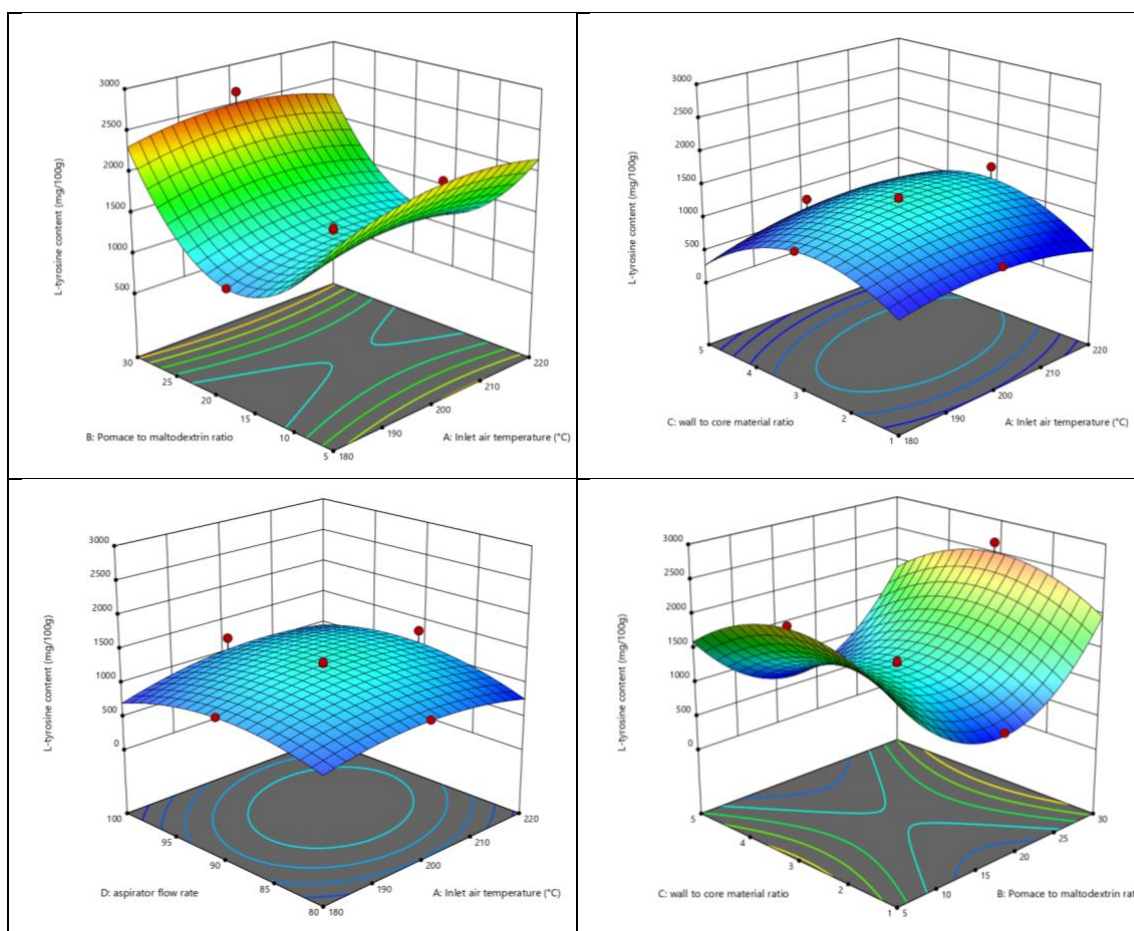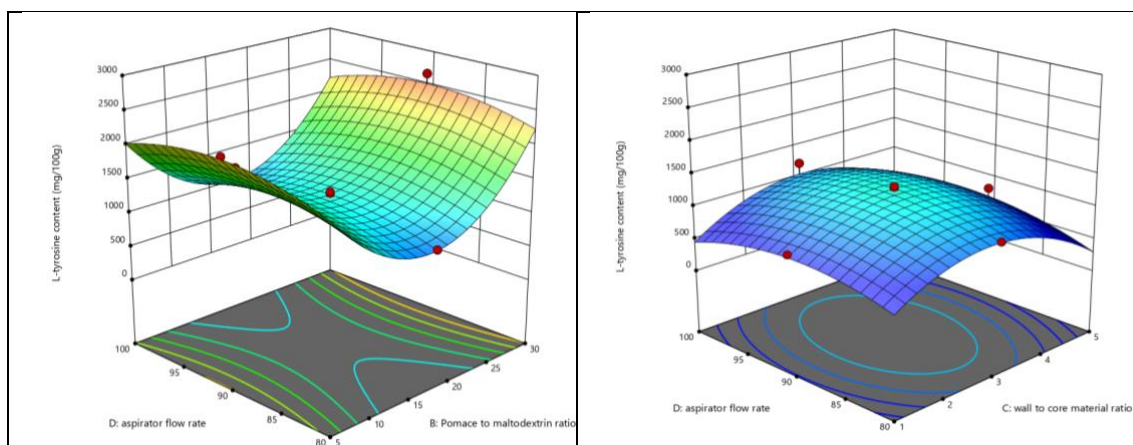
**Figure 4.31: Effect of interaction between different encapsulation variables on L-tyrosine content in encapsulated powder**

## 4.6.8 Optimization of encapsulation parameters

The models developed for encapsulation efficiency, yield, moisture content, and bioactive compound retention were used to identify the optimal conditions for the spray drying process. The optimization process aimed to maximize encapsulation efficiency and yield while minimizing moisture content and maximizing the retention of bioactive compounds.

Using the quadratic models, the optimized conditions were determined to be:

Inlet air temperature: 212 °C

Pomace-to-maltodextrin ratio: 30:1

Wall-to-core material ratio: 1:1

Aspirator flow rate: 100 Nm³/hr

Under these optimized conditions, the encapsulation efficiency was maximized at 21.29±1.23%, with a high yield of 30.12±1.46% and minimal moisture content of 8.10±0.284%. Furthermore, bioactive compound retention was significantly enhanced, with dopamine, L-DOPA and L-tyrosine content reaching 50.13±6.22 mg/100g, 342±18.14 mg/100g, and 1391±121.39 mg/100g, respectively (table 4.24). XIC were shown in figure 4.32.
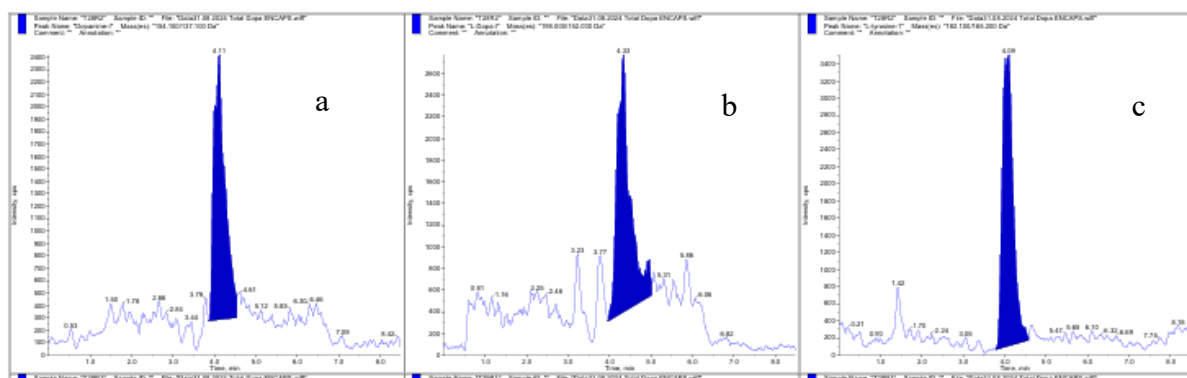
**Figure 4.32: XIC for dopamine (a), L-dopa (b) and L-tyrosine in powder obtained at optimal conditions**

**Picture 4.5: Encapsulated powder for all treatments designed by RSM-Face centred Central Composite Design**

| Parameters | Predicted value | Actual value |
|---|---|---|
| Encapsulation efficiency (%) | 19.01±1.50 | 21.29±1.23 |
| Encapsulation yield (%) | 30.23±1.38 | 30.12±1.46 |
| Moisture content (%) | 9.47±0.28 | 8.10±0.284 |
| Dopamine content (mg/100g) | 38.34±7.82 | 50.13±6.22 |
| L-dopa content (mg/100g) | 316.89±25.15 | 342±18.14 |
| L-tyrosine content (mg/100g) | 1524.88±148.94 | 1391±121.39 |

**Table 4.24: Validation of the predicted values for encapsulation efficiency, encapsulation yield, moisture content, dopamine content, L-dopa content and L-tyrosine content in encapsulated powder**

## 4.7 Physicochemical characterisation of encapsulated powder

### 4.7.1 Physical properties of powder

The encapsulated powder produced in the study displayed several key physicochemical properties, as shown in Table 4.25, including powder yield, bulk density, tapped density, particle density, porosity, flowability, cohesiveness, and solubility. Each of these properties plays a critical role in determining the functionality, stability, and applicability of encapsulated powders in food and nutraceutical industries. Below is an in-depth analysis of these parameters.

### 4.7.1.1. Powder Yield (%)

The powder yield refers to the percentage of the total solid content recovered after the spray-drying. In this study, yield of powder about 31.10%. Spray drying is known for its efficiency in producing fine powders with high retention of active compounds. However, the yield obtained is relatively moderate, possibly due to losses in the spray-dryer chamber or adhesion of powder to the drying walls, as discussed in similar studies (Quek et al., 2007).

### 4.7.1.2. Bulk Density (g/cm³)

Bulk density is the mass of powder per unit volume, including void spaces. The bulk density observed in this study (0.474 g/cm³) falls within typical values reported for spray-dried powders (Tonon et al., 2008). Higher bulk density can lead to more efficient packaging, reducing storage and transportation costs. However, excessive density could negatively affect the powder's rehydration properties and flowability.

### 4.7.1.3. Tapped Density (g/cm³)

Tapped density is measured by subjecting the powder to mechanical tapping, which compacts the material. The observed increase in density from bulked (0.474 g/cm³) to tapped (0.633 g/cm³) suggests that the powder particles are prone to rearrangement and compaction. A higher tapped density can indicate poor flow properties, which might impact the ease of use in formulations (Fitzpatrick et al., 2004).

### 4.7.1.4. Particle Density (g/cm³)

Particle density, or true density, excludes the void spaces between particles and refers to the density of the solid particles themselves. The high particle density observed (4.968 g/cm³) is indicative of a compact structure of the encapsulated material. This is likely due to the spray-drying process, which tends to form dense particles. High particle density can enhance powder stability and prevent particle breakage during handling, making the encapsulated powder ideal for industrial processing (Saénz et al., 2009).

### 4.7.1.5. Porosity (%)

Porosity is calculated as the fraction of the volume of voids over the total volume of the powder. High porosity (87.14%) suggests that the powder contains significant air spaces, which can influence its flowability and dissolution rate. The high porosity also implies that the powder may be less dense and more prone to moisture absorption, which could affect shelf life (Peighambardoust et al., 2011). However, this high porosity can improve the reconstitution properties, allowing the encapsulated bioactive compounds to be easily released in aqueous solutions.

**4.7.1.6. Flowability (%)**

Flowability refers to the ease with which the powder flows. A Carr index (flowability) value of 25.07% indicates fair to passable flow properties (Carr, 1965). Lower flowability can be attributed to the cohesiveness of the powder or irregular particle shapes, as seen in many spray-dried powders. Flowability is a crucial factor in powder handling during packaging and processing, especially in automated systems where free-flowing powders are necessary to prevent blockages (Fitzpatrick et al., 2004).

**4.7.1.7. Cohesiveness**

Cohesiveness is another important parameter, which reflects the tendency of powder particles to stick together. With a cohesiveness value of 1.335, the powder shows moderate cohesiveness, which can affect its flowability. Higher cohesiveness can result from electrostatic forces or moisture content in the powder, which could lead to clumping during storage and processing. Spray-dried powders often have higher cohesiveness due to small particle sizes and the presence of bioactive compounds (Adhikari et al., 2007).

**4.7.1.8. Solubility (%)**

Solubility is a critical parameter, especially for nutraceutical powders that are intended to be reconstituted in aqueous solutions. A solubility value of 58.52% suggests that the encapsulated powder has a moderate solubility. Solubility of powder increased when there is decrease in particle size (Cano-Chauca et al., 2005). However, encapsulation materials, such as grape pomace, might limit solubility to some extent due to the presence of fibrous or hydrophobic components. Improved solubility is essential for better bioavailability of the encapsulated compounds.

The observed physicochemical properties of the encapsulated powder align with existing literature on spray-dried bioactive compounds. Spray drying, as used in this study, is widely recognized for producing fine powders with good retention of bioactive compounds, moderate solubility, and compact particle structures (Cano-Chauca et al., 2005; Tonon et al., 2008). The balance between bulk density, tapped density, and porosity indicates that the powder has good handling properties but may require optimization for flowability and solubility.

**Table 4.25: Physical parameters of encapsulated powder**

| Parameters | Mean±SD |
|---|---|
| Powder yield | 31.10±1.42 |
| Bulked density | 0.474±0.019 |
| Tapped density | 0.633±0.011 |
| Particle density | 4.968±0.605 |
| Porosity | 87.141±1.460 |
| Flowability | 25.068±1.936 |
| Cohesiveness | 1.335±0.035 |
| Solubility | 58.523±3.109 |

## 4.7.2 Biochemical properties of encapsulated powder

The encapsulated powder derived from banana peel and grape pomace exhibited significant levels of bioactive compounds, as detailed in Table 4.26, including TPC, TFC, AA, TAC and concentrations of dopamine, L-dopa and L-tyrosine. These biochemical parameters are key indicators of the potential health benefits and functionality of the encapsulated powder in food, pharmaceutical, or nutraceutical applications.

### 4.7.2.1. Total Phenolic Content (TPC) (mg GAE/100g)

The total phenolic content (TPC) of the encapsulated powder was found to be 645.788 mg GAE/100g, showing higher content of phenols exhibiting antioxidant properties.. Phenolics are crucial for scavenging free radicals and reducing oxidative stress, contributing to the prevention of chronic diseases such as cancer and cardiovascular issues (Shahidi & Ambigaipalan, 2015). The encapsulation process, particularly the use of grape pomace as a carrier, likely contributed to the high retention of phenolic compounds, as grape pomace is naturally rich in phenolics (Makris et al., 2007).

### 4.7.2.2. Total Flavonoid Content (TFC) (mg QE/100g)

Flavonoids are another important class of bioactive compounds with antioxidant and anti-inflammatory properties. The TFC of 119.614 mg QE/100g reflects the moderate presence of flavonoids in the encapsulated powder. Flavonoids contribute to the overall antioxidant activity and have health benefits, providing cardiovascular protection (Panche et al., 2016). The relatively high TFC in the encapsulated powder suggests that the encapsulation process effectively retained these compounds, similar to findings in other studies involving the encapsulation of bioactive compounds (Bobo-García et al., 2015).

### 4.7.2.3. Total Anthocyanin Content (TAC) (mg/100g)

Anthocyanins are pigments responsible for the red, purple, and blue colours in many fruits and vegetables and they possess potent antioxidant activity. The TAC in the encapsulated powder was 13.017 mg/100g, demonstrating the powder's feature as natural source antioxidants (Wallace, 2011). The relatively high TAC suggests that the encapsulation process effectively preserved these pigments, which are known to degrade during processing and storage. Grape pomace, being rich in anthocyanins, played a crucial role in maintaining the anthocyanin levels in the final encapsulated product (García-Lomillo & González-SanJosé, 2017).

### 4.7.2.4. Antioxidant Activity (AA) (%)

The antioxidant activity (AA) of the encapsulated powder was found to be 89.137%, indicating strong potential for scavenging free radicals and reducing oxidative damage. This high level of AA is attributed to the synergistic effects of phenolics, flavonoids, and anthocyanins present in the powder. The antioxidant potential of phenolic compounds has been widely studied, and their ability to neutralize reactive oxygen species (ROS) makes them highly beneficial in preventing oxidative stress-related diseases (Shahidi & Ambigaipalan, 2015). The use of grape pomace as an encapsulation carrier likely contributed to the high AA due to its rich phenolic and anthocyanin content (Makris et al., 2007).

### 4.7.2.5. Dopamine Content (mg/100g)

Dopamine, a neurotransmitter, plays a significant role in regulating mood, attention, and movement. The dopamine content in the encapsulated powder was found to be 48 mg/100g, which is noteworthy given the bioactive potential of

dopamine in health supplements. Dopamine has been studied for its potential role in neuroprotection, particularly in conditions such as Parkinson's disease (Gao et al., 2002). The encapsulation process appears to have successfully preserved dopamine, possibly due to the protective effects of encapsulation, which minimizes oxidation and degradation during processing and storage (Abdelwahed et al., 2006).

### 4.7.2.6. L-dopa Content (mg/100g)

L-dopa is a precursor to dopamine and is used in the treatment of Parkinson's disease. The L-dopa content in the encapsulated powder (342 mg/100g) suggests that the encapsulated product could have potential neuroprotective effects. Previous studies have shown that L-dopa can enhance dopamine levels in the brain, making it a valuable compound in neurotherapeutics (Nagatsu & Sawada, 2009). The ability of the encapsulation process to retain L-dopa is beneficial, as this compound is sensitive to oxidation, and the use of grape pomace may have provided a protective matrix.

### 4.7.2.7. L-tyrosine Content (mg/100g)

L-tyrosine is an amino acid involved in the production of dopamine, norepinephrine, and epinephrine. The high L-tyrosine content (1345 mg/100g) in the encapsulated powder underscores its potential role in improving mental performance under stressful conditions (Jongkees et al., 2015). L-tyrosine supplementation has been shown to improve cognitive function and stress resilience, making it an important compound in health supplements. The high retention of L-tyrosine in the encapsulated product suggests that the encapsulation process was effective in preserving this bioactive compound.



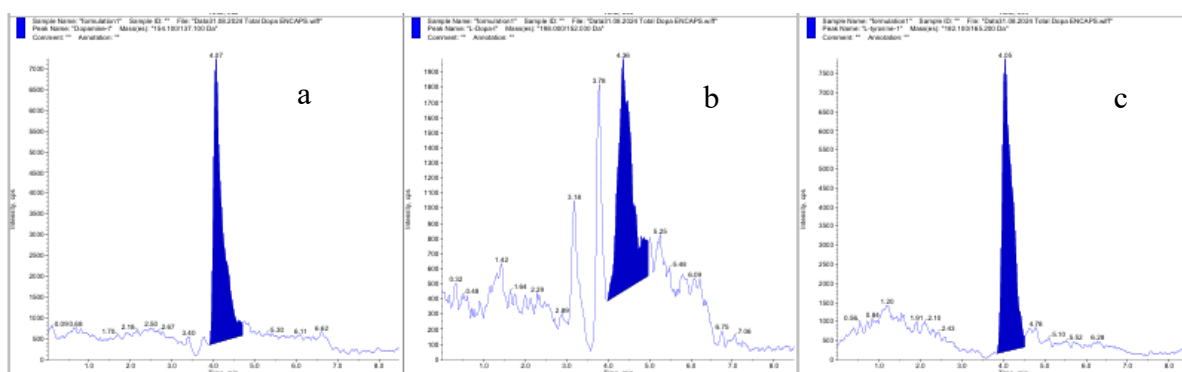**Figure 4.33: XIC for dopamine (a), L-dopa (b) and L-tyrosine in encapsulated powder**

**Table 4.26: Biochemical properties of encapsulated powder**

| Parameters | Mean ±SD |
|---|---|
| TPC | 645.788±1.397 |
| TFC | 119.614±1.479 |
| TAC | 130.165±0.001 |
| AA | 89.137±0.125 |
| Dopamine Content | 48±18.384 |
| L-dopa content | 342±7.071 |
| L-tyrosine content | 1345±63.640 |

# Summary and conclusion

## 5.1 Summary

The study, entitled "Encapsulation of Ultrasound Extracted Bioactive Compounds of Banana Peel with Grape Pomace," was conducted to develop an efficient method for stabilizing bioactive compounds extracted from banana peels through encapsulation using grape pomace powder. Conducted at the Department of Horticulture, Lovely Professional University, Punjab, and ICAR-National Research Centre for Grapes, Pune, this research aims to provide a method for optimizing the utilization of agricultural waste. The focus of the study was on the extraction, drying and encapsulation processes and their effect on biochemical composition and physical properties.

**Objective-01**

## 5.1.1 Physicochemical properties of Banana Peel and Grape Pomace

The physicochemical properties of banana peel revealed high moisture content, phenolic content (373.25 ± 2.99 mg GAE/100g), flavonoid content (169.38 ± 2.18 mg QE/100g), and antioxidant activity (45.57 ± 1.45%). This highlights the peel's potential for waste valorisation. Similarly, grape pomace showed even higher phenolic content (584.95 ± 0.95 mg GAE/100g) and antioxidant activity (89.66 ± 0.93%), emphasizing its use as a carrier for bioactive compounds. Anthocyanins in grape pomace (60.29 ± 0.34 mg M3G/100g) also suggest potential in food and cosmetic applications. It indicated the potential of both commodities as natural corce of phytochemicals

## 5.1.2 Drying Kinetics and degradation kinetics of banana peel

The experiment revealed that drying time decreased as temperature increased, with moisture content reducing significantly from 92.65% to 1.65 Midilli et al. model fitted well to the data. Degradation kinetics showed that total phenolic content (TPC), total flavonoid content (TFC), and antioxidant activity (AA) degraded faster at higher temperatures, following first-order kinetics. The half-life of TPC was longest at lower temperatures, indicating better preservation of phenolic compounds at lower drying

temperatures. Furthermore, the study analysed the impact of drying on key bioactive compounds like dopamine, noradrenaline, L-phenylalanine, and L-tyrosine. These compounds showed a significant decrease in concentration with increased drying temperature. For instance, dopamine content reduced by 50.73% at 70°C. The degradation rate of L-phenylalanine and L-tyrosine was higher than that of dopamine and noradrenaline, likely due to their role in dopamine biosynthesis. Overall, higher temperatures accelerated the degradation of bioactive compounds, emphasizing the importance of temperature control during drying.

### 5.1.3 Drying and degradation kinetics of grape pomace

Moisture content of fresh GP was 72.69%, which decreased to 3.74% after drying. Midilli et al model fitted well to the data. The study also examined effective moisture diffusivity, which increased with higher temperatures, and calculated activation energy (Ea) at 42.79 kJ/mol. The impact of drying temperatures (40°C to 80°C) on TPC, TFC, TAC, and AA was evaluated., with TFC showing the fastest degradation. Anthocyanins in GP were highly temperature-sensitive, with the highest degradation occurring at both low (40°C due to extended drying) and high temperatures. The study highlights that drying between 50°C and 60°C is optimal for preserving anthocyanins. Lastly, the anthocyanin profiles revealed the presence of 16 compounds, with malvidin-3-O-glucoside being the most prevalent.

### Objective-02

### 5.1.4 Extraction of bioactive compounds from banana peel

Extraction parameters such as sonication time, solid-to-liquid ratio, sonication power, and solvent concentration were fine-tuned. The quadratic models developed were highly significant (p < 0.0001) and demonstrated a strong fit, with $R^2$ values above 90% for all compounds, indicating high predictive accuracy.

For TPC extraction, the most significant factors were sonication time, solid-to-liquid ratio, and solvent concentration. The optimal yield of TPC (89.3 mg GAE/100g) was achieved with a 13.8-minute sonication time, a solid-to-liquid ratio of 8 mg/100mL, 400W sonication power, and 50% ethanol concentration. These findings align with previous studies indicating that a balanced ethanol-water mixture enhances phenolic compound solubility. The study also showed that sonication power improves

extraction but must be carefully controlled to prevent the degradation of thermosensitive compounds.

Dopamine and L-DOPA extraction were strongly influenced by similar parameters, with the highest yields of dopamine (15.03 mg/100g) and L-DOPA (21.64 mg/100g) obtained under the same optimal conditions. However, the role of sonication power and solvent concentration was more pronounced for these compounds, especially for dopamine. L-tyrosine extraction followed similar trends, with the highest yield (21.64 mg/100g) also achieved under these conditions.

**Objective-03**

**5.1.5 Encapsulation of bioactive compounds of banana peel with grape pomace**

A central part of the study involved optimizing key parameters such as inlet air temperature, the pomace-to-maltodextrin ratio, the wall-to-core material ratio, and the aspirator flow rate. The results indicated that the encapsulation efficiency was significantly influenced by these variables, with the highest efficiency (33.67%) achieved at an inlet air temperature of 180°C, a pomace-to-maltodextrin ratio of 30:1, and a wall-to-core material ratio of 5:1. These conditions helped enhance the formation of a protective encapsulation matrix, which improved the overall efficiency of the process.

The yield of the encapsulated powder was another critical factor examined in the study. The maximum yield (50.78%) was obtained at an inlet air temperature of 220°C and a 5:1 wall-to-core material ratio. This finding suggests that the core material, grape pomace, played a crucial role in wall formation due to its polyphenolic content. Although the aspirator flow rate also had an impact on yield, the composition of the feed material was more significant. Additionally, the study found that the interaction between inlet air temperature and aspirator flow rate affected the drying rate, further influencing the final powder recovery. Moisture content was another important parameter that was optimized. Lower moisture content in the encapsulated powder was desirable to ensure shelf-life stability and reduce microbial growth. The lowest moisture content (6.96%) was recorded under conditions of higher air temperatures and higher aspirator flow rates, which improved water evaporation. These conditions helped to create a stable, low-moisture product. The interaction between pomace-to-maltodextrin ratio and wall-to-core material ratio also

significantly influenced moisture content, with higher maltodextrin concentrations reducing the residual moisture in the final product.

The study also focused on maximizing the retention of bioactive compounds, including dopamine, L-DOPA, and L-tyrosine. The highest dopamine content (90.46 mg/100g) was obtained at an inlet air temperature of 180°C and a pomace-to-maltodextrin ratio of 5:1. For L-DOPA, the maximum retention (2655 mg/100g) occurred at a 30:1 pomace-to-maltodextrin ratio, while for L-tyrosine, the optimal conditions were similar, achieving the highest content at 2655 mg/100g. These findings suggest that grape pomace, rich in phenolic compounds, helped to stabilize these bioactive compounds, which is essential for preserving sensitive materials.

Finally, the optimization of all parameters led to the development of a robust encapsulation process. The optimal conditions included an inlet air temperature of 212°C, a pomace-to-maltodextrin ratio of 30:1, a wall-to-core material ratio of 1:1, and an aspirator flow rate of 100 Nm³/hr. Under these conditions, encapsulation efficiency, yield, and bioactive compound retention were maximized, while moisture content was minimized. The study demonstrated that careful control of spray drying parameters could significantly enhance the effectiveness of encapsulation for bioactive compound preservation.

### 5.1.6 Physicochemical characterisation of encapsulated powder

The encapsulated powder produced in the study demonstrated important physicochemical and biochemical properties, making it a valuable product for food, pharmaceutical, and nutraceutical industries. Physicochemical parameters such as powder yield, bulk density, tapped density, particle density, porosity, flowability, cohesiveness and solubility were analysed. The powder yield of 31.10% indicated moderate efficiency, with potential losses attributed to adhesion inside the dryer. Bulk density (0.474 g/cm³) and tapped density (0.633 g/cm³) suggested that the powder has moderate flowability and compactness, while the particle density (4.968 g/cm³) and high porosity (87.14%) indicated a structurally compact powder with air spaces that influence flow and dissolution. Flowability was rated as fair, and cohesiveness was moderate, suggesting potential improvements for handling. A solubility of 58.52% reflected moderate reconstitution potential, influenced by encapsulation materials.

The biochemical analysis of the powder revealed high concentrations of bioactive compounds, including TPC< TFC and TAC, all known for their antioxidant properties. The TPC was notably high at 645.79 mg GAE/100g, while the TFC and TAC were 119.61 mg QE/100g and 13.02 mg/100g, respectively, contributing to the antioxidant activity of 89.14%. Neuroactive compounds like dopamine (48 mg/100g), L-dopa (342 mg/100g), and L-tyrosine (1345 mg/100g) were also retained, enhancing the powder's potential for neuroprotective applications. The encapsulation process effectively preserved these compounds, leveraging the antioxidant-rich properties of grape pomace used as a carrier. These findings position the encapsulated powder as a promising functional ingredient with substantial health benefits, particularly in promoting antioxidant activity and supporting neurological health.

This study successfully demonstrated that banana peel and grape pomace are valuable sources of bioactive compounds that can be utilized in nutraceutical applications. The encapsulation of ultrasound-extracted banana peel compounds with grape pomace provides a promising approach to stabilize and enhance the bioavailability of these compounds. The drying and extraction processes were optimized to maximize the recovery of phenolic compounds while minimizing degradation. The use of grape pomace as a natural carrier for bioactive compounds further emphasizes the sustainable nature of this approach. Overall, this research contributes to the valorisation of agricultural waste and promotes the development of sustainable nutraceutical products.

## 5.2 Conclusion

The study has proven that banana peel and grape pomace are rich sources of phytochemicals, including phenolics, flavonoids, and antioxidants. These compounds have significant health benefits and can be incorporated into functional foods, cosmetics, and pharmaceuticals. Through ultrasound-assisted extraction, the recovery of these compounds was optimized, ensuring minimal degradation during the process.

The drying process was crucial in determining the retention of bioactive compounds, and it was shown that higher drying temperatures lead to faster drying times but also increased degradation rates. The encapsulation of bioactive compounds using grape pomace powder provided a sustainable approach to stabilize and preserve the active ingredients.

Mathematical models were employed to describe the drying and extraction processes accurately, and these models' provided insights into the optimal conditions for maximizing bioactive compound recovery. The models also predicted the degradation kinetics of the compounds, allowing for a deeper understanding of the effects of temperature and other factors on the stability of bioactive compounds.

In conclusion, this research has successfully demonstrated the potential of using agricultural by-products, such as banana peel and grape pomace, to develop nutraceutical products. The encapsulation of bioactive compounds using grape pomace as a carrier provides a sustainable and effective solution for stabilizing these compounds, making them more suitable for industrial applications. The findings of this study contribute to the field of sustainable agriculture by offering innovative solutions for waste valorisation and promoting the development of functional products with health benefits.

# Bibliography

Abbaspour-Gilandeh, Y., Kaveh, M., & Jahanbakhshi, A. (2019). The effect of microwave and convective dryer with ultrasound pre-treatment on drying and quality properties of walnut kernel. *Journal of Food Processing and Preservation*, 43(11), e14178.

Abdelwahed, W., Degobert, G., Stainmesse, S., & Fessi, H. (2006). Freeze-drying of nanoparticles: formulation, process and storage considerations. *Advanced drug delivery reviews*, 58(15), 1688-1713.

Aboul-Enein, A. M., Salama, Z. A., Gaafar, A. A., Aly, H. F., Abou-Elella, F., & Ahmed, H. A. (2016). Identification of phenolic compounds from banana peel (*Musa paradaisica* L.) as antioxidant and antimicrobial agents. *Journal of chemical and pharmaceutical research*, 8(4), 46-55.

Adhikari, B., Howes, T., Bhandari, B. R., & Troung, V. (2004). Effect of addition of maltodextrin on drying kinetics and stickiness of sugar and acid-rich foods during convective drying: experiments and modelling. *Journal of food Engineering*, 62(1), 53-68.

Agama-Acevedo, E., Sañudo-Barajas, J. A., Vélez De La Rocha, R., González-Aguilar, G. A., & Bello-Perez, L. A. (2016). Potential of plantain peels flour (*Musa paradisiaca* L.) as a source of dietary fiber and antioxidant compound. *CyTA-Journal of Food*, 14(1), 117-123.

Ahmed, M., I. A., Özcan, M. M., Al Juhaimi, F., Babiker, E. F. E., Ghafoor, K., Banjanin, T., ... & Alqah, H. A. (2020). Chemical composition, bioactive compounds, mineral contents, and fatty acid composition of pomace powder of different grape varieties. *Journal of Food Processing and Preservation*, 44(7), e14539.

Akar, G., & Barutçu Mazı, I. (2019). Color change, ascorbic acid degradation kinetics, and rehydration behaviour of kiwifruit as affected by different drying methods. *Journal of food process engineering*, 42(3), e13011.

Akbulut, M., Çoklar, H., Bulut, A. N., & Hosseini, S. R. (2024). Evaluation of black grape pomace, a fruit juice by-product, in shalgam juice production: Effect on phenolic compounds, anthocyanins, resveratrol, tannin, and in vitro antioxidant activity. *Food Science and Nutrition*. https://doi.org/10.1002/fsn3.4104

Akdaş, S., & Başlar, M. (2015). Dehydration and degradation kinetics of bioactive compounds for mandarin slices under vacuum and oven drying conditions. *Journal of Food Processing and Preservation*, 39(6), 1098-1107.

Altemimi, A., Watson, D. G., Choudhary, R., Dasari, M. R., & Lightfoot, D. A. (2016). Ultrasound assisted extraction of phenolic compounds from peaches and pumpkins. *PloS one*, 11(2), e0148758.

Alzate Acevedo, S., Díaz Carrillo, Á. J., Flórez-López, E., & Grande-Tovar, C. D. (2021). Recovery of banana waste-loss from production and processing: a contribution to a circular economy. *Molecules*, 26(17), 5282.

Ampah, J., Dzisi, K. A., Addo, A., & Bart-Plange, A. (2022). Drying kinetics and chemical properties of mango. *International Journal of Food Science*, 2022(1), 6243228.

Antonić, B., Jančíková, S., Dordević, D., & Tremlová, B. (2020). Grape pomace valorization: A systematic review and meta-analysis. *Foods*, 9(11), 1627. https://doi.org/10.3390/foods9111627

Araújo, C. D. S., Vimercati, W. C., Macedo, L. L., Saraiva, S. H., Teixeira, L. J. Q., da Costa, J. M. G., & Pimenta, C. J. (2022). Encapsulation of phenolic and antioxidant compounds from spent coffee grounds using spray-drying and freeze-drying and characterization of dried powders. *Journal of Food Science*, 87(9), 4056-4067.

Avhad, M. R., & Marchetti, J. M. (2016). Mathematical modelling of the drying kinetics of Hass avocado seeds. *Industrial Crops and Products*, 91, 76–87.

Awele Okolie, J. , Henry, O. and Epelle, E. (2016) Determination of the Antioxidant Potentials of Two Different Varieties of Banana Peels in Two Different Solvents. *Food and Nutrition Sciences*, 7, 1253-1261. doi: 10.4236/fns.2016.713115.

Azmir, J., Zaidul, I. S. M., Rahman, M. M., Sharif, K. M., Mohamed, A., Sahena, F., ... & Omar, A. K. M. (2013). Techniques for extraction of bioactive compounds from plant materials: A review. *Journal of food engineering*, 117(4), 426-436.

Babbar, N., Oberoi, H. S., Uppal, D. S., & Patil, R. T. (2011). Total phenolic content and antioxidant capacity of extracts obtained from six important fruit residues. *Food research international*, 44(1), 391-396.

Başlar, M., Karasu, S., Kiliçli, M., Us, A. A., & Sağdiç, O. (2014). Degradation kinetics of bioactive compounds and antioxidant activity of pomegranate arils during the drying process. *International Journal of Food Engineering*, 10(4), 839-848.

Bennett, R. N., Shiga, T. M., Hassimotto, N. M., Rosa, E. A., Lajolo, F. M., & Cordenunsi, B. R. (2010). Phenolics and antioxidant properties of fruit pulp and cell wall fractions of postharvest banana (*Musa acuminata* Juss.) cultivars. *Journal of agricultural and food chemistry*, 58(13), 7991-8003.

Bhandari, B. R., Datta, N., & Howes, T. (1997). Problems associated with spray drying of sugar-rich foods. *Drying technology*, 15(2), 671-684.

Bobo-García, G., Davidov-Pardo, G., Arroqui, C., Vírseda, P., Marín-Arroyo, M. R., & Navarro, M. (2015). Intra-laboratory validation of microplate methods for total phenolic content and antioxidant activity on polyphenolic extracts, and

comparison with conventional spectrophotometric methods. *Journal of the Science of Food and Agriculture*, 95(1), 204-209.

Bordiga, M., Travaglia, F., & Locatelli, M. (2019). Valorisation of grape pomace: an approach that is increasingly reaching its maturity–a review. *International Journal of Food Science & Technology*, 54(4), 933-942. https://doi.org/10.1111/ijfs.14118

Boyano-Orozco, L., Gallardo-Velázquez, T., Meza-Márquez, O. G., & Osorio-Revilla, G. (2020). Microencapsulation of rambutan peel extract by spray drying. Foods, 9(7), 899.

Brahmi, F., Mateos-Aparicio, I., Mouhoubi, K., Guemouni, S., Sahki, T., Dahmoune, F., ... & Boulekbache-Makhlouf, L. (2023). Kinetic modelling of convective and microwave drying of potato peels and their effects on antioxidant content and capacity. *Antioxidants*, 12(3), 638.

Caliskan, G., & Dirim, S. N. (2016). The effect of different drying processes and the amounts of maltodextrin addition on the powder properties of sumac extract powders. *Powder technology*, 287, 308-314.

Cano-Chauca, M., Stringheta, P. C., Ramos, A. M., & Cal-Vidal, J. (2005). Effect of the carriers on the microstructure of mango powder obtained by spray drying and its functional characterization. *Innovative Food Science & Emerging Technologies*, 6(4), 420-428.

Carr, R. L. (1965). Evaluating flow properties of solids. *Chemical Engineering*, 72(1), 163-168.

Carrera, C., Ruiz-Rodríguez, A., Palma, M., & Barroso, C. G. (2012). Ultrasound assisted extraction of phenolic compounds from grapes. *Analytica chimica acta*, 732, 100-104.

Chabuck, Z. A. G., Al-Charrakh, A. H., Hindi, N. K. K., & Hindi, S. K. K. (2013). Antimicrobial effect of aqueous banana peel extract, Iraq. Res. Gate. *Pharm. Sci*, 1, 73-5..

Chemat, F., Rombaut, N., Sicaire, A. G., Meullemiestre, A., Fabiano-Tixier, A. S., & Abert-Vian, M. (2017). Ultrasound assisted extraction of food and natural products. Mechanisms, techniques, combinations, protocols and applications. A review. *Ultrasonics sonochemistry*, 34, 540-560.

Chemat, F., Vian, M. A., Fabiano-Tixier, A. S., Nutrizio, M., Jambrak, A. R., Munekata, P. E., ... & Cravotto, G. (2020). A review of sustainable and intensified techniques for extraction of food and natural products. *Green Chemistry*, 22(8), 2325-2353.

Chintagunta, A. D., Kumar, N. S., Kolla, J., Kadam, G. B., Kumar, P. N., Shabeer, A., ... & Kumar, S. J. (2022). In silico optimization of anthocyanin extraction from gladious flower extracts and evaluation of its antioxidant potential. *Biomass Conversion and Biorefinery*, 1-11. https://doi.org/10.1007/s13399-022-03653-0

Clemente, G., Sanjuán, N., Cárcel, J. A., & Mulet, A. (2014). Influence of Temperature, Air Velocity, and Ultrasound Application on Drying Kinetics of Grape Seeds. *Drying Technology*, 32(1), 68–76. https://doi.org/10.1080/07373937.2013.811592

Conte, A., Panza, O., & Del Nobile, M. A. (2024). Modeling the dehydration kinetic of grape pomace. *LWT*, 198, 116021.

da Silva Júnior, M. E., Araújo, M. V. R. L., Martins, A. C. S., dos Santos Lima, M., Da Silva, F. L. H., Converti, A., & Maciel, M. I. S. (2023). Microencapsulation by spray-drying and freeze-drying of extract of phenolic compounds obtained from ciriguela peel. *Scientific Reports*, 13(1), 15222.

Dahmoune, F., Remini, H., Dairi, S., Aoun, O., Moussi, K., Bouaoudia-Madi, N., ... & Madani, K. (2015). Ultrasound assisted extraction of phenolic compounds from *P. lentiscus* L. leaves: Comparative study of artificial neural network (ANN) versus degree of experiment for prediction ability of phenolic compounds recovery. *Industrial Crops and Products*, 77, 251-261.

Dai, J., & Mumper, R. J. (2010). Plant phenolics: extraction, analysis and their antioxidant and anticancer properties. *Molecules*, 15(10), 7313-7352.

Demiray, E., & Tulek, Y. (2015). Color degradation kinetics of carrot (D aucus carota L.) slices during hot air drying. *Journal of Food Processing and Preservation*, 39(6), 800-805.

Demiray, E., & Tulek, Y. (2017). Degradation kinetics of β-carotene in carrot slices during convective drying. *International Journal of Food Properties*, 20(1), 151-156.

Demiray, E., Tulek, Y., & Yilmaz, Y. (2013). Degradation kinetics of lycopene, β-carotene and ascorbic acid in tomatoes during hot air drying. *LWT-Food Science and Technology*, 50(1), 172-176.

Dhake, K., Jain, S. K., Jagtap, S., & Pathare, P. B. (2023). Effect of Pretreatment and Temperature on Drying Characteristics and Quality of Green Banana Peel. *AgriEngineering*, 5(4), 2064-2078.

Dönmez, A., & Kadakal, Ç. (2024). Hot-air drying and degradation kinetics of bioactive compounds of gilaburu (*Viburnum opulus* L.) fruit. *Chemical Industry and Chemical Engineering Quarterly*, 30(1), 59–72. https://doi.org/10.2298/CICEQ220614011D

Doymaz, I., & Akgün, N. A. (2009). Study of thin-layer drying of grape wastes. *Chemical Engineering Communication*s, 196(7), 890–900. https://doi.org/10.1080/00986440802668422

Eastman, J. E., & Moore, C. O. (1984). U.S. Patent No. 4,465,702. Washington, DC: U.S. Patent and Trademark Office.

Elik, A., Armağan, H. S., Göğüş, F., Oboturova, N., Nagdalian, A., Smaoui, S., & Shariati, M. A. (2023). Impact of radio frequency-assisted hot air drying on drying

kinetics behaviors and quality features of orange peel. *Biomass Conversion and Biorefinery*, 13(16), 15173–15183. https://doi.org/10.1007/s13399-023-04336-0

Emaga, T. H., Bindelle, J., Agneesens, R., Buldgen, A., Wathelet, B., & Paquot, M. (2011). Ripening influences banana and plantain peels composition and energy content. *Tropical Animal Health and Production*, 43(1). https://doi.org/10.1007/s11250-010-9671-6

Escobar-Avello, D., Avendaño-Godoy, J., Santos, J., Lozano-Castellón, J., Mardones, C., von Baer, D., ... & Gómez-Gaete, C. (2021). Encapsulation of phenolic compounds from a grape cane pilot-plant extract in hydroxypropyl beta-cyclodextrin and maltodextrin by spray drying. *Antioxidants*, 10(7), 1130.

Esfanjani, F., Jafari, S.M., 2016. Biopolymer nano-particles and natural nano-carriers for nano-encapsulation of phenolic compounds. *Colloids Surfaces B Biointerfaces* 146, 532–543.

Fang, S., Wang, Z., & Hu, X. (2009). Hot air drying of whole fruit Chinese jujube (Zizyphus jujuba Miller): Thin-layer mathematical modelling. *International Journal of Food Science and Technology,* 44(9), 1818–1824. https://doi.org/10.1111/j.1365-2621.2009.02005.x

FAO (2024). Food and Agriculture Organization, https://www.fao.org/in-action/seeking-end-to-loss-and-waste-of-food-along-production-chain/en/

FAOSTAT (2019). Crops. Available at http://www.fao.org/faostat/en/#data/QC

FAOSTAT (2022). Food and Agriculture organisation. Available on-https://www.fao.org/faostat/en/#data/QCL accessed on 07/05/2024 & 12.43 pm.

Fatemeh, S. R., Saifullah, R., Abbas, F. M. A., & Azhar, M. E. (2012). Total phenolics, flavonoids and antioxidant activity of banana pulp and peel flours: influence of variety and stage of ripeness. *International food research journal*, 19(3).

Fernandes, L., Casal, S., Pereira, J. A., Saraiva, J. A., & Ramalhosa, E. (2017). Edible flowers: A review of the nutritional, antioxidant, antimicrobial properties and effects on human health. *Journal of Food Composition and Analysis*, 60, 38-50.

Fernandez, M.de los A., ´Espino, M., Gomez, F. J. V., & Silva, M. F. (2018). Novel approaches mediated by tailor-made green solvents for the extraction of phenolic compounds from agro-food industrial by-products. *Food Chemistry*, 239, 671–678. https://doi.org/10.1016/j.foodchem.2017.06.150

Fernando, L., Ferreira, D., Pirozi, R., Ramos, A. M., Antônio, J., & Pereira, M. (2012). Modelagem matemática da secagem em camada delgada de bagaço de uva fermentado. In Pesq. agropec. bras (Issue 6).

Ferreira, L. F. D., Pirozi, M. R., Ramos, A. M., & Pereira, J. A. M. (2012). Modelagem matemática da secagem em camada delgada de bagaço de uva fermentado. *Pesquisa Agropecuária Brasileira*, 47, 855-862.

Fidrianny, I., Kiki Rizki, R., & Insanu, M. (2014). In vitro antioxidant activities from various extracts of banana peels using abts, dpph assays and correlation with phenolic, flavonoid, carotenoid content. *International Journal of Pharmacy and Pharmaceutical Sciences*, 6(8), 299–303.

Fitzpatrick, J. J., Iqbal, T., Delaney, C., Twomey, T., & Keogh, M. K. (2004). Effect of powder properties and storage conditions on the flowability of milk powders with different fat contents. *Journal of food Engineering*, 64(4), 435-444.

Gafuma, S., Byarugaba-Bazirake, G. W., & Mugampoza, E. (2018). Textural Hardness of Selected Ugandan Banana Cultivars under Different Processing Treatments. *Journal of Food Research*, 7(5). https://doi.org/10.5539/jfr.v7n5p98

Gao, H. M., Jiang, J., Wilson, B., Zhang, W., Hong, J. S., & Liu, B. (2002). Microglial activation-mediated delayed and progressive degeneration of rat nigral dopaminergic neurons: relevance to Parkinson's disease. *Journal of neurochemistry*, 81(6), 1285-1297.

García Batista, R. M., Quevedo Guerrero, J. N., & Socorro Castro, A. R. (2020). Practices for the use of solid waste in banana plantations and results of its implementation. Universidad y Sociedad, 12(1).

García-Lomillo, J., & González-SanJosé, M. L. (2017). Applications of wine pomace in the food industry: Approaches and functions. *Comprehensive reviews in food science and food safety*, 16(1), 3-22.

Ghafoor, K., Choi, Y. H., Jeon, J. Y., & Jo, I. H. (2009). Optimization of ultrasound-assisted extraction of phenolic compounds, antioxidants, and anthocyanins from grape (*Vitis vinifera*) seeds. *Journal of agricultural and food chemistry*, 57(11), 4988-4994.

Ghandehari Yazdi, A. P., Barzegar, M., Sahari, M. A., & Ahmadi Gavlighi, H. (2021). Encapsulation of pistachio green hull phenolic compounds by spray drying. *Journal of Agricultural Science and Technology*, 23(1), 51-64.

Gharsallaoui, A., Roudaut, G., Chambin, O., Voilley, A., & Saurel, R. (2007). Applications of spray-drying in microencapsulation of food ingredients: An overview. *Food research international*, 40(9), 1107-1121.

Gonzalez-Centeno, M. R., Jourdes, M., Femenia, A., Simal, S., Rossello, C., & Teissedre, P. L. (2013). Characterization of polyphenols and antioxidant potential of white grape pomace byproducts (*Vitis vinifera* L.). *Journal of Agricultural and Food Chemistry*, 61(47), 11579-11587.

Goyal, R. K., Kingsly, A. R. P., Manikantan, M. R., & Ilyas, S. M. (2007). Mathematical modelling of thin layer drying kinetics of plum in a tunnel dryer. *Journal of Food Engineering*, 79(1), 176–180. https://doi.org/10.1016/j.jfoodeng.2006.01.041

Guiné, R. P., Barroca, M. J., Gonçalves, F. J., Alves, M., Oliveira, S., & Correia, P. M. (2015). Effect of drying on total phenolic compounds, antioxidant activity,

and kinetics decay in pears. *International Journal of Fruit Science*, 15(2), 173-186.

Hernández-Carranza, P., Ávila-Sosa, R., Guerrero-Beltrán, J. A., Navarro-Cruz, A. R., Corona-Jiménez, E., & Ochoa-Velasco, C. E. (2016). Optimization of antioxidant compounds extraction from fruit by-products: Apple pomace, orange and banana peel. *Journal of food processing and preservation*, 40(1), 103-115.

Hikal, W. M., Said-Al Ahl, H. A., Bratovcic, A., Tkachenko, K. G., Sharifi-Rad, J., Kačániová, M., ... & Atanassova, M. (2022). Banana peels: A waste treasure for human being. *Evidence-Based Complementary and Alternative Medicine*, (1), 7616452.

Hogervorst, J. C., Miljić, U., & Puškaš, V. (2017). Extraction of Bioactive Compounds from Grape Processing By-Products. In Handbook of Grape Processing By-Products: Sustainable Solutions (pp. 105–135). Elsevier Inc. https://doi.org/10.1016/B978-0-12-809870-7.00005-3

Ibrahim, M. M., El-Zawawy, W. K., Jüttke, Y., Koschella, A., & Heinze, T. (2013). Cellulose and microcrystalline cellulose from rice straw and banana plant waste: Preparation and characterization. *Cellulose*, 20(5). https://doi.org/10.1007/s10570-013-9992-5

Ince, A. E., Şahin, S., & ŞÜMNÜ, S. G. (2013). Extraction of phenolic compounds from melissa using microwave and ultrasound. *Turkish Journal of Agriculture and Forestry*, 37(1), 69-75.

Iora, S. R., Maciel, G. M., Zielinski, A. A., da Silva, M. V., Pontes, P. V. D. A., Haminiuk, C. W., & Granato, D. (2015). Evaluation of the bioactive compounds and the antioxidant capacity of grape pomace. *International Journal of Food Science & Technology*, 50(1), 62-69.

Islam, M. R., Kamal, M. M., Kabir, M. R., Hasan, M. M., Haque, A. R., & Hasan, S. M. K. (2023). Phenolic compounds and antioxidants activity of banana peel extracts: Testing and optimization of enzyme-assisted conditions. *Measurement: Food*, 10. https://doi.org/10.1016/j.meafoo.2023.100085

Jafari, S. M., Assadpoor, E., He, Y., & Bhandari, B. (2008). Re-coalescence of emulsion droplets during high-energy emulsification. *Food hydrocolloids*, 22(7), 1191-1202.

Jha, A. K., & Sit, N. (2020). Drying characteristics and kinetics of colour change and degradation of phytocomponents and antioxidant activity during convective drying of deseeded *Terminalia chebula* fruit. *Journal of Food Measurement and Characterization*, 14(4), 2067–2077. https://doi.org/10.1007/s11694-020-00454-9

Jiang, N., Ma, J., Ma, R., Zhang, Y., Chen, P., Ren, M., & Wang, C. (2023). Effect of slice thickness and hot-air temperature on the kinetics of hot-air drying of Crabapple slices. *Food Science and Technology* (Brazil), 43. https://doi.org/10.1590/fst.100422

Jinapong, N., Suphantharika, M., & Jamnong, P. (2008). Production of instant soymilk powders by ultrafiltration, spray drying and fluidized bed agglomeration. *Journal of food engineering*, 84(2), 194-205.

Jongkees, B. J., Hommel, B., Kühn, S., & Colzato, L. S. (2015). Effect of tyrosine supplementation on clinical and healthy populations under stress or cognitive demands—A review. *Journal of psychiatric research*, 70, 50-57.

Jović, T., Elez Garofulić, I., Čulina, P., Pedisić, S., Dobroslavić, E., Cegledi, E., ... & Zorić, Z. (2023). The Effect of Spray-Drying Conditions on the Characteristics of Powdered Pistacia lentiscus Leaf Extract. *Processes*, 11(4), 1229.

Kaderides, K., & Goula, A. M. (2017). Development and characterization of a new encapsulating agent from orange juice by-products. *Food Research International*, 100, 612-622.

Kaderides, K., & Goula, A. M. (2019). Encapsulation of pomegranate peel extract with a new carrier material from orange juice by-products. *Journal of Food Engineering*, 253, 1-13.

Kaderides, K., Goula, A. M., & Adamopoulos, K. G. (2015). A process for turning pomegranate peels into a valuable food ingredient using ultrasound-assisted extraction and encapsulation. *Innovative Food Science & Emerging Technologies*, 31, 204-215.

Kaveh, M., Amiri Chayjan, R., & Nikbakht, A. M. (2017). Mass transfer characteristics of eggplant slices during length of continuous band dryer. *Heat and Mass Transfer/Waerme- Und Stoffuebertragung*, 53(6), 2045–2059. https://doi.org/10.1007/s00231-016-1961-8

Kaveh, M., Rasooli Sharabiani, V., Amiri Chayjan, R., Taghinezhad, E., Abbaspour-Gilandeh, Y., & Golpour, I. (2018). ANFIS and ANNs model for prediction of moisture diffusivity and specific energy consumption potato, garlic and cantaloupe drying under convective hot air dryer. *Information Processing in Agriculture*, 5(3), 372–387. https://doi.org/10.1016/j.inpa.2018.05.003

Kaya, S., & Kahyaoglu, T. (2007). Moisture sorption and thermodynamic properties of safflower petals and tarragon. *Journal of Food Engineering*, 78(2), 413–421. https://doi.org/10.1016/j.jfoodeng.2005.10.009

Kim, T. H., Hampton, J. G., Opara, L. U., Hardacre, A. KBrahmi., & Mackay, B. R. (2002). Effects of maize grain size, shape and hardness on drying rate and the occurrence of stress cracks. *Journal of the Science of Food and Agriculture*, 82(10), 1232–1239. https://doi.org/10.1002/jsfa.1166

Khalangre, A., Mirza, A., Sharma, A. K., Shaikh, N., & Shabeer, T. A. (2024). Effect of drying temperature on preservation of banana peel and its impact on degradation of targeted phytochemical by LC-Orbitrap-MS analysis. *Biomass Conversion and Biorefinery*, 1-16.

Kooli, S., Fadhel, A., Farhat, A., & Belghith, A. (2007). Drying of red pepper in open sun and greenhouse conditions. Mathematical modeling and experimental

validation. *Journal of Food Engineering*, 79(3), 1094–1103. https://doi.org/10.1016/j.jfoodeng.2006.03.025

Kumar K, S. (2015). Drying Kinetics of Banana Peel. *Journal of Food Processing & Technology*, 6(11). https://doi.org/10.4172/2157-7110.1000514

Kumar, K. S., Bhowmik, D., Duraivel, S., & Umadevi, M. (2012). Traditional and medicinal uses of banana. Journal of pharmacognosy and phytochemistry, 1(3), 51-63.

Ky, I., & Teissedre, P. L. (2015). Characterisation of Mediterranean grape pomace seed and skin extracts: Polyphenolic content and antioxidant activity. *Molecules*, 20(2), 2190-2207.

Lefebvre, T., Destandau, E., & Lesellier, E. (2021). Selective extraction of bioactive compounds from plants using recent extraction techniques: A review. *Journal of Chromatography A*, 1635, 461770.

Li, Y., Zhu, J., Li, S., Guo, Z., & Van der Bruggen, B. (2020). Flexible aliphatic–aromatic polyamide thin film composite membrane for highly efficient organic solvent nanofiltration. *ACS applied materials & interfaces*, 12(28), 31962-31974.

Liyana-Pathirana, C., & Shahidi, F. (2005). Optimization of extraction of phenolic compounds from wheat using response surface methodology. *Food chemistry*, 93(1), 47-56.

Madamba, P. S., Driscollb, R. H., & Buckleb, K. A. (1996). The Thin-layer Drying Characteristics of Garlic Slices. *Journal of Food Engineering* (Vol. 29).

Mahdavi, S.A., Jafari, S.M., Ghorbani, M., Assadpoor, E., (2014). Spray-drying microencapsulation of anthocyanins by natural biopolymers: a review. *Dry. Technol*. 32, 509–518.

Makris, D. P., Boskou, G., & Andrikopoulos, N. K. (2007). Polyphenolic content and in vitro antioxidant characteristics of wine industry and other agri-food solid waste extracts. *Journal of Food Composition and Analysis*, 20(2), 125-132.

Martín-Gómez, J., Varo, M. Á., Mérida, J., & Serratosa, M. P. (2020). Influence of drying processes on anthocyanin profiles, total phenolic compounds and antioxidant activities of blueberry (*Vaccinium corymbosum*). *LWT*, 120. https://doi.org/10.1016/j.lwt.2019.108931

Méndez-Lagunas, L., Rodríguez-Ramírez, J., Cruz-Gracida, M., Sandoval-Torres, S., & Barriada-Bernal, G. (2017). Convective drying kinetics of strawberry (Fragaria ananassa): Effects on antioxidant activity, anthocyanins and total phenolic content. *Food Chemistry,* 230, 174–181. https://doi.org/10.1016/j.foodchem.2017.03.010

Mghazli, S., Ouhammou, M., Hidar, N., Lahnine, L., Idlimam, A., & Mahrouz, M. (2017). Drying characteristics and kinetics solar drying of Moroccan rosemary leaves. *Renewable Energy*, 108, 303–310. https://doi.org/10.1016/j.renene.2017.02.022

Midilli, A., Kucuk, H., & Yapar, Z. (2002). A new model for single-layer drying. *Drying Technology*, 20(7), 1503–1513. https://doi.org/10.1081/DRT-120005864

Mishra, S., Prabhakar, B., Kharkar, P. S., & Pethe, A. M. (2022). Banana peel waste: An emerging cellulosic material to extract nanocrystalline cellulose. *ACS omega*, 8(1), 1140-1145.

Moura, H. V., de Figueirêdo, R. M. F., de Melo Queiroz, A. J., de Vilela Silva, E. T., Esmero, J. A. D., & Lisbôa, J. F. (2021). Mathematical modeling and thermodynamic properties of the drying kinetics of trapiá residues. *Journal of Food Process Engineering*, 44(8). https://doi.org/10.1111/jfpe.13768

Mphahlele, R. R., Fawole, O. A., Makunga, N. P., & Opara, U. L. (2016). Effect of drying on the bioactive compounds, antioxidant, antibacterial and antityrosinase activities of pomegranate peel. *BMC Complementary and Alternative Medicine*, 16(1). https://doi.org/10.1186/s12906-016-1132-y

Mphahlele, R. R., Pathare, P. B., & Opara, U. L. (2019). Drying kinetics of pomegranate fruit peel (cv. Wonderful). *Scientific African*, 5, e00145.

Munin, A., Edwards-Lévy, F., (2011). Encapsulation of natural poly-phenolic compounds: a review. *Pharmaceutics* 3, 793–829

Muñoz-Bernal, Ó. A., Coria-Oliveros, A. J., de la Rosa, L. A., Rodrigo-García, J., del Rocío Martínez-Ruiz, N., Sayago-Ayerdi, S. G., & Alvarez-Parrilla, E. (2021). Cardioprotective effect of red wine and grape pomace. *Food Research International*, 140, 110069. https://doi.org/10.1016/j.foodres.2020.110069

Nagatsu, T., & Sawada, M. (2009). L-dopa therapy for Parkinson's disease: past, present, and future. *Parkinsonism & related disorders*, 15, S3-S8.

Niamnuy, C., Nachaisin, M., Poomsa-ad, N., & Devahastin, S. (2012). Kinetic modelling of drying and conversion/degradation of isoflavones during infrared drying of soybean. *Food Chemistry*, 133(3), 946-952.

Oliveira, D. E. C., Resende, O., Smaniotto, T. A. S., Campos, R. C., & Chaves, T. H. (2012). Cinética de Secagem dos Grãos de Milho. Revista Brasileira de Milho e Sorgo, 11(2), 190–201. https://doi.org/10.18512/1980-6477/rbms.v11n2p190-201

Onache, P. A., Geana, E. I., Ciucure, C. T., Florea, A., Sumedrea, D. I., Ionete, R. E., & Tița, O. (2022). Bioactive phytochemical composition of grape pomace resulted from different white and red grape cultivars. *Separations*, 9(12), 395. https://doi.org/10.3390/separations9120395

Ouyang, M., Cao, S., Huang, Y., & Wang, Y. (2021). Phenolics and ascorbic acid in pumpkin (Cucurbita maxima) slices: effects of hot air drying and degradation kinetics. *Journal of Food Measurement and Characterization*, 15, 247-255.

Page, G. E. (1949) Factors Influencing the maximum rates of air-drying shelled corn in thin layers. M. S. Thesis, Purdue University, USA.

Paini, M., Aliakbarian, B., Casazza, A. A., Lagazzo, A., Botter, R., & Perego, P. (2015). Microencapsulation of phenolic compounds from olive pomace using spray drying: A study of operative parameters. *LWT-Food Science and Technology*, 62(1), 177-186.

Panche, A. N., Diwan, A. D., & Chandra, S. R. (2016). Flavonoids: an overview. *Journal of nutritional science*, 5, e47.

Park, N., Cho, S. D., Chang, M. S., & Kim, G. H. (2022). Optimization of the ultrasound-assisted extraction of flavonoids and the antioxidant activity of Ruby S apple peel using the response surface method. *Food Science and Biotechnology*, 31(13), 1667-1678.

Parry, J. W., Li, H., Liu, J. R., Zhou, K., Zhang, L., & Ren, S. (2011). Antioxidant activity, antiproliferation of colon cancer cells, and chemical composition of grape pomace. *Food and nutrition Sciences*, 2(6), 530-540.

Peighambardoust, S. H., Tafti, A. G., & Hesari, J. (2011). Application of spray drying for preservation of lactic acid starter cultures: a review. *Trends in food science & technology*, 22(5), 215-224.

Phaiphan, A. (2022). Ultrasound assisted extraction of pectin from banana peel waste as a potential source for pectin production. *Acta Scientiarum Polonorum Technologia Alimentaria*, 21(1), 17-30.

Pollini, L., Tringaniello, C., Ianni, F., Blasi, F., Manes, J., & Cossignani, L. (2020). Impact of ultrasound extraction parameters on the antioxidant properties of Moringa oleifera leaves. *Antioxidants*, 9(4), 277.

Popescu, M., Iancu, P., Plesu, V., Bildea, C. S., & Manolache, F. A. (2023). Mathematical Modeling of Thin-Layer Drying Kinetics of Tomato Peels: Influence of Drying Temperature on the Energy Requirements and Extracts Quality. *Foods*, 12(20), 3883.

Pu, Y., Ding, T., Wang, W., Xiang, Y., Ye, X., Li, M., & Liu, D. (2018). Effect of harvest, drying and storage on the bitterness, moisture, sugars, free amino acids and phenolic compounds of jujube fruit (*Zizyphus jujuba* cv. Junzao). *Journal of the Science of Food and Agriculture*, 98(2), 628–634. https://doi.org/10.1002/jsfa.8507

Quek, S. Y., Chok, N. K., & Swedlund, P. (2007). The physicochemical properties of spray-dried watermelon powders. *Chemical Engineering and Processing: Process Intensification*, 46(5), 386-392.

Ranjbar-Slamloo, Y., & Fazlali, Z. (2020). Dopamine and Noradrenaline in the Brain; Overlapping or Dissociate Functions? *Frontiers in Molecular Neuroscience*, 12. https://doi.org/10.3389/fnmol.2019.00334

Rebello, L. P. G., Ramos, A. M., Pertuzatti, P. B., Barcia, M. T., Castillo-Muñoz, N., & Hermosín-Gutiérrez, I. (2014). Flour of banana (Musa AAA) peel as a source of antioxidant phenolic compounds. *Food Research International*, 55, 397-403.

Ribeiro, L. F., Ribani, R. H., Francisco, T. M. G., Soares, A. A., Pontarolo, R., & Haminiuk, C. W. I. (2015). Profile of bioactive compounds from grape pomace (Vitis vinifera and Vitis labrusca) by spectrophotometric, chromatographic and spectral analyses. *Journal of chromatography B*, 1007, 72-80.

Robert, P., Gorena, T., Romero, N., Sepulveda, E., Chavez, J., & Saenz, C. (2010). Encapsulation of polyphenols and anthocyanins from pomegranate (Punica granatum) by spray drying. *International journal of food science & technology*, 45(7), 1386-1394.

Rockenbach, I. I., Rodrigues, E., Gonzaga, L. V., Caliari, V., Genovese, M. I., Gonçalves, A. E. D. S. S., & Fett, R. (2011). Phenolic compounds content and antioxidant activity in pomace from selected red grapes (*Vitis vinifera* L. and *Vitis labrusca* L.) widely produced in Brazil. *Food Chemistry*, 127(1), 174-179.

Rodrigues, L. M., Romanini, E. B., Silva, E., Pilau, E. J., da Costa, S. C., & Madrona, G. S. (2020). Camu-camu bioactive compounds extraction by ecofriendly sequential processes (ultrasound assisted extraction and reverse osmosis). *Ultrasonics sonochemistry*, 64, 105017.

Rodrigues, R. P., Sousa, A. M., Gando-Ferreira, L. M., & Quina, M. J. (2023). Grape pomace as a natural source of phenolic compounds: solvent screening and extraction optimization. *Molecules*, 28(6), 2715.

Rodrigues, S., & Pinto, G. A. (2007). Ultrasound extraction of phenolic compounds from coconut (Cocos nucifera) shell powder. Journal of food engineering, 80(3), 869-872.

Rodrigues, S., Fernandes, F. A., de Brito, E. S., Sousa, A. D., & Narain, N. (2015). Ultrasound extraction of phenolics and anthocyanins from jabuticaba peel. *Industrial Crops and Products*, 69, 400-407.

Rodrigues, S., Pinto, G. A., & Fernandes, F. A. (2008). Optimization of ultrasound extraction of phenolic compounds from coconut (Cocos nucifera) shell powder by response surface methodology. *Ultrasonics Sonochemistry*, 15(1), 95-100.

Rodríguez De Luna, S. L., Ramírez-Garza, R. E., & Serna Saldívar, S. O. (2020). Environmentally friendly methods for flavonoid extraction from plant material: Impact of their operating conditions on yield and antioxidant properties. *The Scientific World Journal*, 2020(1), 6792069.

Rodsamran, P., & Sothornvit, R. (2019). Extraction of phenolic compounds from lime peel waste using ultrasonic-assisted and microwave-assisted extractions. *Food bioscience*, 28, 66-73.

Saeed, I. E., Sopian, K., & Abidin, Z. Z. (2008). Drying characteristics of roselle (1): mathematical modeling and drying experiments. *Agricultural Engineering International: CIGR Journal*.

Saénz, C., Tapia, S., Chávez, J., & Robert, P. (2009). Microencapsulation by spray drying of bioactive compounds from cactus pear (*Opuntia ficus*-indica). *Food chemistry*, 114(2), 616-622.

Şahin, S., & Şamlı, R. (2013). Optimization of olive leaf extract obtained by ultrasound-assisted extraction with response surface methodology. *Ultrasonics sonochemistry*, 20(1), 595-602.

Sant'Anna, V., Christiano, F. D. P., Marczak, L. D. F., Tessaro, I. C., & Thys, R. C. S. (2014). The effect of the incorporation of grape marc powder in fettuccini pasta properties. *LWT*, 58(2), 497–501. https://doi.org/10.1016/j.lwt.2014.04.008

Sant'Anna, V., Cassini, A. S., Marczak, L. D. F., & Tessaro, I. C. (2014). Kinetic modeling, total phenolic content and colour changes of mango peels during hot air drying. *Latin American applied research*, 44(4), 301-306.

Šelo, G., Planinić, M., Tišma, M., Martinović, J., Perković, G., & Bucić-Kojić, A. (2023). Bioconversion of Grape Pomace with Rhizopus oryzae under Solid-State Conditions: Changes in the Chemical Composition and Profile of Phenolic Compounds. *Microorganisms*, 11(4), 956. https://doi.org/10.3390/microorganisms11040956

Shahidi, F., & Ambigaipalan, P. (2015). Phenolics and polyphenolics in foods, beverages and spices: Antioxidant activity and health effects–A review. *Journal of functional* foods, 18, 820-897.

Sharma, Y., Chauhan, A., Bala, K., & Nagar, A. (2016). Comparative study of different parts of fruits of Musa Sp. on the basis of their antioxidant activity. *Der Pharmacia Lettre*, 8, 88-100.

Shishir, M. R. I., & Chen, W. (2017). Trends of spray drying: A critical review on drying of fruit and vegetable juices. *Trends in food science & technology*, 65, 49-67..

Sid, S., Alam, M., Islam, M., Kumar, Y., Mor, R. S., Kishore, A., & Kumar, N. (2023). Characterization and quality attributes of spray-dried Kinnow peel powder using maltodextrin and gum arabic. *Journal of Food Process Engineering*, 46(12), e14488.

Singh, B., Singh, J. P., Kaur, A., & Singh, N. (2016). Bioactive compounds in banana and their associated health benefits–A review. Food chemistry, 206, 1-11.

Singhal, M., & Ratra, P. (2013). Antioxidant activity, total flavonoid and total phenolic content of musa acuminate peel extracts. *Global Journal of Pharmacology*, 7(2), 118-122.

Socaci, S. A. (2017). In D. O. Ruginˇ a (Ed.), Antioxidant compounds recovered from food wastes. Intech Open. https://doi.org/10.5772/intechopen.69124.

Sokač, T., Gunjević, V., Pušek, A., Tušek, A. J., Dujmić, F., Brnčić, M., ... & Redovniković, I. R. (2022). Comparison of drying methods and their effect on the

stability of Graševina grape pomace biologically active compounds. *Foods*, 11(1), 112.https://doi.org/10.3390/foods11010112

Sridhar, K., & Charles, A. L. (2022). Mathematical modeling to describe drying behavior of kyoho (Vitis labruscana) skin waste: drying kinetics and quality attributes. *Processes*, 10(10), 2092. https://doi.org/10.3390/pr10102092

Sugesta, M. Y. I., Wibowo, R. S., Alfiah, M., Reza, M., & Sjaifullah, A. (2024). Extraction of Polyphenols from Horn Banana Peel (Musa Paradisiaca var. Typica) Using the Ultrasound Assisted Extraction Method. *Journal of Biobased Chemicals*, 4(1), 1-20.

Sulaiman, S. F., Yusoff, N. A. M., Eldeen, I. M., Seow, E. M., Sajak, A. A., Supriatno, & Ooi, K. L. (2011). Correlation between total phenolic and mineral contents with antioxidant activity of eight Malaysian bananas (*Musa sp*.). *Journal of Food Composition and Analysis*, 24(1), 1-10.

Sundaram, S., Anjum, S., Dwivedi, P., & Rai, G. K. (2011). Antioxidant activity and protective effect of banana peel against oxidative hemolysis of human erythrocyte at different stages of ripening. *Applied biochemistry and biotechnology*, 164, 1192-1206.

Syukriani, L., Febjislami, S., Lubis, D. S., Hidayati, R., Asben, A., Suliansyah, I., & Jamsari, J. (2021). Physicochemical characterization of peel, flesh and banana fruit cv. raja [Musa paradisiaca]. In IOP Conference Series: Earth and Environmental Science (Vol. 741, No. 1, p. 012006). IOP Publishing.

Tabaraki, R., Heidarizadi, E., & Benvidi, A. (2012). Optimization of ultrasonic-assisted extraction of pomegranate (*Punica granatum* L.) peel antioxidants by response surface methodology. *Separation and Purification Technology*, 98, 16-23.

Teles, A. S. C., Chávez, D. W. H., Gomes, F. D. S., Cabral, L. M. C., & Tonon, R. V. (2017). Effect of temperature on the degradation of bioactive compounds of Pinot Noir grape pomace during drying. *Brazilian Journal of Food Technology*, 21.

Thiruvalluvan, M., Gupta, R., & Kaur, B. P. (2024). Optimization of ultrasound-assisted extraction conditions for the recovery of phenolic compounds from sweet lime peel waste. *Biomass Conversion and Biorefinery*, 1-23.

Tibolla H., Pelissari F., Martins J., Vicente A., and Menegalli F. (2018). Cellulose nanofibers produced from banana peel by chemical and mechanical treatments: Characterization and cytotoxicity assessment. *Food Hydrocoll*. 75:192–201. doi: 10.1016/j.foodhyd.2017.08.027.

Tonon, R. V., Brabet, C., & Hubinger, M. D. (2008). Influence of process conditions on the physicochemical properties of açai (*Euterpe oleraceae* Mart.) powder produced by spray drying. *Journal of food engineering*, 88(3), 411-418

Toprakçı, İ., Güngör, K. K., Torun, M., & Şahin, S. (2024). Spray-drying microencapsulation of plum peel bioactives using Arabic gum and maltodextrin as coating matrix. *Food Bioscience*, 61, 104824.

Tulek, Y. (2011). Drying Kinetics of Oyster Mushroom (*Pleurotus ostreatus*) in a Convective Hot Air Dryer. https://www.researchgate.net/publication/267945964

UNEP (2022) United Nations Environment Programme. https://www.unep.org/thinkeatsave/get-informed/worldwide-food-waste.

Gaware, T. J., Sutar, N., & Thorat, B. N. (2010). Drying of tomato using different methods: comparison of dehydration and rehydration kinetics. *Drying Technology*, 28(5), 651-658.

Vardin, H., & Yilmaz, F. M. (2018). The effect of blanching pre-treatment on the drying kinetics, thermal degradation of phenolic compounds and hydroxymethyl furfural formation in pomegranate arils. *Italian journal of food science*, 30(1).

Verma, L. R., Bucklin, R. A., Endan, J. B., Wratten, F. T., Member, A., & Asae, A. (1985). Effects of Drying Air Parameters on Rice Drying Models.

Vo, T. P., Nguyen, N. T. U., Le, V. H., Phan, T. H., Nguyen, T. H. Y., & Nguyen, D. Q. (2023). Optimizing ultrasonic-assisted and microwave-assisted extraction processes to recover phenolics and flavonoids from passion fruit peels. *ACS omega*, 8(37), 33870-33882.

Voora, V., Larrea, C., & Bermudez, S. (2020). Global Market Report: Bananas SUSTAINABLE COMMODITIES MARKETPLACE SERIES 2019.

Vu, H. T., Scarlett, C. J., & Vuong, Q. V. (2017). Optimization of ultrasound-assisted extraction conditions for recovery of phenolic compounds and antioxidant capacity from banana (Musa cavendish) peel. *Journal of food processing and preservation*, 41(5), e13148.

Vu, H. T., Scarlett, C. J., & Vuong, Q. V. (2018). Phenolic compounds within banana peel and their potential uses: A review. Journal of functional foods, 40, 238-248.

Vu, Hang T., Christopher J. Scarlett, and Quan V. Vuong (2020) Encapsulation of phenolic-rich extract from banana (*Musa cavendish*) peel. *Journal of food science and technology,* 57 : 2089-2098.

Wachirasiri, P., Julakarangka, S., & Wanlapa, S. (2009). The effects of banana peel preparations on the properties of banana peel dietary fibre concentrate. Songklanakarin *Journal of Science & Technology*, 31(6).

Wallace, T. C. (2011). Anthocyanins in cardiovascular disease. *Advances in nutrition*, 2(1), 1-7.

Wanderley, R. de O. S., de Figueirêdo, R. M. F., Queiroz, A. J. de M., dos Santos, F. S., Paiva, Y. F., Ferreira, J. P. de L., de Lima, A. G. B., Gomes, J. P., Costa, C. C., da Silva, W. P., Santos, D. da C., & Maracajá, P. B. (2023). The Temperature

Influence on Drying Kinetics and Physico-Chemical Properties of Pomegranate Peels and Seeds. *Foods*, 12(2). https://doi.org/10.3390/foods12020286

Wang, L., & Weller, C. L. (2006). Recent advances in extraction of nutraceuticals from plants. *Trends in Food Science & Technology*, 17(6), 300-312.

Wang, R., Zhang, W., He, R., Li, W., & Wang, L. (2021). Customized deep eutectic solvents as green extractants for ultrasonic-assisted enhanced extraction of phenolic antioxidants from dogbane leaf-tea. *Foods*, 10(11), 2527.

Wang, S., Lin, A. H. M., Han, Q., & Xu, Q. (2020). Evaluation of direct ultrasound-assisted extraction of phenolic compounds from potato peels. *Processes*, 8(12), 1665.

Westerman, P. W., White, G. M., Ross, I. J., & Asae, A. (1973). Relative Humidity Effect on the High-Temperature Drying of Shelled Corn.

Wisniak, J., & Polishuk, A. (1999). Analysis of residuals—a useful tool for phase equilibrium data analysis. *Fluid Phase Equilibria*, 164(1), 61-82.

Yaldiz, O., Ertekin, C., & Uzun, H. I. (2001). Mathematical modeling of thin layer solar drying of sultana grapes. *Energy*, 26(5), 457-465.

Zhang, J., Zhang, C., Chen, X., & Quek, S. Y. (2020). Effect of spray drying on phenolic compounds of cranberry juice and their stability during storage. *Journal of Food Engineering*, 269, 109744.

Zhang, Y., Pechan, T., & Chang, S. K. (2018). Antioxidant and angiotensin-I converting enzyme inhibitory activities of phenolic extracts and fractions derived from three phenolic-rich legume varieties. *Journal of Functional Foods*, 42, 289-297.

Zhou, T., Xu, D. P., Lin, S. J., Li, Y., Zheng, J., Zhou, Y., ... & Li, H. B. (2017). Ultrasound-assisted extraction and identification of natural antioxidants from the fruit of *Melastoma sanguineum* Sims. *Molecules*, 22(2), 306.

Žlabur, J. Š., Opačić, N., Žutić, I., Voća, S., Poštek, M., Radman, S., ... & Uher, S. F. (2021). Valorization of nutritional potential and specialized metabolites of basil cultivars depending on cultivation method. *Agronomy*, 11(6), 1048.

Zogzas, N. P., Maroulis, Z. B., & Marinos-Kouris, D. (1996). Moisture diffusivity data compilation in foodstuffs. *Drying Technology*, 14(10), 2225–2253. https://doi.org/10.1080/07373939608917205